The Official Journal of the Chinese Stomatological Association (CSA)

Chinese Journal of Dental Research

CJDR

VOLUME 25 NUMBER 3 2022

Chinese Journal of Dental Research

The Official Journal of the Chinese Stomatological Association (CSA)

Chinese Journal of Dental Research

The Official Journal of the Chinese Stomatological Association (CSA)

Original article

Original article

Case report

Chinese Journal of Dental Research

CN 10-1194/R • ISSN 1462-6446 • eISSN 1867-5646 • Quarterly

The Official Journal of the Chinese Stomatological Association
Co-sponsor: Peking University School of Stomatology, Quintessenz Verlag

Publication Department

Production Manager: Megan Platt (London, UK)
Managing Editor: Xiao Xia ZHANG (Beijing, P.R. China)

Address: 4F, Tower C, Jia 18#, Zhongguancun South Avenue, HaiDian District, 100081, Beijing, P.R. China.
Tel: 86 10 82195785, **Fax:** 86 10 62173402
Email: editor@cjdrcsa.com

Manuscript submission: Information can be found on the Guidelines for Authors page in this issue. To submit your outstanding research results more quickly, please visit: http://mc03.manuscriptcentral.com/cjdr

Administrated by: China Association for Science and Technology
Sponsored by: Chinese Stomatological Association and Popular Science Press
Published by: Popular Science Press
Printed by: Beijing ARTRON Colour Printing Co Ltd
Subscription (domestically) by Post Office

Chinese Journal of Dental Research is indexed in MEDLINE.

For more information and to download the free full text of the issue, please visit
www.quint.link/cjdr
http://www.cjdrcsa.com

Acknowledgements

We would like to express our gratitude to the peer reviewers for their great support to the journal in 2021.

Abi Rached-Junior, Fuad Jacob (Brazil)
Agudelo-Suárez, Andrés (Colombia)
Ahmed, Sarfraz (Pakistan)
Al-Moraissi, Essam (Yemen)
Antunes, Jose Leopoldo Ferreira (Brazil)
Ardeshirylajimi, Abdolreza (Iran)
Atarbashi-Moghadam, Fazele (Iran)
Azañedo, Diego (Peru)
Baghaei, Kaveh (Iran)
Bauer, Jose (Brazil)
Bayindir, Funda (Turkey)
Beldüz Kara, Nihal (Turkey)
Bhawal, Ujjal (Japan)
Buyuk, Suleyman (Turkey)
Chen, Bin (China)
Chen, Fa Ming (China)
Chen, Su (China)
Chen, Zhi (China)
Chrcanovic, Bruno R (Sweden)
Chu, Chun Hung (Hong Kong, China)
Coban, Gokhan (Turkey)
Corchuelo, Jairo (Colombia)
Cristiane, Koga-Ito (Brazil)
Cynthia, Evangeline (India)
Dai, Ning (China)
Dhirawat, Jotikasthira (Thailand)
Erdemir, Uğur (Turkey)
Erdogan, Ozgur (Turkey)
Estrela, Carlos (Brazil)
Fan, Yuan (China)
Fan, Zhi Peng (China)
Feng, Hai Lan (China)
Figueiredo, Rui (Spain)
Fu, Kai Yuan (China)
Ge, Wen Shu (China)
Ghahraman, Leila (Iran)
Ghelichi-Ghojogh, Muosa (Iran)
Graf, Daniel (Canada)
Gu, Xin Hua (China)
Gu, Yan (China)
Gunpinar, Sadiye (Turkey)
Güzel, Rezan (Turkey)
Hajeer, Mohammad Y (Syria)
Hari, Petsos (Germany)
He, Chuang Long (China)
Hou, Ben Xiang (China)
Huang, Cui (China)
Huang, Ding Ming (China)
Huang, Xiao Feng China
Jia, Ling Fei (China)
Jiang, Jiu Hui (China)
Jiang, Qian Zhou (China)
Jiang, Shao Yun (China)
Jin, Li Jian (Hong Kong, China)
Kallarakkal, Thomas (Malaysia)
Khurana, Prakhar (India)
Köseoğlu, Serhat (Turkey)
Koşumcu, Sevim (Turkey)
Kowash, Mawlood
(United Arab Emirates)
Kum, Kee-Yeon (South Korea)
Kurt, Ayça (Turkey)
León, Jorge Esquiche (Brazil)
León-Manco, Roberto (Peru)
Li, Gang (China)
Li, Hong Bo (China)
Li, Mei (New Zealand)
Liang, Yu Hong (China)
Lin, Huan Cai (China)
Liu, Da Wei (China)
Liu, Deng Gao (China)
Liu, Jian Zhang (China)
Liu, Ou Sheng (China)
Liu, Xiao Hua (United States)
Liu, Xue Nan (China)
Lorenzo, Susana (Brazil)
Lu, Rui fang (China)
Mai, Sui (China)
Menini, Maria (Italy)
Mohtasham, Nooshin (Iran)
Nokhbatolfoghahaei, Hanieh (Iran)
Ozturk, Taner (Turkey)
Paksoy, Tugce (Turkey)
Pan, Shao Xia (China)
Pan, Ya Ping (China)
Pan, Yong Chu (China)
Panda, Saurav (India)
Patil, Nikita (India)
Peng, Xian (China)
Pimkhaokham, Atiphan (Thailand)
Rajabi, Abdolhalim (Iran)
Rengifo-Reina, Herney A (Colombia)
Rezaei Rad, Maryam (Iran)
Rirattanapong, Praphasri (Thailand)
Rong, Qi Guo (China)
Rossi-Fedele, Giampiero (Australia)
Schuch, Helena Silveira (Brazil)
Sharma, Divyas (India)
Shokri, Abbas (Iran)
Souza, Erick Miranda (Brazil)
Sriram, Srikanthan (India)
Sun, Hong Chen (China)
Sun, Zhi Peng (China)
Tahmaseb, Ali (Netherlands)
Tavakoly , Belin (Iran)
Tuner, Jan (Sweden)
Umemura, Naoki (Japan)
Üstün, Kemal (Turkey)
Wang, Chun Xiao (China)
Wang, Xiao Yan (China)
Wang, Yi Xiang (China)
Wax, MK (United States)
Yan, Fu Hua (China)
Yang, Kai (China)
Yang, Rui Li (China)
Yildirim, Handan (Turkey)
Yiu, Cynthia Kar Yung
(Hong Kong, China)
Zeng, Dong Lin (China)
Zhang, Cheng Fei (Hong Kong, China)
Zhang, Lei (China)
Zheng, Shu Guo (China)
Zhou, Yong Sheng (China)
Zhou, Zhi Bo (China)

Editorial Office
Chinese Journal of Dental Research

Features of the Sensorimotor Cortex Altered after Tooth Loss and Subsequent Implant Placement in the Maxilla of Rats

Sheng Hao XUE[1#], Jian LI[1#], Jing Wen YANG[1], Zhong Ning LIU[1], Ting JIANG[1]

Objective: *To investigate the synergistic changes of the astrocytes and neurons in the sensorimotor cortex during the process of implant osseointegration after insertion.*
Methods: *A total of 75 rats were allocated into three groups (n = 25): non-operated, extraction and implant. The rats in the latter two groups underwent extraction surgery of three maxillary right molars. One month later, the implant group received one titanium implant in the healed extraction socket. The rats were sacrificed on days 1, 3, 7, 14 and 28 after implantation. The brain sections, including sensory centre S1 and motor centre M1, were selected for further immunofluorescence for measurement of the synergistic morphological and quantitative changes of astrocytes and neurons.*
Results: *In layer IV of S1, the number of astrocytes in the implant group showed a descending trend with time; on days 1, 3, 7 and 14, the number of astrocytes in both the extraction group and the implant group was significantly higher than that in the non-operated group, and there was no difference between the extraction group and the implant group; however, on day 28, the number of astrocytes in the implant group was significantly lower than that in the extraction group. In layer V of M1, on days 7, 14 and 28, the number of astrocytes in the implant group was significantly lower than that in the extraction group; on days 14 and 28, the number of astrocytes in the extraction group was significantly higher than that in the non-operated group. In layer IV of S1 or layer V of M1, the number of neurons showed no significant changes between the three groups.*
Conclusion: *The astrocytes in the face sensorimotor cortex were activated as a reaction to oral environment changes. This kind of neuroplasticity can be reversed by oral rehabilitation with dental implants. The motor cortex may be intimately related to osseointegration and osseoperception.*
Key words: *motor cortex, neuroplasticity, oral implant, osseointegration, sensory cortex*
Chin J Dent Res 2022;25(3):169–177; doi: 10.3290/j.cjdr.b3317969

The sensory signal pathway of natural teeth starts from the Ruffini body in the periodontal ligament. After tooth loss, the transmission of mechanical sensory signals from the periodontal ligament disappears, which affects the deep sensory signals of muscle spindle and temporomandibular joint proprioceptors and interrupts the sensory feedback pathway[1]. Thus, the complete reconstruction of the same shape, structure, function and sensory perception as normal natural teeth is considered the ultimate goal of dental prostheses[2]. Dental implants have innovated traditional restoration methods, offering satisfactory rehabilitation effects approximate to the appearance of natural teeth[3,4]. In clinical application, however, the tactile sensory ability of implant-supported dentures has been found to be far less than that of natural teeth, only 1/50 to 1/10 of the latter[5]. Consequently, there have been clinical cases of unsuc-

1 Department of Prosthodontics, Peking University School and Hospital of Stomatology, National Clinical Research Centre for Oral Diseases, National Engineering Laboratory for Digital and Material Technology of Stomatology, Beijing Key Laboratory of Digital Stomatology, Beijing, China.
# These two authors contributed equally to this work.

Corresponding authors: Dr Jian LI and Dr Ting JIANG, Department of Prosthodontics, Peking University School and Hospital of Stomatology, 22# Zhongguancun South Avenue, HaiDian District, Beijing 100081, P.R. China. Tel: 86-10-8219539. Email: pkujianli@126.com; jt_ketizu@163.com

This work was supported by the National Natural Science Foundation of China (nos. 81100771, 81771045 and 82170928).

cessful implants due to excessive bite force, with failure manifesting itself mainly as mechanical complications and early excessive vertical bone resorption. Thus, the question of how to improve the tactile sensory ability of dental implants has become an urgent issue to be solved in clinical application.

In the 1990s, Brånemark proposed the concept of osseoperception, which was amended gradually before a consensus was reached in academic circles in 2005[6]: the sensation arising from mechanical stimulation of a bone-anchored prosthesis, transduced by mechanoreceptors that may include those located in muscle, joint, mucosal, cutaneous and periosteal tissues, and a change in central neural processing in maintaining sensorimotor function. In other words, the osseoperception of dental implants encompasses not only the information from the peripheral nervous system, but also the perception of the central nervous system, namely the cerebral cortex[7]. However, it has not been fully clarified whether this tactile sensation perceived by implants comes from the establishment of a specific feedback regulatory pathway from the peripheral to the central nervous system. The clarification of this pathway will be of great significance to the strategies and methods to improve osseoperception; however, so far there has been little knowledge about the changes in the microstructure of the sensory conduction pathway at different stages of the implant osseointegration process due to a lack of systematic observation.

Some studies have reported that changes in the oral environment would cause structural and functional neuroplasticity in the central cortex, including the reduction of the number of neurons[8,9], the change of synaptic function[9], the deformation of astrocytes[10] and the reduction in the volume of the brain area controlling the oral and maxillofacial region[11]. Many studies have also shown that when degenerative changes occur in the oral cavity (such as chronic pain, dysfunction, noxious stimulus and cancer)[10-12], they cause proliferation or activation of astrocytes in the corresponding sensory cortex. It has been reported that the number of astrocytes in the hippocampal region of rats increased significantly after tooth loss[10].

At the same time, some studies have suggested that implants could partially reverse the neuroplastic changes of the central nervous system caused by tooth loss. A study using functional magnetic resonance imaging (fMRI) showed that electrical stimulation of implants could activate the cortical somatosensory area corresponding to natural teeth and a wide range of bilateral external areas[13]. Some researchers compared the brain fMRI among three groups of patients who underwent rehabilitation of an implant-supported fixed denture, implant-supported overdenture or mucosal-supported denture, respectively, and found that the blood oxygen–related signals in the primary sensory centre (S1)/motor centre (M1) of patients with implant-supported fixed dentures were significantly higher than those of the other two groups[14]. Another study found that after extraction of the right maxillary molars in rats, the activated area of M1 in the cerebral motor cortex decreased when the anterior abdomen of digastric muscle and genioglossus muscle contracted[15]. After restoration with implants, the changes in M1 were reversed and caused the activation of the wider cortical area, which suggested neuroplastic changes in M1[15]; however, these studies did not investigate the cellular or molecular changes in the cortex or observe the synergic linkage between the osseointegration process and cortical neurons or astrocytes, which would offer the possibility of explaining how osseointegrated implants develop osseoperception.

The oromaxillofacial sensory/motor centre (face-S1/face-M1, hereinafter referred to as S1/M1) plays an important role in coordinating oromaxillofacial sensory/motor function[16]. Many studies have shown that in subprimates and primates, S1 mainly undertakes oral and maxillofacial sensory function and partly participates in the control of oral and maxillofacial movement. M1 mainly outputs motor information to brainstem motor neurons and receives many sensory inputs to assist its role in motor behaviour[17]. Therefore, this study aimed to establish a time-axis animal model to explore the changes in the morphology and number of neurons and astrocytes in S1/M1 region during osseointegration to understand the difference in neuroplastic changes between S1 and M1 and the changes' temporal and spatial linkage with the osseointegration process. This research also aimed to provide indispensable basic data to build up some neurogenic strategies to improve osseointegration and osseoperception of dental implants.

Materials and methods

Experimental animals and groups

The animal experiments were approved by the experimental animal welfare ethics committee of Peking University (license no. LA2013-76). Seventy-five 6-week-old Sprague Dawley male rats weighing 220 ± 15 g were selected and provided by Beijing SPEF Experimental Animal Technology (experimental animal production license: SCXK [Beijing] 2019-001]). All specific path-

ogen free (SPF) rats were fed in the experimental animal room of Peking University Hospital and School of Stomatology. The feeding conditions were temperature 22 ± 1°C, humidity 50% ± 5%, daytime/night 12 hours alternately, and they consumed a mashed chow diet and water ad libitum from the adaptation period.

After the 7-day adaptation period, the rats were randomly divided into three groups: non-operated, extraction and implant (25 rats per group). The rats in the extraction and implant groups underwent extraction of the three right maxillary molars under anaesthesia, and the masticatory function of the left maxillary and mandibular teeth was retained. One month after tooth extraction, the rats in the implant group received one titanium implant in the healed extraction socket of the maxillary right first molar. Since osseointegration of implants in the maxilla of rodents has been confirmed to complete in around 28 days after implantation[18], the rats were sacrificed on days 1, 3, 7, 14 and 28 after implantation (taking the day of implantation as baseline, five rats in each subgroup were sacrificed on day 1, five on day 3, five on day 7, five on day 14 and five on day 28) (Fig 1).

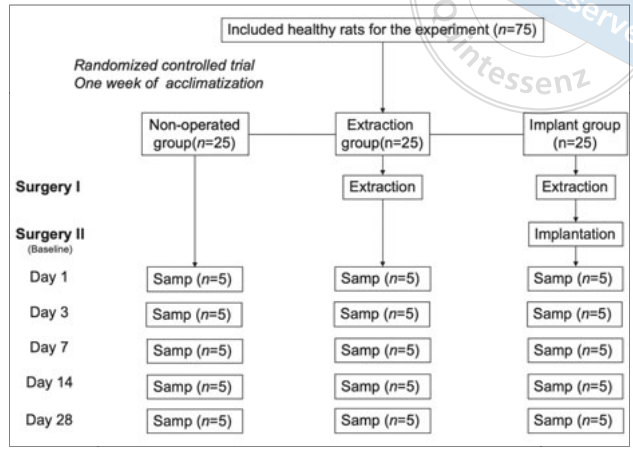

Fig 1 Groups of experimental animals. The implant group (n = 25) underwent both extraction and implant insertion surgery while the extraction group only underwent the former. Baseline was set as the day of implant placement, and the five time points for animal euthanasia and sampling were on days 1, 3, 7, 14 and 28 after implant surgery. Samp, sample.

Surgical protocol

The molar extraction and implant surgery were carried out under aseptic conditions. The gingival tissue around three maxillary right molars was detached with a probe and the teeth were luxated using Ventura forceps (Belevor, Shenzhen, China). One month later, prior to implant surgery, the extraction sites were evaluated through gross examination for adequate soft tissue healing. Then, in the rats in the implant group, the healed edentulous alveolar crest was surgically exposed with a scalpel, then a bone cavity was prepared with a low-speed drill into the healed extraction site of the maxillary right first molar, and a titanium miniscrew implant (MCTBIO, Gyeonggi-do, South Korea; 1.2 mm diameter, 3.0 mm length) was inserted in the cavity (Fig 2). Primary implant stability (a prerequisite for successful bone healing around dental implants) was confirmed manually. The implant head remained non-submerged and was occluded with the mandibular first molar. Bilateral occlusion was checked to verify the existence of occlusal contacts between the implant and the opposing tooth, as well as between the opposing teeth on the contralateral side. Since an increased occlusal load would interfere with bone healing around the implants, maxillomandibular occlusal contact was checked clinically every other day after insertion to ensure no excessive occlusal loading occurred on the implants.

The previous literature pointed out that the mesial root of the maxillary molars in rats was the thickest and was a suitable site for implant placement[19]. The recommended diameter of the drill hole was 1.5 mm and intraosseous length was 2.0 mm[19]. The bone–implant contact rate reached 55.1% ± 8.9% 28 days after implantation, and there was no significant difference in the osseointegration rate between 28 and 56 days[19].

Execution of animals and tissue handling

The rats were sacrificed by intraperitoneal injection of an excess of 1% sodium pentobarbital solution and then placed on an ice table. The head skin was quickly peeled off and the skull was separated. The brain was taken out intact and put in 4% paraformaldehyde to be fixed for 24 hours, then transferred to 30% sucrose solution for at least 2 days. After the specimens sank to the bottom, they were transferred to 0.01 mol/L phosphate-buffered saline (PBS) solution and placed on the prepared freezing table. After the tissue was frozen, serial frozen slices with a thickness of 40 μm were made using Leica CM1950 Cryostats (Leica, Wetzlar, Germany).

Immunofluorescence

Referring to the rat brain stereotactic map[20], the coronal slices at a distance of 2.0 mm from the anterior bregma were selected (Fig 3); the first and second of every three consecutive slices were used for neurons and astrocytes, and the third slice was discarded. Five slices

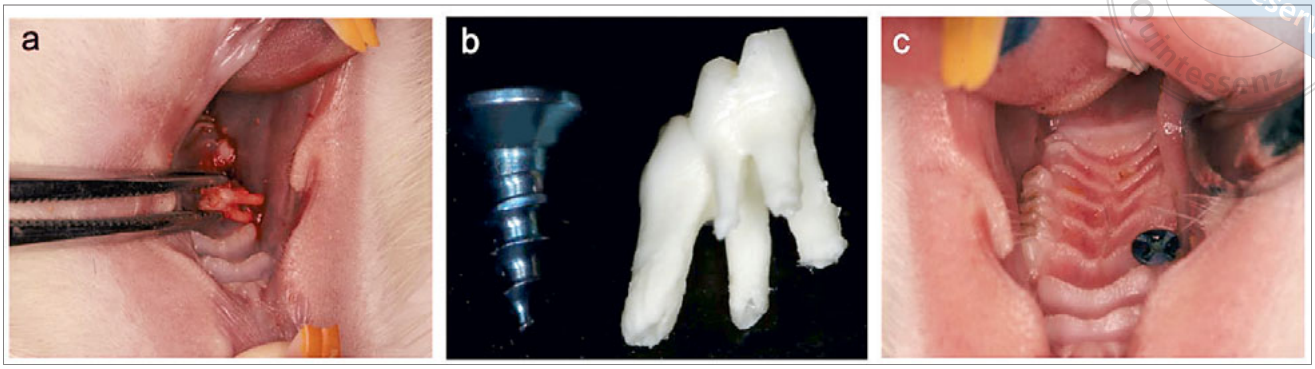

Fig 2 Implantation model in rats' maxilla. **(a and b)** Three maxillary right molars were luxated using a modified dental instrument. **(c)** A titanium miniscrew implant (1.2 mm diameter, 3.0 mm length) was inserted to restore the maxillary right first molar after 1 month of healing from extraction.

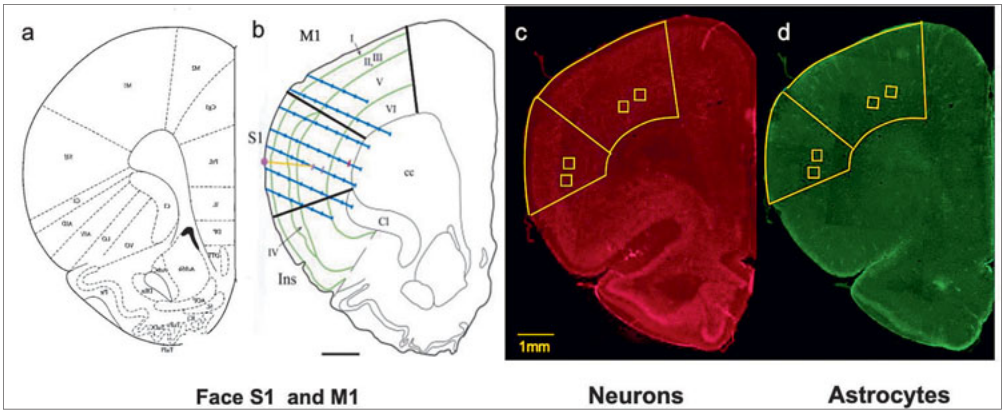

Fig 3 Schematic diagrams of S1/M1 in coronal sections. **(a and b)** S1/M1 in coronal sections of rats' brain. **(c)** Staining of neurons in layer IV of S1 and layer V of M1. **(d)** Staining of astrocytes in layer IV of S1 and layer V of M1.

were obtained for neurons and astrocytes for free-floating immunofluorescence staining. NeuN (1:1000; Proteintech, Rosemont, IL, USA) was used as the marker for neurons and GFAP (1:1000; Proteintech) was the marker for astrocytes. Nonspecific antigens were blocked using goat serum. The sections were placed in the primary antibody and incubated overnight in a refrigerator at 4°C. The fluorescent secondary antibody corresponding to the source species of the primary antibody was diluted with PBS according to the instructions and incubated at room temperature for 3 hours, then the mounting was completed using mounting medium with 4',6-diamidino-2-phenylindole (DAPI) to stain the nucleus. The target proteins were observed with green fluorescence (fluorescein isothiocyanate, FITC) or red fluorescence (tetramethylrhodamine, TRITC) and the nucleus with blue fluorescence (DAPI) (Fig 4).

The neurons and astrocytes could be observed in the same slice at the same time, then two areas of interest (AOI) under the 200-fold lens were selected: one was layer IV of S1 (orofacial sensory centre) and the other was layer V of M1 (orofacial motor centre). After that, two 425 μm × 425 μm square areas for measurement were randomly selected in the AOI. The morphology of neurons and astrocytes was observed, and the number was calculated using Image-Pro Plus software (version 6.0, Media Cybernetics, Rockville, MD, USA).

Tissue staining around the implant

In the implant group, a specimen block containing 3 to 5 mm thick bone around the implant was separated from the maxilla and immersed in 10% formalin at 4°C for 24 hours. It was then immersed in 20% ethylenediaminetetraacetic acid (EDTA) and decalcified at 37°C for 2 months until the implant could be removed easily from the specimen with surgical forceps. Continuous coronal sections with a thickness of 4 μm along the central axis of the implant were prepared after gradient dehydration and paraffin embedding. Masson staining was used to observe the bone remodelling around the implant (Fig 5). The BioQuant Osteo Bone Biology Research System (Biosan, Brussels, Belgium) was used to measure the outline of the screw surface on one side of the

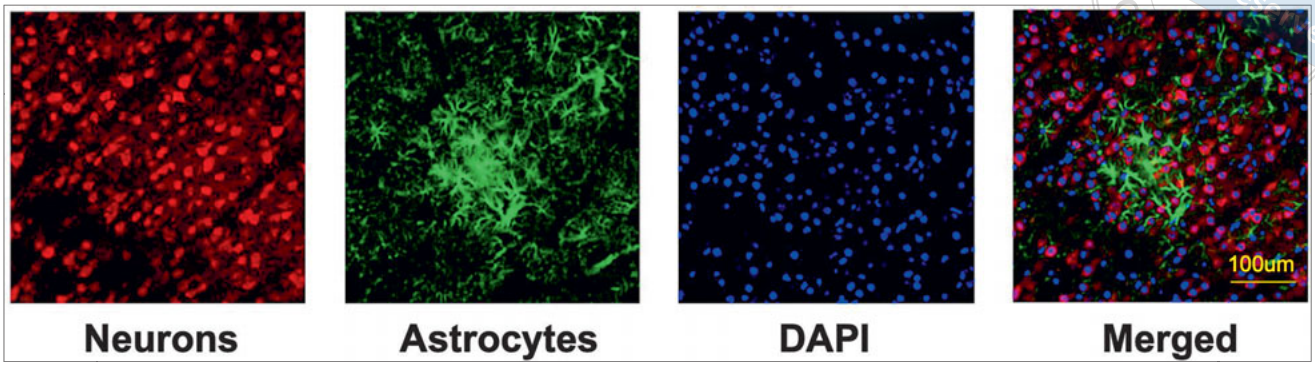

Fig 4 Images of neurons, astrocytes, DAPI and their merger observed using a laser confocal microscope. Neurons were stained as irregular circles, separated from each other (red fluorescence); the astrocytes were star-shaped, with many long and branched protrusions from the cell bodies; DAPI staining showed the nucleus. When neuron staining marked by NeuN and astrocyte staining marked by GFAP were merged, it showed the protrusions of astrocytes were stretched and filled among the cell bodies of neurons and their protrusions.

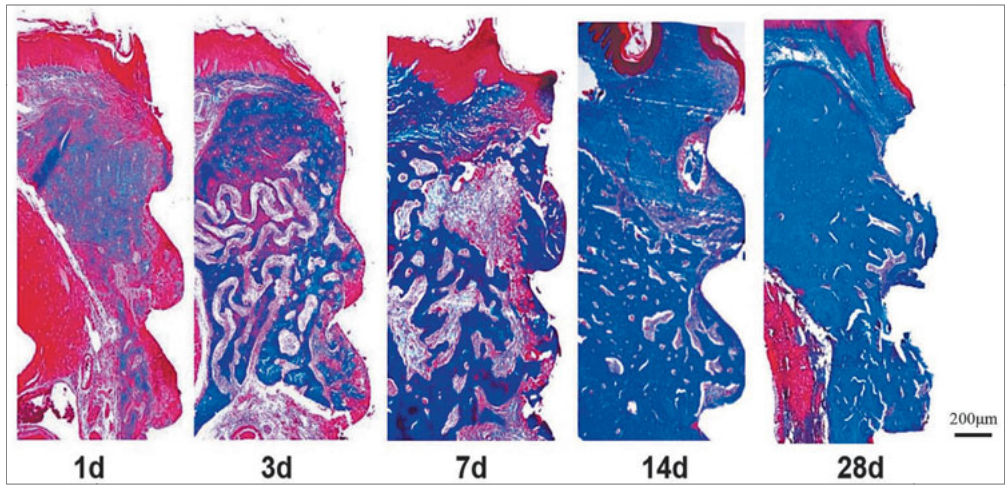

Fig 5 Implant osseointegration on days 1, 3, 7, 14 and 28 by Masson staining.

implant and the length of the contacted bone, then the ratio of the aforementioned two values was calculated and expressed as the percentage of the bone–implant outline contact (BIOC) rate in this experiment.

Statistical analyses

All data were expressed as mean ± standard deviation. The differences in the numbers of neurons and astrocytes were assessed among three groups at the same time point and among different time points within each group. The differences in BIOC were also assessed among different time points in the implant group. First, the homogeneity of variance was tested using a Bartlett test. If the variance was homogeneous, an analysis of variance (ANOVA) was performed using SPSS 27.0 (IBM, Armonk, NY, USA); otherwise, a Kruskal-Wallis (rank-sum) test was employed. The differences in the variables between two time points or two groups were tested using the Student-Neuman-Keuls method. The level of significance was set at $P < 0.05$.

Results

Under red fluorescence, the neurons were quasicircular, separated from each other and had a certain orientation, and protrusions could be seen in the cell bodies. Under green fluorescence, the astrocytes were stellate, emitting long and branched processes from the bodies. In the merged images, the processes of astrocytes extended and filled between the bodies and processes of neurons, separating the latter.

In layer IV of S1, there was no significant difference in the morphology or number of neurons among the implant group, extraction group and non-operated group at five different time points (days 1, 3, 7, 14 and 28). The manifestation of astrocytes was significantly different. Firstly, at the five time points, the morphology

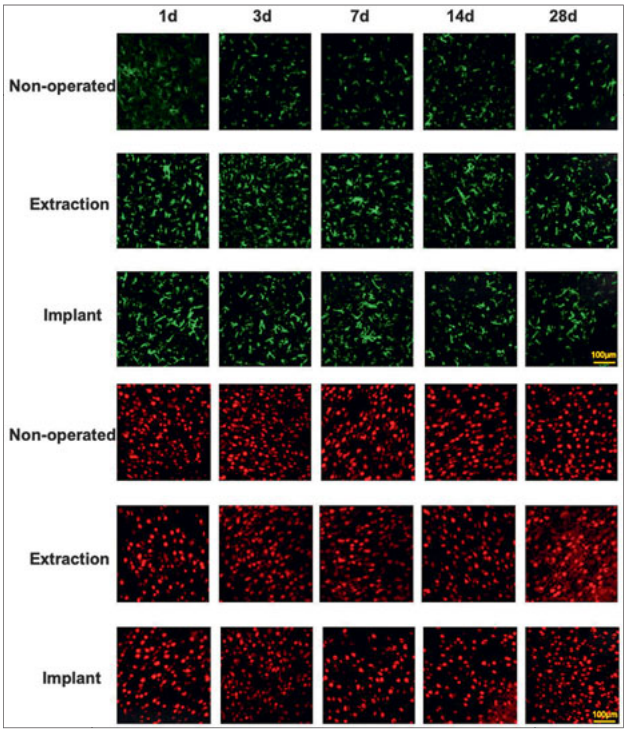

Fig 6 Staining of astrocytes (green fluorescence) and neurons (red fluorescence) in layer IV of S1 on days 1, 3, 7, 14 and 28.

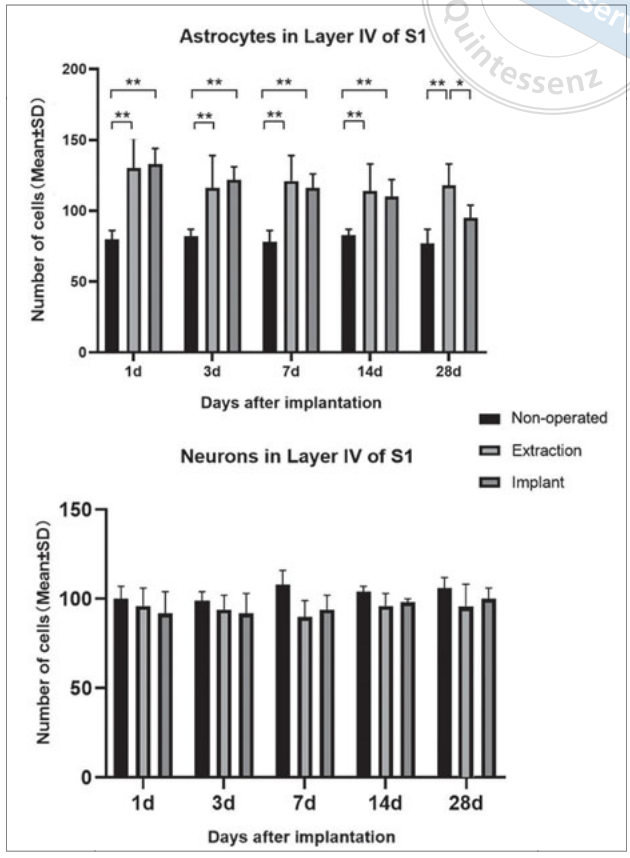

Fig 7 Comparison of the number of astrocytes and neurons in layer IV of S1 among groups. **(a)** On days 1, 3, 7 and 14, the number of astrocytes in both the extraction group and implant group was significantly higher than that in the non-operated group; however, on day 28, the number of astrocytes in the implant group was significantly lower than that in the extraction group. **(b)** There was no significant change in the number of neurons among the three groups. $^{*}P < 0.01$, $^{**}P < 0.05$.

of astrocytes in the extraction group was different from that in the non-operated group, with increased volume, antennae and swelling morphology, and the number was significantly higher too ($P < 0.01$). As for the implant group, the number of astrocytes was also significantly higher than that of the non-operated group on days 1, 3, 7 and 14 ($P < 0.01$), but significantly lower than that of the extraction group on day 28 ($P = 0.03$). No significant difference was found between the implant group and the non-operated group on day 28 ($P > 0.05$); the neurons and astrocytes showed a similar morphology and swelling was significantly reduced compared with the extraction group (Figs 6 and 7).

There was no significant difference in the morphology and number of neurons in layer V of M1 among the three groups at the five time points. The number of astrocytes in the extraction group was significantly higher than that in the non-operated group on days 14 and 28, whereas in the implant group it was significantly lower than that of the extraction group on days 7, 14 and 28. Unlike layer IV of S1, the number of astrocytes in the implant group was even slightly lower than that of the non-operated group on day 28 (Figs 8 and 9).

In layer IV of S1 and layer V of M1, the number of astrocytes in the implant group showed a downward trend with time. In layer IV of S1, the number of astrocytes on day 28 was significantly lower than that on days 1, 3 and 7 (Figs 6 and 7); in layer V of M1, the number of astrocytes on day 28 was significantly lower than that on days 1 and 3 (Figs 8 and 9). However, the BIOC rate showed an obvious upward trend with time, from 36.52% ± 11.17% on day 1 to 85.11% ± 4.02% on day 28. On day 1, the original bone trabeculae were found to have been destroyed due to implant surgery. On days 3 and 7, the early stages of bone remodelling, the inflammatory fibrous tissue began to transform into cartilage callus until the hard callus formed on day 14, and finally the bone remodelling matured further on day 28 (Fig 5). The number of astrocytes in S1 and M1 changed inversely with the BIOC rate (Fig 10).

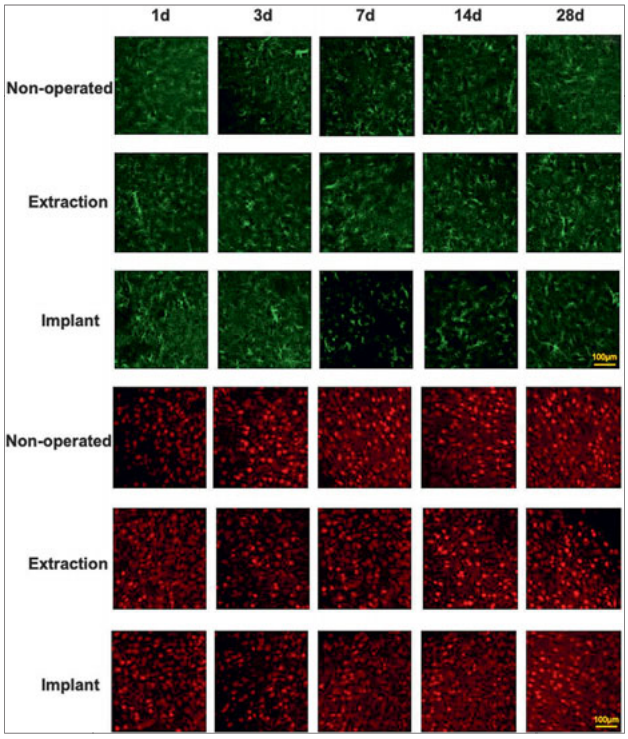

Fig 8 Staining of astrocytes (green fluorescence) and neurons (red fluorescence) in layer V of M1 on days 1, 3, 7, 14 and 28.

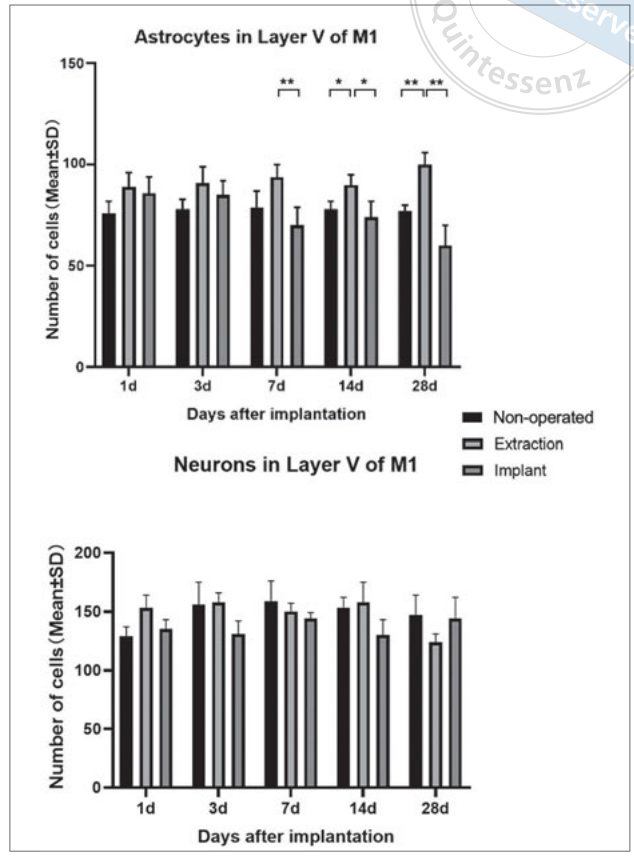

Fig 9 Comparison of the number of astrocytes and neurons in layer V of M1. **(a)** On days 7, 14 and 28, the number of astrocytes in the implant group was significantly lower than that in the extraction group, and on days 14 and 28, the number of astrocytes in the extraction group was significantly higher than in the non-operated group. **(b)** There was a lack of an obvious change in the number of neurons among the three groups. $^{*}P < 0.01$, $^{**}P < 0.05$.

Discussion

In this study, a randomised controlled animal model was established. The synergistic changes of neurons and astrocytes in the sensory motor cortex were observed to explore the cortical neuroplasticity in the process of implant osseointegration. The selected observation areas were S1 and M1, which were responsible for the regulation of oral and maxillofacial sensation and movement. The study drilled further down into specific layers: layer IV of S1, which was the main cortex receiving sensory input from the thalamic somatosensory nucleus and some spherical endothelial layers, and layer V of M1, which was the main output layer, relaying signals to affect the brainstem motor neurons[21]. By analysing the phenomenon of cortical neuroplasticity, this experiment hoped to explore the origin of osseoperception and lay a foundation to promote the tactile sensory ability of implants in future clinical practice. In addition, the basic data obtained in this experiment seeks to have guiding significance for follow-up experiments.

First, the results of this study suggested that tooth loss caused the neuroplastic changes in S1 and M1, which were manifested in the morphological and quantitative changes of astrocytes. In this study, compared with the non-operated group, astrocytes in the extraction group showed "activation"[22] on days 1, 3, 7, 14 and 28 in layer IV of S1 and on days 14 and 28 in layer V of M1. Studies have shown that when degenerative stimuli (such as chronic pain, dysfunction and cancer) were transmitted into the central nervous system, they caused the proliferation and activation of astrocytes in the corresponding sensory cortex, which was regarded as the defensive change of astrocytes[10-12,23,24]. The astrocytes in the hippocampus increased significantly following loss of molar teeth in SAMP8 mice[10]. In the present study, the functional degeneration caused by tooth loss was speculated to be the defensive change of astrocytes to the change of oral environment.

Second, the restoration of masticatory function by osseointegrated implants can partially reverse the plastic changes of S1 and M1 related to tooth loss. On day 28, there was no significant difference in the number

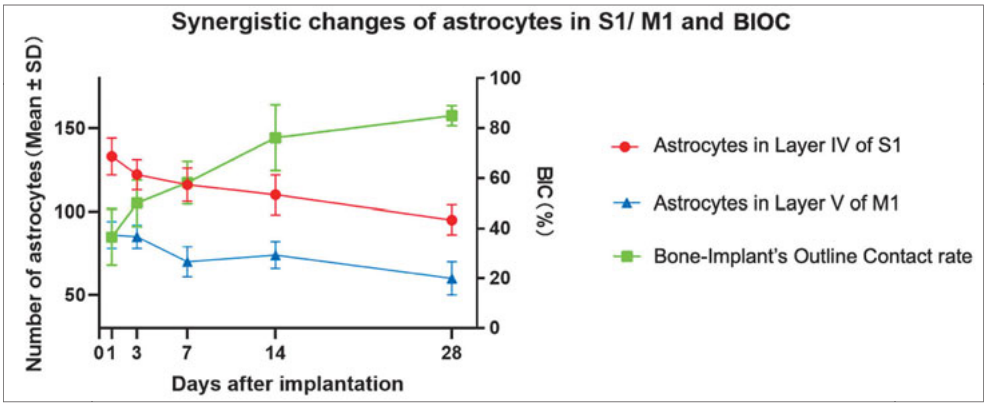

Fig 10 Synergistic changes of the number of astrocytes in S1/ M1 and BIOC rate. The number of astrocytes in layer V of M1 and layer IV of S1 showed a decreasing trend from day 1 to day 28 while the BIOC rate increased from 36.52% ± 11.17% to 85.11% ± 4.02%.

of astrocytes between the implant group and the non-operated group in layer IV of S1, and even in layer V of M1, the number of astrocytes in the implant group was less than that in the non-operated group.

Compared with the extraction group, the number of astrocytes in S1 and M1 in the implant group decreased, and the morphology of cell swelling was reversed. The results also showed that the osseointegration was completed on day 28 after implantation, and the implant in the first maxillary molar area restored the masticatory function to a certain extent.

In addition, there was a slight difference between S1 and M1. Although the number of astrocytes in S1 in the implant group was significantly less than that in the extraction group on day 28 ($P = 0.03$), the P value was not as significant as that of M1 ($P < 0.01$). The number of astrocytes in M1 was even slightly less than that of the non-operated group, which showed more obvious changes in the motor cortex after implantation. It is speculated that M1 has a closer relationship with the establishment of implant osseoperception, but the internal mechanism still needs to be explored further.

Finally, the results suggest that attention should be paid to the metabolic coupling between neurons and astrocytes in the cerebral cortex when exploring osseoperception, which might be related to the establishment and development of the tactile sensibility of dental implants. In this experiment, there was no significant change in the morphology and number of neurons of S1 and M1 among the three groups. It was speculated that more microscopic changes might have taken place in neurons, such as changes in synaptic structure or number, cell branches or cell size, and this needs to be confirmed by further research. Previous studies mentioned that the signal changes in the S1/M1 area of patients' brain after implant restoration could be observed by fMRI[13,14], which means neurons must play an indispensable role in the changes in haemodynamics in this area. This study has proved that neuroplasticity of neurons did not occur in the quantitative level, so it is particularly important to observe the microstructure of neurons further. Astrocytes play a key role in the maintenance of neuronal function. From the developmental regulation of synapse formation to the maintenance of synapses in disease, astrocytes are key participants in the homeostasis of the central nervous system, they can act as a doorkeeper for water, ions (such as potassium and calcium), glutamate and the second messenger through their channels and receptors on the surface. At the same time, they can provide energy for neurons, shuttle lactic acid and amino acids to neurons through and maintain the energy metabolism of neurons[25]. The close supporting relationship between astrocytes and neurons may also partly explain the significant changes of astrocytes and no significant change of neurons in the present study because astrocytes are more sensitive to environmental changes. It is therefore necessary to further clarify the molecular mechanism of energy metabolic coupling between neurons and astrocytes in the establishment of implant osseoperception.

Conclusion

In conclusion, after tooth loss, the astrocytes in the face sensorimotor cortex were activated as a reaction to changes in the oral environment. This kind of neuroplasticity can be reversed to some extent by oral rehabilitation with a dental implant. With regard to the differences in the response altered by implant placement between the sensory cortex and motor cortex, the motor cortex might be more intimately related to osseointegration and osseoperception of dental implants. Further experiments

are required to elucidate the inner mechanism of energy metabolic coupling between neurons and astrocytes in the establishment of implant osseoperception.

Conflicts of interest

The authors declare no conflicts of interest related to this study.

Author contribution

Drs Sheng Hao XUE and Jian LI were involved in the conception, design, writing and editing of the manuscript; Drs Jing Wen YANG and Zhong Ning LIU contributed to the data collection and analyses; Dr Ting JIANG was responsible for the conception, design, communication with editors and editing of the manuscript. All authors agreed with the final version.

(Received Sep 30, 2021; accepted Nov 11, 2021)

References

1. Sessle BJ, Yao D, Nishiura H, et al. Properties and plasticity of the primate somatosensory and motor cortex related to orofacial sensorimotor function. Clin Exp Pharmacol Physiol 2005;32:109–114.
2. Negahdari R, Ghavimi M, Ghanizadeh M, Bohlouli S. Active tactile sensibility of three-unit implant-supported FPDs versus natural dentition. J Clin Exp Dent 2019;11:e636–e641.
3. Huang Y, Jacobs R, Van Dessel J, Bornstein MM, Lambrichts I, Politis C. A systematic review on the innervation of peri-implant tissues with special emphasis on the influence of implant placement and loading protocols. Clin Oral Implants Res 2015;26:737–746.
4. Huang Y, Bornstein MM, Lambrichts I, Yu HY, Politis C, Jacobs R. Platelet-rich plasma for regeneration of neural feedback pathways around dental implants: A concise review and outlook on future possibilities. Int J Oral Sci 2017;9:1–9.
5. Enkling N, Nicolay C, Utz KH, Jöhren P, Wahl G, Mericske-Stern R. Tactile sensibility of single-tooth implants and natural teeth. Clin Oral Implants Res 2007;18:231–236.
6. Klineberg I, Calford MB, Dreher B, et al. A consensus statement on osseoperception. Clin Exp Pharmacol Physiol 2005;32:145–146.
7. Mishra SK, Chowdhary R, Chrcanovic BR, Brånemark PI. Osseoperception in dental implants: A systematic review. J Prosthodont 2016;25:185–195.
8. Onozuka M, Watanabe K, Mirbod SM, et al. Reduced mastication stimulates impairment of spatial memory and degeneration of hippocampal neurons in aged SAMP8 mice. Brain Res 1999;826:148–153.
9. Kubo KY, Murabayashi C, Kotachi M, et al. Tooth loss early in life suppresses neurogenesis and synaptophysin expression in the hippocampus and impairs learning in mice. Arch Oral Biol 2017;74:21–27.
10. Onozuka M, Watanabe K, Nagasaki S, et al. Impairment of spatial memory and changes in astroglial responsiveness following loss of molar teeth in aged SAMP8 mice. Behav Brain Res 2000;108:145–155.
11. Avivi-Arber L, Seltzer Z, Friedel M, et al. Widespread volumetric brain changes following tooth loss in female mice. Front Neuroanat 2017;10:121.
12. Zhou B, Zuo YX, Jiang RT. Astrocyte morphology: Diversity, plasticity, and role in neurological diseases. CNS Neurosci Ther 2019;25:665–673.
13. Habre-Hallage P, Dricot L, Jacobs R, van Steenberghe D, Reychler H, Grandin CB. Brain plasticity and cortical correlates of osseoperception revealed by punctate mechanical stimulation of osseointegrated oral implants during fMRI. Eur J Oral Implantol 2012;5:175–190.
14. Yan C, Ye L, Zhen J, Ke L, Gang L. Neuroplasticity of edentulous patients with implant-supported full dentures. Eur J Oral Sci 2008;116:387–393.
15. Avivi-Arber L, Lee JC, Sood M, et al. Long-term neuroplasticity of the face primary motor cortex and adjacent somatosensory cortex induced by tooth loss can be reversed following dental implant replacement in rats. J Comp Neurol 2015;523:2372–2389.
16. Holmes NP, Tamè L, Beeching P, et al. Locating primary somatosensory cortex in human brain stimulation studies: Experimental evidence. J Neurophysiol 2019;121:336–344.
17. Avivi-Arber L, Martin R, Lee JC, Sessle BJ. Face sensorimotor cortex and its neuroplasticity related to orofacial sensorimotor functions. Arch Oral Biol 2011;56:1440–1465.
18. Fujii N, Ohnishi H, Shirakura M, Nomura S, Ohshima H, Maeda T. Regeneration of nerve fibres in the peri-implant epithelium incident to implantation in the rat maxilla as demonstrated by immunocytochemistry for protein gene product 9.5 (PGP9.5) and calcitonin gene-related peptide (CGRP). Clin Oral Implants Res 2003;14:240–247.
19. Du Z, Lee RS, Hamlet S, Doan N, Ivanovski S, Xiao Y. Evaluation of the first maxillary molar post-extraction socket as a model for dental implant osseointegration research. Clin Oral Implants Res 2016;27:1469–1478.
20. Zhuge Qixun. Stereotactic Atlas of Rat Brain, ed 3. Beijing: People's Medical Publishing House, 2005.
21. Tzeng SF, Kahn M, Liva S, De Vellis J. Tumor necrosis factor-alpha regulation of the Id gene family in astrocytes and microglia during CNS inflammatory injury. Glia 1999;26:139–152.
22. Pekny M, Wilhelmsson U, Pekna M. The dual role of astrocyte activation and reactive gliosis. Neurosci Lett 2014;565:30–38.
23. Sofroniew MV. Astrocyte reactivity: Subtypes, states, and functions in CNS innate immunity. Trends Immunol 2020;41:758–770.
24. Pekny M, Pekna M. Reactive gliosis in the pathogenesis of CNS diseases. Biochim Biophys Acta 2016;1862:483–491.
25. Khakh BS, Sofroniew MV. Diversity of astrocyte functions and phenotypes in neural circuits. Nat Neurosci 2015;18:942–952.

Comments on "Features of Sensorimotor Cortex Altered after Teeth Loss and Subsequent Implants Placement in the Maxilla of Rats"

Xu Liang DENG[1,2]

The study by Xue et al investigated neurological changes within the S1 and M1 areas of the sensorimotor cortex during the process of dental implant osseointegration to shed light on the establishment and development of tactile sensibility of dental implants. They found that tooth extraction resulted in an increase in the number of astrocytes with no change to the number of neurons, and that osseointegration of dental implants reversed such histological changes within the S1 and M1 regions of the sensorimotor cortex. It was thus concluded that astrocytes within the sensorimotor cortex were activated in response to loss of masticatory function after tooth extraction, and that restoration of masticatory function through implant osseointegration could reverse such pathological neurological changes. This study thus paves the way for further research into how ossteointegration and osseoperception of dental implants are affected by the interaction between astrocytes and neurons, and corresponding changes to neuron microstructure within the sensorimotor cortex. Other interesting aspects of this study that can be further explored are how the observed neurological changes within the sensorimotor cortex are associated with detrimental changes that occur within the oral cavity when extracted teeth are not replaced by dental implants. These include alveolar bone loss and the extrusion, tilting and shifting of other teeth into the space left behind by the missing tooth. These could in turn lead to the development of new therapeutic strategies and prophylactic measures to prevent such detrimental changes from occurring within the oral cavity, particularly during the lengthy period between tooth extraction and final osseointegration of dental implants. An even more interesting but speculative topic for further research is the possible role that these observed neurological changes might play in the link between masticatory activity and glucose homeostasis, which may have implications for type II diabetes.

Chin J Dent Res 2022;25(3):178; doi: 10.3290/j.cjdr.b3317989

Xu Liang DENG, DDS, PhD
Professor of Prosthodontics, Researcher of dental materials and tissue engineering at Peking University School and Hospital of Stomatology
Associate Dean of Peking University School and Hospital of Stomatology since 2014

Prof Deng is chair of the NMPA Key Laboratory for Dental Materials, deputy director of the National Engineering Research Center of Oral Biomaterials and Digital Medical Devices and deputy director of the Beijing Laboratory of Biomedical Materials. In 2013, he was inducted as a Young Leading Scientist of Scientific and Technological Innovation of the Chinese Ministry of Science and Technology. In 2014, Deng was awarded funding from the NSFC Distinguished Young Scholars Programme. In 2015, he was inducted as distinguished professor of the Changjiang Scholars Programme. In 2016, he received the Shulan Medical Youth Award and Guanghua Engineering Science and Technology Prize. To date, Prof Deng has authored over 180 publications, and has successfully obtained 28 Chinese patents and a series of Class III medical device registrations.

1 Department of Geriatric Dentistry, Peking University School and Hospital of Stomatology, Beijing, 100081, PR China.
2 National Engineering Research Center of Oral Biomaterials and Digital Medical Devices, NMPA Key Laboratory for Dental Materials, Beijing Laboratory of Biomedical Materials, Peking University School and Hospital of Stomatology, Beijing, 100081, PR China.

Correspondence: Prof Xu Liang DENG, #22 Zhongguancun South Avenue, Haidian District, Beijing, 100081, P.R. China. Tel: 86-10-82195637; Fax: 86-10-82195581. Email: kqdengxuliang@bjmu.edu.cn

References

1. Hamamoto Y, Ouhara K, Miyagawa T, et al. Masticatory dysfunction in patients with diabetic neuropathy: A cross-sectional study. PLoS One 2022;17(6):e0269594.
2. Yerlikaya-Schatten G, Trimmal L, Rosicky I, et al. Effects of gum chewing on glycaemic control in women with gestational diabetes mellitus: A randomized controlled trial. Impact of chewing on hyperglycaemia in women with GDM. Eur J Obstet Gynecol Reprod Biol 2020;247:61–65.

Comparative Study of Temporomandibular Articular Fossa Bone Surface and the Envelope Surface of the Condyle Movement

Ke Nan CHEN[1#], Jing WANG[1#], Jun Peng CHEN[1], Jun Lin WANG[1], Yu Chun SUN[2], Xiang Liang XU[1], Chuan Bin GUO[1]

Objective: *To investigate the differences between temporomandibular articular fossa bone surface and the envelope surface of the mandibular condyle movement.*
Methods: *Thirty-four healthy adults underwent skull base and mandible scans using CBCT and performed mandibular border movement using the mandibular movement recording system. Landmarks of the fossa and tubercle were indicated and distance and angle parameters were measured on the 3D models reconstructed from the CBCT. The condyle movement envelope surfaces were formed according to models reconstructed from CBCT and the mandibular movement trajectory using computer simulation. The highest and lowest points of the envelope surface were indicated to create parameters. The data were analysed using a paired t test in SPSS (version 24.0, IBM, Armonk, NY, USA).*
Results: *The mandibular fossa bone surface was statistically different to the envelope surface for the height of the first peak of the envelope surface (3.280 ± 1.319 mm) and depth of the mandibular fossa (6.338 ± 2.389 mm) (the ratio was 51.75%), the height of the second peak of the envelope surface (1.463 ± 0.745 mm) and the height of the tubercle (2.000 ± 0.968 mm) (the ratio was 73.15%), and the downwards angle of the envelope surface (25.933 ± 7.539 degrees) and the posterior slope angle of the articular tubercle (35.059 ± 5.224 degrees) (the ratio was 73.97%).*
Conclusion: *The downwards angle of the envelope surface was statistically significantly smaller than the posterior slope angle of the articular tubercle, suggesting that the condyle movement is flatter than the mandibular fossa bone surface.*

Key words: *artificial fossa component, condyle movement, envelope surface, mandibular fossa bone surface, temporomandibular joint*
Chin J Dent Res 2022;25(3):179–187; doi: 10.3290/j.cjdr.b3317993

1 Department of Oral and Maxillofacial Surgery, Peking University School and Hospital of Stomatology, National Centre of Stomatology, National Clinical Research Centre for Oral Diseases, National Engineering Research Centre of Oral Biomaterials and Digital Medical Devices, Beijing Key Laboratory of Digital Stomatology, Research Centre of Engineering and Technology for Computerised Dentistry, Ministry of Health, NMPA Key Laboratory for Dental Materials, Beijing, P.R. China.
2 Centre of Digital Dentistry, Peking University School and Hospital of Stomatology, Beijing, P.R. China.
# These two authors contributed equally to this work.

Corresponding authors: Prof Chuan Bin GUO and Associate Prof Xiang Liang XU, Department of Oral and Maxillofacial Surgery, Peking University School and Hospital of Stomatology, #22 Zhongguancun South Avenue, Haidian District, Beijing, 100081, P.R. China. Tel: 86-10-82195398; Fax: 86-10-82195710. Email: guodazuo@sina.com; kqxxl@126.com

This work was supported by grants from the Beijing Municipal Science and Technology Commission (grant number Z201100005520055) and the National Key R&D Programme of China (grant number 2019YFB1706900).

The temporomandibular joint (TMJ) is one of the most complex joints in the human body and plays an important role in the functions of chewing, swallowing and speaking[1-4]. Although the TMJ is comprised of only two bones, McKay et al[5] consider it as a double joint because the articular disc covers the condyle and interposes below the fossa, dividing the joint cavity into superior and inferior compartments. The movement of the TMJ is usually divided into translation and rotation: the upper compartment, the discotemporal compartment, in which the condyle–disc complex translates on the posterior slope of the articular eminence, and the lower compartment, the discomandibular compartment, in which the mandibular condyle rotates on the lower aspect of the articular disc[6]. The superior portion of the disc is in contact with the posterior surface of the articular tubercle, with the function of preventing the disc from slipping during mouth opening. The inferior portion has the task of avoiding excessive rotational movements of the disk relative to the mandibular condyle[1].

The morphology of the TMJ[7,8] and research about movement of the condyle have been well documented in some studies[2,4,9,10]. As the condyle moves out of centric relation, it descends along the posterior slope of the articular eminence of the mandibular fossa[11]. From an anatomical perspective, the articular facet of the TMJ includes the mandibular fossa and anterior articular tubercle; however, from a functional perspective, the anterior boundary of the TMJ is the front end of the anterior slope of the articular tubercle, where the border movement of the condyle can reach. The TMJ facet is the posterior aspect of the articular eminence (articular slope), the anterior slope of the mandibular condyle and the anterior segment (anterior to the Glaser fissure) of the mandibular fossa. It has been proposed that sagittal guidance of the condyle is related to the height and slope of the posterior surface of the articular tubercle[11]. As cited in Singh et al[11], glossary of prosthodontic terms defines condylar guidance as "mandibular guidance generated by the condyle and articular disc traversing the contour of the glenoid fossae". Considering the articular discs and the bone cartilage between the condyle and fossa bone are flexible and prone to deformation when mastication or movement causes compression, there should be a difference between the path of condylar movement and the posterior slope of the articular tubercle.

Based on the anatomical structures of the TMJ and the relevant literature, it is hypothesised that the shape of the envelope surface is not significantly different from the mandibular fossa bone surface. Few articles have investigated the difference between condyle movement and mandibular fossa bone surface quantitatively. One important reason for this is that movement data for the TMJ cannot be obtained directly. Most of the previous studies on the movement of the mandibular condylar process obtained the movement trajectory of the condylar process through landmark points, but this method did not accurately reflect the 3D movement shape of the condylar process[12,13]. In a previous study by the present authors, the 3D envelope surface of the condylar process movement was investigated and the concept of the condyle movement functional surface was identified, including a 3D motion range of the condylar process[14]. The condylar movement envelope surface is a fusion of condylar digital models at different positions during mandibular movement that represents the 3D boundary range that the condylar process can reach. The condylar envelope surface can be measured quantitatively so that information on condylar movement can be obtained by measuring the envelope surface. In addition, by measuring it quantitatively, information on biological condyle movement can be obtained. The envelope surface of condylar movement recorded from normal adults could be applied when designing an artificial joint replacement system with the help of 3D printing technology, resulting in a more physiological design of the artificial TMJ.

The present study aims to preliminarily explore a quantitative method for measuring the envelope surface of condylar process movement and compare it with the mandibular fossa bone surface. This study provides a reliable data basis for the above hypothesis and more information on the movement of the condyle in the physiological state.

Materials and methods

Subjects

This study was approved by the Bioethics Committee of Peking University School and Hospital of Stomatology, Beijing, China (no. Pkussirb-201947091). Twenty-five women (aged 26.22 ± 1.922 years) and nine men (aged 25.48 ± 2.95 years) were selected according to the following inclusion criteria:

- no systemic disease;
- facial symmetry;
- no history of maxillofacial trauma or surgery;
- no history of orthodontic treatment;
- no TMJ discomfort, such as pain, clicking, limited mouth opening or any history of TMJ treatment;
- no abnormal habits, such as bruxism or clenching;

Table 1 Landmarks and parameters of the articular fossa bone surface.

Landmarks and parameters	Abbreviation	Definition
Orbitale	O	Lowest point on the lower edge of the cranial orbit
Porion	P	Highest point on the external auditory canal
Frankfurt horizontal plane	FH plane	Determined by left porion, right porion and the midpoint of orbitales
Fossa	F	Highest point of the articular fossa
Tubercle	T	Lowest point of the articular tubercle
Starting point of the articular tubercle	Ta	Anterior starting point of the articular tubercle
Posterior slope angle of the articular tubercle	Angle α	Angle between the line passing through point F and point T and the FH plane
Anterior slope angle of the articular tubercle	Angle β	Angle between the line passing through point T and point Ta and the FH plane
Fossa depth	Y_{F-T}	Distance between point F and point T in Y-axis direction
Tubercle height	Y_{T-Ta}	Distance between point T and point Ta in Y-axis direction

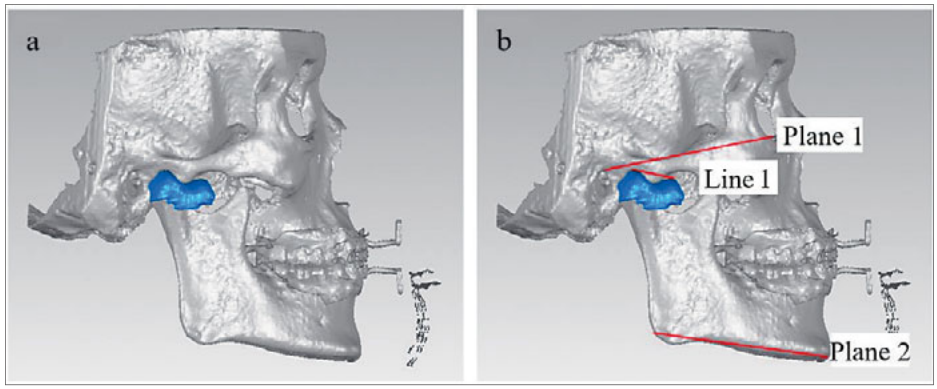

Fig 1 **(a)** Registration model and acquisition of the envelope surface (blue part). **(b)** The FH plane (plane 1), the mandibular body plane (plane 2) and the line connecting the two peaks of the envelope surface (line 1), the mandibular body angle and the MBP-ES angle (the angle between the envelope surface and the mandibular body plane) can be obtained; the angle between FH plane and line 1 can be calculated.

- full dentition and a Class I occlusal relationship.

Each volunteer underwent a clinical examination to assess TMJ function, occlusion and facial form. The examination was carried out by three trained professional doctors separately and assessed whether the TMJ experienced clicking, pain or an opening restriction, as well as no obvious deviation and abnormality of the mandibular movement during opening. Informed consent was obtained from all participants.

Imaging data collection

All volunteers underwent skull base and mandible CBCT scans (NewTom VG, NewTom, Imola, Italy; voxel size 0.3 mm, field of view 16 cm × 16 cm) at the intercuspal position (ICP) to obtain DICOM data. The CBCT was imported into ProPlan CMF 3.0 (Materialise, Leuven, Belgium) in DICOM format. Separation of the maxilla and mandible was achieved by selecting the appropriate bone tissue threshold in the software, and the reconstructed maxilla and mandible were exported in stereolithography (STL) format.

Parameters of the mandibular fossa bone surface

The CBCT of the ICP was imported into ProPlan CMF 3.0 in DICOM format to measure the parameters of the mandibular fossa bone surface. The landmarks of the articular facet were indicated and the direction was defined as perpendicular to the Frankfurt horizontal plane (FH plane) as the Y-axis. The distances from the indicated points and FH plane, the posterior slope of the articular tubercle (angle α) and the anterior slope of the articular tubercle (angle β) could be measured directly and fossa depth (distance between point F and point T in the Y-axis direction, Y_{F-T}) and tubercle height (distance between point T and point Ta in Y-axis direction, Y_{T-Ta}) can be calculated as shown in Table 1 and Fig 1.

3D splint printing

The 3D morphological data and relative position in intercuspal occlusion of the maxillary and mandibular dentition of volunteers were obtained using a TRIOS 3 intraoral scanner (3Shape, Copenhagen, Denmark) in the ICP. Two splints were created to attach the maxillary and mandibular eight anterior teeth in Geomagic Studio

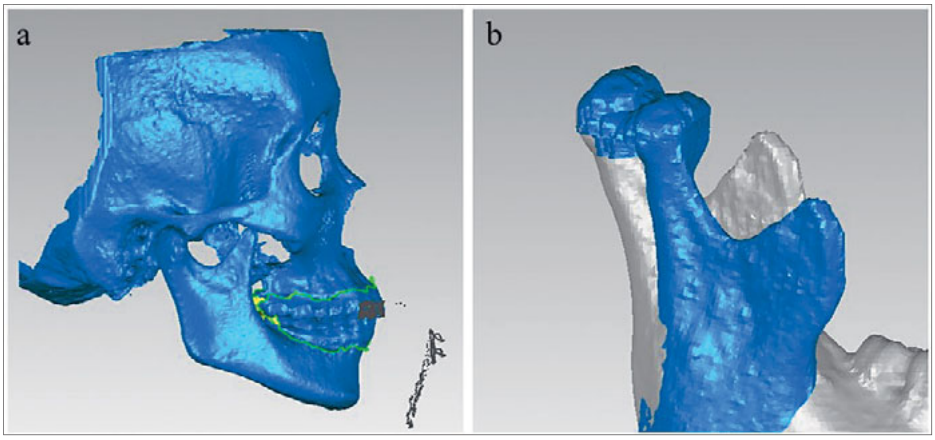

Fig 2 **(a)** Registration models. **(b)** The positions of the condyle at each moment were saved in the same 3D coordinated system merged to construct the envelope surface.

(3D Systems, Rock Hill, SC, USA) using the scanned dentition model. The splints were obtained using a 3D printer (SHINO I, SHINO, Beijing, China; nozzle diameter 0.3 mm, thickness 0.1 mm).

Mandibular movement trajectory collection

Volunteers performed border movements with a splint on their teeth with landmarks stuck to it. The movement trajectory of the target was measured at 120 HZ using the mandibular movement recording system PN300 (GeoVision, Taipei, Taiwan) and the result was represented by the coordinate points in the coordinate system. The core binocular vision device in the PN300 system was two digital cameras. Movement information data saved in a TXT file were opened in Geomagic Studio 2012, creating a point cloud of the maxillary dentition and mandibular trajectory. The curve present in the 3D coordinated system was obtained by connecting the coordinate points resulting from the movement trajectory of the mandibular movement. The coordinated point and 3D curve were imported into Geomagic Studio 2012 and transformed into STL format. The error in the 3D real-time, computerised, binocular, tracking system was 0.1 mm[15].

Obtaining the envelope surface

The models of the skull, mandible and mandibular movement trajectories were registered in Geomagic Studio, as shown in Fig 2a. The mandibular movement was simulated according to the collected trajectory and the positions of the condyle at each moment were saved in the same 3D coordinated system. They were imported into Geomagic Studio in PLY format and merged to construct the envelope surface, as shown in Fig 2b.

Processing of the models

The envelope surface and maxillary and mandibular models were imported into Geomagic Studio in STL format in the same coordinated system, as shown in Fig 1a. The FH plane and Y-axis were the same as the models in ProPlan CMF. The mandibular body angle was defined as the angle between the FH plane and the mandibular body plane, as shown in Fig 1b. The angle between the mandibular body plane and the line crossing two peaks of the envelope surface (MBP-ES angle) can be measured directly. The angle between the line crossing two peaks of the envelope surface and the FH plane can be calculated from the MBP-ES angle and mandibular body angle. The calculation method involved comparing the mandibular body plane with the line crossing two peaks; when the mandibular body plane is flatter, it equals mandibular body angle plus MBP-ES angle; when the mandibular plane is steeper, it equals mandibular body angle minus MBP-ES angle. The landmarks of the envelope surface were indicated and parameters were measured and calculated as shown in Table 2 and Fig 3.

Results

Shape of the envelope surface

All the envelope surfaces showed a 'two-peak' shape. The second peak was lower than the first, and the depression between the two peaks was roughly below the

Table 2 Landmarks and parameters of the envelope surface.

Landmarks and parameters	Abbreviation	Definition
Condylion at ICP	F1	Highest point of the first peak
Lowest point of the envelope surface	T1	Lowest point between two peaks
Condylion of end position	Ta1	Highest point of the second peak
Height of first peak	Y_{F1-T1}	Distance between point F1 and T1 in the y-axis direction
Height of second peak	Y_{T1-Ta1}	Distance between point T1 and Ta1 in the y-axis direction
Downwards angle of the envelope surface	Angle α_1	Angle between the line F1-T1 and FH plane
Upwards angle of the envelope surface	Angle β_1	Angle between the line T1-Ta1 and FH plane

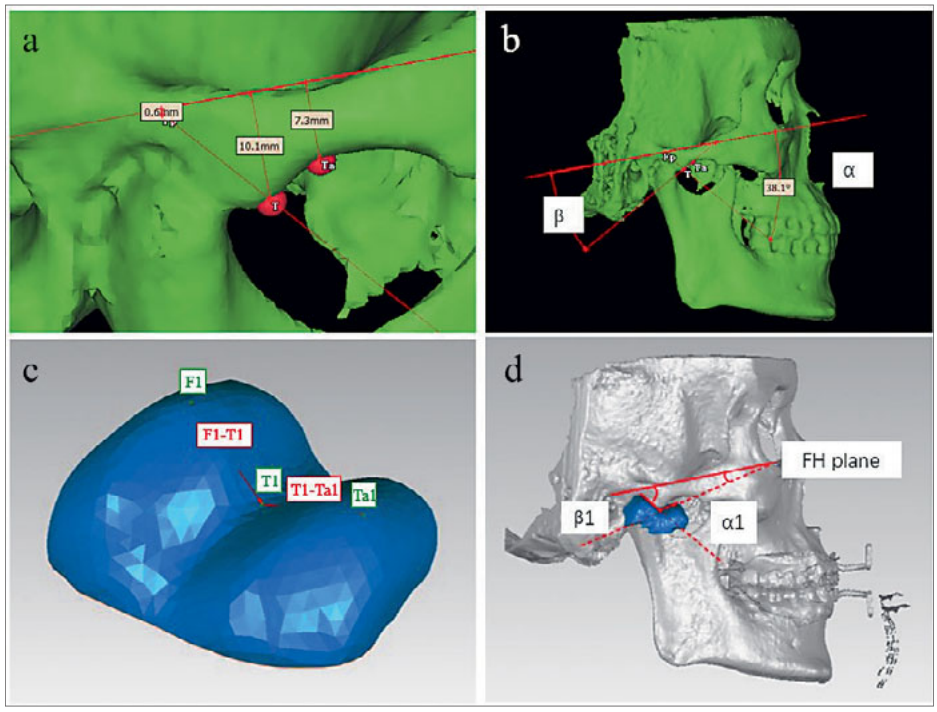

Fig 3 Landmarks of the articular fossa bone surface **(a)** and envelope surface **(c)**; angles of the articular fossa bone surface **(b)** and envelope surface **(d)**. F, highest point of the articular fossa; T, lowest point of the articular tubercle; Ta, the anterior starting point of the articular tubercle; angle α, posterior slope angle of the articular tubercle; angle β, anterior slope angle of the articular tubercle; F1, highest point of the first peak; T1, lowest point between two peaks; Ta1, highest point of the second peak; angle α_1, downwards angle of the envelope surface; angle β_1, upwards angle of the envelope surface.

articular tubercle in the registration model. The condyle moves forwards and downwards from the ICP forming the first peak and downwards surface, then crosses the lowest point of the articular tubercle and moves upwards slightly, forming the upwards surface and the second peak of the envelope surface[4].

Data analysis

The results of the measurement of the above parameters are shown in Table 3. A paired *t* test analysis was performed, the results of which are shown in Table 4 and Fig 4.

Parameters of the mandibular fossa bone surface of the TMJ and the envelope surface were measured and analysed. A paired *t* test was performed between parameters of the mandibular fossa bone surface and the envelope surface. The statistical results showed that angle α and angle α_1, Y_{F-T} and Y_{F1-T1}, Y_{T-Ta} and Y_{T1-Ta1} were statistically different with $P = 0.000$, $P = 0.000$ and $P = 0.007$, respectively, which indicated significant differences between the envelope surface and the articular facet in angle α and angle α_1, as well as the vertical distances. There was no statistical difference between angle β and angle β_1. Statistically different parameters were further subjected to the following ratio calculations: angle α_1 / angle α = 73.97%, Y_{F-T} / Y_{F1-T1} = 51.75%, Y_{T-Ta} / Y_{T1-Ta1} = 73.15%. The ratio illustrated that the condyle moved half of the fossa depth in vertical distance. Angle α_1 was 10 degrees smaller than angle α, which is nearly 30% smaller than the angle of the mandibular fossa bone surface.

Discussion

The articular facet of the TMJ includes the mandibular fossa and articular tubercle. Corbett et al[16] and Mack[17] found that the condyle followed the surface of the man-

Table 3 Data analysis of the articular fossa bone surface of the TMJ and the envelope surface.

Parameters	Min	Max	Mean ± SD
Angle α, degrees	23.40	45.30	35.059 ± 5.224
Angle β, degrees	1.00	28.30	14.277 ± 6.679
$Y_{F\text{-}T}$, mm	2.70	10.90	6.338 ± 2.389
$Y_{T\text{-}Ta}$, mm	0.10	3.80	2.000 ± 0.968
Angle α_l, degrees	11.12	41.84	25.933 ± 7.539
Angle β_l, degrees	1.98	29.56	15.192 ± 6.178
$Y_{Fl\text{-}Tl}$, mm	1.21	6.51	3.280 ± 1.319
$Y_{Tl\text{-}Tal}$, mm	0.23	3.89	1.463 ± 0.745

Table 4 Paired *t* test between the parameters of the articular facet and envelope surface.

Parameters	Mean ± SD	t	*P* value
Angle α_1, degrees	25.933 ± 7.539	5.582	0.000
Angle α, degrees	35.059 ± 5.224		
Angle β_1, degrees	15.192 ± 6.178	−0.722	0.475
Angle β, degrees	14.277 ± 6.679		
$Y_{F1\text{-}T1}$, mm	3.280 ± 1.319	6.395	0.000
$Y_{F\text{-}T}$, mm	6.338 ± 2.389		
$Y_{T1\text{-}Ta1}$, mm	1.463 ± 0.745	2.869	0.007
$Y_{T\text{-}Ta}$, mm	2.000 ± 0.968		

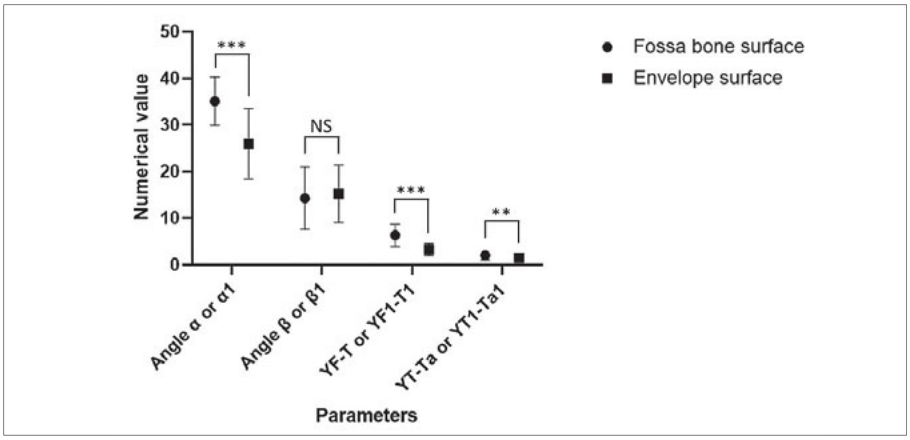

Fig 4 Parameters of the articular facet and envelope surface. $^{**}P < 0.01$, $^{***}P < 0.001$. NS, not significant

dibular fossa closely during mandibular movement. It has been proposed that sagittal condylar guidance coincides more or less with the posterior slope of the articular tubercle[11]; however, the physiological movement of the TMJ is also affected by the shape and deformation of the articular disc, restrictions of capsule and ligament, traction of muscles and other factors[17]. A more accurate assessment is as follows: the condylar path is determined by the bony fossa, the muscles responsible for mandibular movements and their nerve controls, the occlusal relationship, the shape and movements of the disc and the limitations of ligaments[11]. Theoretically, the condyle movement is related to the mandibular fossa bone surface but not completely consistent. The differences between the fossa and the condyle movement path are rarely studied. In the present study, these parameters were measured and compared statistically.

The morphology of the TMJ has been measured with different landmarks and parameters[7,8]. Common parameters of the mandibular fossa bone surface include the diameter and angle of the fossa and the height of the articular tubercle. In the present study, several sagittal landmarks and related parameters closely related to the movement of the condyle were selected. All the envelope surfaces exhibited a 'two-peak' shape. The second peak was lower than the first, and the depression between the two was roughly below the articular tubercle in the registration model. The highest point of the mandibular fossa (F) corresponds to the condylion in the centric relation position (F1), which is also the first peak's highest point of the envelope surface. The downwards angle of the envelope surface (angle α_1) is formed by the forwards and downwards movement of the condyle in the guidance of the posterior slope of the articular tubercle (angle α) anatomically. The condyle then moves across the lowest point of the articular tubercle (T) and upwards a little until it reaches the maximum opening point, resulting in the formation of the second peak. Thus, the lowest point of the envelope surface (T1) corresponds to point T. Fossa depth, articular tubercle height, the posterior slope of the articular tubercle and the anterior slope of the articular tubercle were measured through points F, T and Ta. The results for fossa depth are consistent with previous studies[7,8]. The definition of tubercle height in the present study is different from that given in the previous literature because the FH plane was set as the reference plane for the measurement of the envelope surface and articular

facet to make the parameters comparable. The angle α measured in this study was relatively consistent with the results of the previous literature[18].

The method of using landmark points to study the condylar process or mandibular movement has become more accurate as instruments have developed; however, the difference in the selection of landmark points causes differences in the results of the movement trajectory[12,13], and this method cannot reflect the influence of the 3D shape of the condylar process on movement trajectory. Koolstra et al[19] first introduced the concept of the envelope surface of the incisors and studied the incisor movement with the aim of evaluating the influence of the temporomandibular ligaments and the passive tension muscles on the envelope surface. Later, Huang et al[14] took the 3D shape of the condyle into consideration and analysed the 3D shape of the movement of the functional surface of the mandibular condyle. They found that the condylar movement envelope surface was the reachable range of the condylar process during mandibular border movement[14]. Thirty-four healthy adults were included in the present study and the obtained envelope surfaces presented a 'two-peak' shape, which is consistent with Huang et al[14] and may be influenced by the morphology of the articular tubercle. The first peak of the envelope surface is formed when the condyle is in the centric position as the condyle moves forwards and downwards, crosses the lowest point of the articular tubercle and then moves upwards slightly[4], forming the second peak of the envelope surface.

Results of measurements for parameters of the mandibular fossa bone surface of the TMJ and the envelope surface in this study quantitatively verified our hypothesis that the shape of the envelope surface is not significantly different from the mandibular fossa bone surface. Paired *t* test results and mean values showed that the parameters of the envelope surface are significantly smaller than the mandibular fossa bone surface, with a ratio between 50% and 75%. The data showed significant differences between the envelope surface and the articular facet with the vertical distance of the condyle moving only 51% of the fossa depth. The downwards angle of the envelope surface was 10 degrees smaller than the posterior slope angle of the articular tubercle, which is nearly 30% smaller than the mandibular fossa.

These results indicate that the tissue between the condyle and the mandibular fossa has a very important influence on the movement of the condyle. During the forwards and downwards movement of the condyle, the posterior slope of the articular tubercle still played a guiding role; however, the articular disc and other flexible tissues influenced the shape of the upper functional surface of the condyle movement, resulting in smaller downwards angles of the envelope surface than the bony slope angles of the mandibular fossa. This difference reflected the cushioning function of the structures between the mandibular fossa bone surface and the condyle process. The mismatches between the mandibular fossa and the mandibular condyle are mitigated by the articular disc, which also has the role of ensuring the congruence of the articular surfaces. The result between angle β and angle β_l was not significantly different ($P = 0.475 > 0.05$). From a physiological and anatomical perspective, this part of the bone structure had little effect on the movement of the condyle because the condyle could not reach the anterior starting point of the tubercle in the physiological status.

At present, the design of an artificial TMJ replacement system, consisting of two rigid prosthetic components, rarely includes reconstruction of the articular disc and other tissues[20]. The present results indicated that the articular disc played a highly important role in the process of condyle movement, which affected the design of the artificial TMJ. The mandibular fossa bone surface cannot replicate the envelope surface of condyle movement in the physiological status[21]. Given that the TMJR system could not replicate the reconstruction and simulation of soft tissues, such as the joint disc, at this stage, it is important to consider how the TMJR system mimics the movement of a healthy TMJ. The results of clinical trials of the TMJ system by Yang's team[22] which was designed based on the bony shape of healthy Chinese adults also suggested that artificial joints that conform to anatomical shapes still cannot still simulate the movement of a healthy TMJ[23]. Although a finite element analysis study of a custom-made temporal component that fitted the mandibular fossa bone surface showed that the geometry of the fossa promoted better load transfer of the condyle distally, this study mentioned that the design according to the fossa surface did not correspond to joint physiological movements[24].

Based on the current design of the TMJR system and the present results, it is suggested that the mandibular fossa should act as a guide for the movement of the artificial joint head. Previous studies pointed out that the 3D morphology of condylar movement could be used for the design of an artificial TMJ fossa[14,25]. Xu et al[25] designed a TMJ prosthesis that obtained the condylar movement surface of a canine as the articular surface of the fossa component, with a good result for strain distribution in the finite element analysis. The artificial TMJR system, based on the design of the condyle movement envelope surface, is more suitable for the

rigid artificial prosthesis design without flexible tissue repair, such as the joint disc, at present. The purpose of the envelope surface is to provide a theoretical basis for the functional surface of the artificial joint fossa. It is hoped that the movement of the artificial joint head can be guided and supported by the reconstructed condyle movement envelope surface after the removal of the articular disc to achieve physiological mandibular movement.

Conclusion

The downwards angle of the envelope surface was statistically significantly smaller than the posterior slope angle of the articular tubercle, suggesting that the condyle movement is gentler than the mandibular fossa bone surface of the TMJ. The envelope surface of condylar movement could be helpful for the geometrical design of the fossa component in an artificial TMJR system, which may play a role in guiding the movement of the condyle component in a manner similar to that of a healthy joint.

Conflicts of interest

The authors declare no conflicts of interest related to this study.

Author contribution

Drs Ke Nan CHEN and Jing WANG conceived and designed the study, contributed to the data acquisition, analysis and interpretation and drafted the manuscript, and contributed equally to this article; Drs Jun Peng CHEN, Jun Lin WANG and Jun Qi JIANG contributed to the data collection; Dr Yu Chun SUN provided devices for the experiment; Dr Xiang Liang XU and Prof Chuan Bin GUO critically revised the manuscript for important intellectual content and gave final approval, and contributed equally to this article.

(Received Apr 24, 2022; accepted Jun 20, 2022)

References

1. Bordoni B, Varacallo M. Anatomy, Head and Neck, Temporomandibular Joint. StatPearls. Treasure Island (FL): StatPearls Publishing; 2022.
2. Krohn S, Joseph AA, Voit D, et al. Multi-slice real-time MRI of temporomandibular joint dynamics. Dentomaxillofac Radiology. 2019;48:20180162.
3. Tubbs RS, Shoja MM, Loukas M. Temporomandibular Joint. Bergman's Comprehensive Encyclopedia of Human Anatomic Variation. Hoboken: John Wiley and Sons, 2016.
4. Chen CC, Lin CC, Hsieh HP, Fu YC, Chen YJ, Lu TW. In vivo three-dimensional mandibular kinematics and functional point trajectories during temporomandibular activities using 3d fluoroscopy. Dentomaxillofac Radiol 2021;50:20190464.
5. McKay GS, Yemm R, Cadden SW. The structure and function of the temporomandibular joint. Br Dent J 1992;173:127–132.
6. Chang CL, Wang DH, Yang MC, Hsu WE, Hsu ML. Functional disorders of the temporomandibular joints: Internal derangement of the temporomandibular joint. Kaohsiung J Med Sci 2018;34:223–230.
7. Zhang LZ, Meng SS, He DM, et al. Three-dimensional measurement and cluster analysis for determining the size ranges of Chinese temporomandibular joint replacement prosthesis. Medicine (Baltimore) 2016;95:e2897.
8. Zhong Z, Sun J, Yu Z, Han Y, Kang C. Morphological study of safe fixation region of temporomandibular joint prosthesis in Chinese northeast population with 3-dimensional computed tomographic image. Medicine (Baltimore) 2020;99:e22779.
9. Krohn S, Frahm J, Mahler A, et al. Biomechanical analysis of temporomandibular joint dynamics based on real-time magnetic resonance imaging. Int J Comput Dent 2020;23:235–244.
10. Gallo LM. Modeling of temporomandibular joint function using MRI and jaw-tracking technologies--Mechanics. Cells Tissues Organs 2005;180:54–68.
11. Singh S, Das S, Bhattacharyya J, Ghosh S, Goel P, Dutta K. A comparative study to correlate between clinically and radiographically determined sagittal condylar guidance in participants with different skeletal relationships. J Indian Prosthodont Soc 2017;17:175–182.
12. Ueda K. Three-dimensional analysis for prediction and assessment of mandibular movement in orthognathic surgery in the ramus. J Maxillofac Surg 1983;11:216–226.
13. Zwijnenburg A, Megens CC, Naeije M. Influence of choice of reference point on the condylar movement paths during mandibular movements. J Oral Rehabil 1996;23:832–837.
14. Huang C, Xu XL, Li LL, Sun YC, Guo CB. A study on reconstruction of the four-dimensional movement model and envelope surface of condyle in normal adults [epub ahead of print 2 September 2021]. Br J Oral Maxillofac Surg doi: 10.1016/j.bjoms.2021.08.006.
15. Zhao T, Yang H, Sui H, Salvi SS, Wang Y, Sun Y. Accuracy of a real-time, computerized, binocular, three-dimensional trajectory-tracking device for recording functional mandibular movements. PLoS One 2016;11:e0163934.
16. Corbett NE, DeVincenzo JP, Huffer RA, Shryock EF. The relation of the condylar path to the articular eminence in mandibular protrusion. Angle Orthod 1971;41:286–292.
17. Mack PJ. A computer analysis of condylar movement as determined by cuspal guidances. J Prosthet Dent 1989;61:628–633.
18. Lee WJ, Park KH, Kang YG, Kim SJ. Automated real-time evaluation of condylar movement in relation to three-dimensional craniofacial and temporomandibular morphometry in patients with facial asymmetry. Sensors (Basel) 2021;21:2591.
19. Koolstra JH, Naeije M, van Eijden TM. The three-dimensional active envelope of jaw border movement and its determinants. J Dent Res 2001;80:1908–1912.
20. Elledge R, Mercuri LG, Attard A, Green J, Speculand B. Review of emerging temporomandibular joint total joint replacement systems. Br J Oral Maxillofac Surg 2019;57:722–728.
21. Gakhal MK, Gupta B, Sidebottom AJ. Analysis of outcomes after revision replacement of failed total temporomandibular joint prostheses. Br J Oral Maxillofac Surg 2020;58:220–224.

22. Zheng J, Chen X, Jiang W, Zhang S, Chen M, Yang C. An innovative total temporomandibular joint prosthesis with customized design and 3D printing additive fabrication: a prospective clinical study. J Transl Med 2019;17:4.
23. Zou L, Zhao J, He D. Preliminary clinical study of Chinese standard alloplastic temporomandibular joint prosthesis. J Craniomaxillofac Surg 2019;47:602–606.
24. Ramos A, Mesnard M. Comparison of load transfers in TMJ replacement using a standard and a custom-made temporal component. J Craniomaxillofac Surg 2014;42:1766–1772.
25. Xu X, Luo D, Guo C, Rong Q. A custom-made temporomandibular joint prosthesis for fabrication by selective laser melting: Finite element analysis. Med Eng Phys 2017;46:1–11.

爱 国　创 新　求 实　奉 献　协 同　育 人

黄大年

1958年8月—2017年1月

叩开“地球门”

巡天探地潜海
向深地深空深海进军

Prevalence of Dental Anomalies Assessed Using Panoramic Radiographs in a Sample of the Turkish Population

Mediha BÜYÜKGÖZE-DİNDAR[1], Meltem TEKBAŞ-ATAY[2]

Objective: *To determine the prevalence, frequency and distribution of dental anomalies that were detectable on panoramic radiographs in a large sample Turkish population, and the associations among the anomalies.*
Methods: *This study was conducted retrospectively on panoramic radiographs of 43,880 patients who were admitted to the Faculty of Dentistry at Trakya University, Edirne, Turkey. Patients' files were examined by two observers and radiographic images of 2265 patients with at least one dental anomaly were included. Dental anomalies were classified as anomalies in the number, structure, position and shape of teeth. The interactions between the groups were analysed using chi-square tests.*
Results: *The study group consisted of 1336 women (59%) and 929 men (41%) with a mean age of 33.3 ± 14.4 years. A total of 2265 patients, with a prevalence of 5.2% (2265/43880), had at least one dental anomaly. The most frequent anomalies were in position (2.7%) and number (2.1%). Structure anomalies were least common, affecting 0.02% of patients. Among the study group of patients with dental anomalies, 12.2% presented more than one kind of anomaly.*
Conclusion: *Position anomalies were the most common dental anomaly, whereas structural anomalies were least common in a Turkish sample. The prevalence of anomalies varies between populations, confirming the role of racial factors.*

Key words: *fused teeth, impacted tooth, panoramic radiography, supernumerary tooth, tooth abnormalities.*
Chin J Dent Res 2022;25(3):189–196; doi: 10.3290/j.cjdr.b3317997

Dental anomalies are defined as deviations from the expected number, shape, position and structure of teeth, and can be congenital, developmental or acquired. Congenital types are inherited and have a genetic basis, developmental types occur at the tooth formation stage, and acquired anomalies occur after tooth development[1]. Anomalies in number, morphology and size are included in developmental anomalies while eruption anomalies that may occur due to early loss of deciduous tooth can be considered as acquired anomalies[2].

Dental anomalies may occur due to various factors, which are generally expressed as genetic, epigenetic and environmental[3]. Complex interactions between these factors during dental development can lead to abnormal changes, which in turn cause dental anomalies. It has been stated that genetic factors such as multifactorial inheritance and environmental factors such as trauma, radiation, infection and hormonal factors may play a significant role in the formation of dental anomalies[4].

Dental anomalies can be seen in simple isolated defects or symptoms of specific syndromes and can result in various problems. While developmental anomalies of enamel can cause problems such as tooth sensitivity and susceptibility to caries, situations such as impacted, supernumerary and missing teeth may lead

1 Health Science Vocational College, Trakya University, Edirne, Türkiye
2 Department of Restorative Dentistry, Faculty of Dentistry, Trakya University, Edirne, Türkiye.

Corresponding author: Dr Mediha BÜYÜKGÖZE DİNDAR, Health and Science Vocational College, Trakya University, Edirne 22030, Türkiye. Tel: 0284-235-78-85; Fax: 0284-235-77-87. Email: medihabuyukgoze@hotmail.com

to orthodontic problems by affecting occlusion[5]. These problems, especially those related to the anterior region, may cause aesthetic issues and also lead to psychological problems[6].

Detailed investigation of dental anomalies is essential to prevent further complications such as malocclusion, aesthetic deformities, periodontal problems, caries lesions and difficulties during extraction and root canal treatment[7]. Thus, radiographic observations play an important role in the differential diagnoses of anomalies as well as clinical examinations. Panoramic radiographs are frequently used in oral examination for diagnostic purposes and can also be used to diagnose dental anomalies[8]. Radiographic evaluation is the most effective method to detect many different anomalies that cannot be noticed only through clinical examination.

Many studies have examined the prevalence of dental anomalies, but the results show inconsistencies for different populations[9-12]. Incidence and degree of expression of dental anomalies in different population groups can provide important information for phylogenic and genetic studies and may assist understanding of variations within and between the different populations[13]. Thus, population-specific prevalence studies are required to provide physicians with information about anomalies that can affect oral health and thereby quality of life. Studies with a large sample size make it possible to detect the rarest types as well as variable types in a specific population in terms of genetic predisposition. Early diagnosis can therefore guide effective management of personal preventive dentistry and dental treatment programmes.

The present study aims to determine the frequency and distribution of dental anomalies that are detectable on panoramic radiographs in a large sample of the Turkish population, and the associations among them.

Materials and methods

The ethical permissions necessary for this study were obtained from the Scientific Research Ethics Committee of Trakya University, Edirne, Turkey (TÜTF-BAEK 2020/243). This cross-sectional study was planned retrospectively on routine panoramic radiographs of 43,880 patients who were admitted to the Faculty of Dentistry at the university between 2015 and 2020. The files of 43,880 patients were examined by two observers, and panoramic radiographs of 2265 patients aged between 12 and 60 years and with at least one dental anomaly who met the inclusion criteria were included. The radiographs examined in this study were taken with the same panoramic radiograph device (PaX-Flex3D, Vatech, Hwaseong, South Korea) at the Department of Radiology at Trakya University. None of the radiographs were exposed specifically for this study.

After examining the anamnesis in the patient files, individuals with systemic diseases, syndromes, tooth extraction due to caries lesions, trauma or orthodontic reasons, large restorations that prevent the observation of crown morphology and insufficient radiograph quality for optimal evaluation that could negatively affect the study were excluded. In addition, third molars, due to their wide morphology and position variations, were also excluded.

The radiographic images were evaluated independently by two different observers on the computer monitor with subdued ambient lighting and anomalies were classified as number (including hypodontia, oligodontia and hyperdontia), structure (including amelogenesis imperfecta, dentinogenesis imperfecta, dentine dysplasia and regional odontodysplasia), position (including transposition, ectopia, impaction and inversion) and shape (including microdontia, macrodontia, fusion, talon cusp, dens invaginatus and taurodontism).

To estimate the reproducibility of the diagnosis, 100 randomly selected radiographs were examined separately by two observers once again and the interobserver agreement was determined. Parameters such as patients' age, sex, type and region of dental anomalies were recorded.

Statistical analysis was performed using SPSS Statistics for Windows, version 23.0 (IBM, Armonk, NY, USA). Descriptive statistics such as frequency distributions and percentages were calculated for the categorical data. Chi-square and Fisher exact tests were used to determine potential differences in the distribution of dental anomalies stratified by sex and age variables and to determine the interaction between different dental anomalies. The correlation coefficient was also used to evaluate the relationship between the number of detected dental anomalies and age. A Cohen kappa statistic was used between the two observers to test the reproducibility of the diagnosis. The level of significance was set at $P < 0.05$ was considered significant.

Results

The distributions of different types and subtypes of dental anomalies are shown in Table 1. The Cohen kappa analysis demonstrated substantial interexaminer agreement (Kappa 0.892). Of the 43,880 panoramic radiographs, 2265 patients had at least one dental anomaly, with a prevalence rate of 5.2%. The study group of patients with dental anomalies consisted of 1336 women (59%) and 929 men (41%) with a mean age of 33.3 ± 14.4 ears.

Table 1 Distribution of different dental anomalies and subtypes.

Type and subtypes of anomalies			Frequency, n (%)	Prevalence, %
Number	Hypodontia	Total	655 (29.0)	1.5
		Missing central incisor	18 (0.9)	0.04
		Missing lateral incisor	307 (13.5)	0.7
		Missing canine	91 (4)	0.2
		Missing premolar	239 (10.6)	0.5
		Missing molar	0 (0.0)	0.0
	Oligodontia		18 (0.9)	0.04
	Hyperdontia	Total	254 (11.0)	0.6
		Supernumerary central incisior	8 (0.4)	0.02
		Supernumerary lateral incisor	14 (0.6)	0.03
		Supernumerary canine	10 (0.4)	0.02
		Supernumerary premolar	82 (3.6)	0.2
		Supernumerary molar	0 (0.0)	0.0
		Mesiodens	54 (2.4)	0.1
		Paramolar	86 (3.8)	0.2
	Total		927 (41.1)	2.1
Position	Transposition		13 (0.6)	0.03
	Ectopia		62 (2.7)	0.1
	Impaction	Total	1077 (47.6)	2.5
		Impacted central incisor	15 (0.7)	0.03
		Impacted lateral incisor	8 (0.4)	0.02
		Impacted canine	853 (37.7)	1.9
		Impacted premolar	130 (5.7)	0.3
		Impacted molar	71 (3.1)	0.2
	Inversion		20 (0.9)	0.05
	Total		1172 (51.8)	2.7
Shape	Microdontia		404 (17.8)	0.9
	Macrodontia		2 (0.1)	0.004
	Fusion-gemination		2 (0.09)	0.004
	Talon cusp		14 (0.6)	0.03
	Dens invaginatus		8 (0.4)	0.02
	Taurodontism		48 (2.1)	0.1
	Total		478 (21.1)	1.1
Structure	Amelogenesis imperfecta		8 (0.4)	0.02
Total			2265 (100.0)	5.2

The most frequent anomalies were impacted teeth (2.5%), hypodontia (1.5%) and microdontia (0.9%). Structural anomalies, affecting 0.02% of patients, were the least common anomaly observed, followed by shape anomalies (1.1%). Among the study group patients, 12.2% presented more than one dental anomaly. A negative correlation was observed between age and the number of anomalies (r = −0,061, $P = 0.004$). As patients got older, the number of anomalies encountered decreased. The occurrence of dental anomalies was statistically significantly higher in women ($P = 0.00$).

The occurrence of missing central incisors was statistically significantly higher in the mandible than the maxilla ($P = 0.01$) and occurred bilaterally ($P = 0.00$). The most common anomaly relating to number was missing lateral incisors (0.7%) and presented statistically significantly frequently in the maxilla ($P = 0.00$). In contrast to missing premolars, missing canines were found to occur statistically significantly more frequently in the maxilla (P = 0.00). No cases of agenesis of the maxillary or mandibular first molars were observed. Supernumerary central and lateral incisors were all located in the maxilla. Although the frequency of supernumerary canines in the maxilla and mandible were similar, supernumerary premolars were significantly more common in the mandible ($P = 0.00$). While mesiodens was statistically significantly higher in women ($P = 0.005$), there was no correlation between paramolar presence and sex.

Fig 1 Radiograph of a case displaying kissing molars.

Fig 3 Radiograph of a case involving complete transposition of the upper left permanent canine and premolar.

Fig 2 Representative radiograph of a supernumerary mandibular microdontic canine with inversion.

Fig 4 Panoramic radiograph of a case displaying amelogenesis imperfecta. Note the generalised crown abnormalities, such as flat occlusal surfaces and the presence of hypoplastic enamel with more radiodensity in contrast to dentine.

Impacted canines were the most common positional anomaly (1.9%) and the maxilla was more often affected than the mandible ($P = 0.00$). The incidence of impaction was rather unilateral ($P = 0.00$); both the right and left sides were affected similarly. On the other hand, impacted premolars were often present in the mandible ($P = 0.00$).

Only five patients (0.005%) presented kissing molar teeth (Fig 1). No statistically significant correlation was detected between inversion (Fig 2), transposition (Fig 3) and sex ($P = 0.147$ and $P = 0.111$, respectively). A positive correlation was detected between inversion and ectopia ($P = 0.016$).

The most common shape anomaly was microdontia (0.9%) and 86.4% of microdontia cases involved the maxillary lateral incisors and were significantly higher in women ($P = 0.00$). Only two patients exhibited macrodontia (0.004%), and all were in mandibular molars.

The most common shape anomaly following microdontia was taurodontism (0.1%). The distribution of taurodontism was similar between arches and all cases were in molars. Fourteen patients (0.03%) had talon cusps and all were in the maxillary lateral incisors. Similarly, all cases exhibiting dens invaginatus were in maxillary lateral incisors. No statistically significant correlation was found between the occurrence of talon cusps, taurodontism, dens invaginatus and sex ($P = 0.454$, $P = 0.063$ and $P = 0.993$, respectively).

Eight patients with evident amelogenesis imperfecta (0.02%) (Fig 4) were detected. No cases of dentinogenesis imperfecta, dentin dysplasia or regional odontodysplasia were observed.

Discussion

The present study investigated the prevalence and association between different dental anomalies in a large sample. Due to the differences in the reported prevalence of anomalies in various racial and ethnic groups, the authors planned to investigate the frequencies

in a sample of Turkish patients in the Thrace region. Although there have been several studies investigating the prevalence of various dental anomalies[10,13-15], only a few studies considered all types and subtypes of dental anomalies, and none have been conducted with such a large randomised sample group.

It has been reported in various studies that the prevalence of dental anomalies is between 1.73% and 74%[1,5,16]. The highest prevalence in the literature was 74.78% as reported by Tongudomporn and Freer[17] and this finding, which was higher than those of previous random sample studies, was explained as a result of orthodontic patients' tendency to have more dental anomalies than the general population. In non-orthodontic patient groups, the prevalence of dental anomalies was reported to be 40.8% by Ezoddini et al[18] in 2007, 34.28% by Gupta et al[19] in 2011, 29% by Shokri et al[20] in 2014, 4.75% by Aren et al[12] in 2015 and 1.8% by Almaz et al[3] in 2017. These conflicting results can be explained primarily by racial differences and sampling techniques, and also by local environmental influences and nutrition. Additionally, with the exception of the differences in the sampled population, other influential factors are the diagnostic methods and the criteria used in the studies. In the present study, the prevalence of dental anomalies diagnosed by panoramic radiographs was approximately 5.2%. This result was consistent with the prevalence rate of 5.46% reported by Altuğ-Atac and Erdem[15]. The fact that the prevalence rates were almost equal indicates that the results of studies conducted in the same ethnic groups will be similar even if the sample groups are different.

Diagnostic methods could affect study results. Developmental dental anomalies can be diagnosed clinically as well as radiographically. When clinical examination and radiographic examination were performed together, as in the study by Gupta et al[19], a higher prevalence rate (34.28%) than in the present study was reported; however, many studies in the literature have shown that most anomalies can be detected by careful radiographic examination[8,18,19]. In addition, a larger sample group can be reached by examining routine panoramic radiographs, and more reliable results can be obtained with a larger sample. Thus, in the present study, anomalies were evaluated by using panoramic radiographs, as in most studies in the literature.

The inclusion of third molars may also increase the prevalence of anomalies. The prevalence was reported to be 36.7% by Patil et al[13] and 45.1% by Afify and Zawawi[21] when third molars were included. Since third molars show more variations than other teeth, the prevalence of anomalies was reported to be higher when they were included. Consequently, third molars were not included in the present study in order not to affect the results.

Studies investigating types and prevalence of dental anomalies reported that the most common anomaly types were position and number[7,13,22], corresponding to the results of this study. In the present study, 12.2% of the study group presented more than one dental anomaly, similar to the rate of 10% reported by Bilge et al[1]; however, these values were lower than the 21.27% reported by Shokri et al[20].

Several studies indicated that dental anomalies were statistically independent of sex[10,14,19]. In contrast, the present study found that women were statistically significantly more prone to exhibiting dental anomalies, as in a study by Pallikaraki et al[22]. Similarly, reports suggest that women display a higher incidence of dental agenesis[23,24].

In the present study, the prevalence of anomalies in terms of number was 2.1%, and the most common of these was hypodontia (1.5%). The reported prevalence of congenitally missing third molars varies between 5% and 37%[25]. When third molars are excluded, the prevalence ranges between 0.15% and 16.2%[25-27]. In line with the results of the present study, it has been reported that in many populations, the most frequently missing teeth, with the exception of the third molars, are the maxillary lateral incisors and mandibular premolars[26]. It is believed that the reduction in the number of teeth and the size of the jaw are part of human evolution and will continue and become more frequent in years to come[19].

In previous studies, it was reported that the prevalence of supernumerary teeth ranges from 0.1% to 3%[8,15]. Similarly, the prevalence reported in the present study was 0.6%. Supernumerary teeth affect the maxilla more than the mandible (8:1)[28], as in the present study. In previous studies, the majority of detected supernumerary teeth were mesiodens[22,29]. Cases involving supernumerary teeth most commonly affect the anterior maxilla, followed by the mandibular premolar region[30]; however, the most common supernumerary teeth in the present study were paramolars (0.2%) and supernumerary premolars (0.2%), followed by mesiodens (0.1%). This suggests that supernumerary teeth may not be depicted clearly in panoramic radiographs due to the narrow focal trough in the anterior maxilla[31].

Transposition is a rare position anomaly that involves the permanent dentition (prevalence 0.3% to 0.4%) and is more frequently seen in the maxilla[32]. In the present study, the prevalence of transpositions was 0.03% and even although it was more commonly detected in the

maxilla, there was no significant difference between the arches. Transposition is commonly encountered with other anomalies, such as aplasia and peg-shaped lateral incisors[33]; however, no relationship was observed in the present study. It has been reported that transposition usually involves the canines, along with either the incisors or premolars[34]. Likewise, in the present study, the canines were involved in most cases. There was also a significant relationship between impacted canines and transposition ($P = 0.000$). Canines affected by transposition tended to remain impacted.

The prevalence of ectopic eruption has been reported to range from 0.01% to 8.9%[7,19,21]. In the present study, the prevalence was determined to be 0.1%, which was in accordance with the findings of Uslu et al[14] and Afify et al[21]. On the other hand, the prevalence of ectopic eruption was considerably lower compared to other studies[19,35]. Although it has been reported in the literature that transpositions constitute a significant part of ectopia, no correlation was found between transposition and ectopia in the present study; however, there was a significant relationship between ectopia and inversion. Inverted teeth were commonly in ectopic positions.

The prevalence of impacted teeth was 2.5%, which was much lower than in the study of Pallikaraki et al[22] who reported a prevalence of 5.4% in Greece. Maxillary canines were found to be the most impacted tooth excluding third molars, supporting previous findings[14,19,22]. It is not surprising that canines, the last erupted teeth in the arches, are most frequently remain impacted due to a lack of space.

Concerning shape anomalies, macrodontia was reported to be less common than microdontia in previous studies[15-22]. Likewise, only two cases of macrodontia were detected in the present study (0.004%), and all were in mandibular molars. The prevalence of microdontia reported in the current study (0.9%) was similar to that reported by Uslu et al[14] (0.7%) and Patil et al[13] (1.0%). However, other authors reported higher prevalence rates of microdontia due to the inclusion of third molars. Consistent with studies in the literature[13,15], the maxillary lateral incisors were the teeth most affected by microdontia in the present study.

The association between the unilateral agenesis of the maxillary lateral incisor and the microdontia of the contralateral incisor is often observed clinically, and a statistically significant relationship was detected in the present study ($P = 0.000$). This situation was explained by the fact that the genetic defect that determined the agenesis had an incomplete expression on the opposite side of the dental arch, causing microdontia[21].

Only a few studies have reported the prevalence of taurodontism, which varies between 0.02% and 46.4%12,[19]. Diagnosis of taurodontism can be difficult in permanent teeth with ongoing root development, and consequently, it has been reported that the prevalence of taurodontism is lower in people aged under 20 years. The prevalence of taurodontism was 0.1% in the present study which was lower than that reported by Pillai et al[36] (4.79%). On the other hand, the reported prevalence in the present study was higher than in the study by Laganà et al[5].

In the literature, it was reported that the prevalence of fusion ranges from 0.0% to 0.8%[1,7]. Similarly, the prevalence of fusion, which affected both sexes equally ($P = 0.652$), was 0.004% in the present study. The prevalence of talon cusps ranges from 1% to 8% in permanent teeth, with a higher frequency in men than women[37]. However, the prevalence was 0.03% in the present study and they were more predominant in maxillary lateral incisors, which is consistent with results reported by Dash et al[37]. Dens invaginatus was also a rare dental anomaly. Despite the reported prevalence ranging from 0.47% to 6.7%[10], it was found to be lower (0.02%) in the present study.

Structural anomalies are reported to be very rare, with a prevalence less than 5/1000[38]. In fact, structural anomalies may be difficult to detect on radiographs and without a clinical observation (mostly in their less severe forms). Nevertheless, eight prominent cases of generalised amelogenesis imperfecta (0.02%) were identified in the present study. Dentinogenesis imperfecta, dentine dysplasia and regional odontodysplasia were not observed, which is not surprising considering the rarity of these anomalies.

Within the limitations of this study, treated anomalies could not be detected; thus, prevalence may be higher than reported. On the other hand, the lack of clinical examination was another limitation of the study. A prospective study with clinical examination would have allowed precise detection of dental anomalies and improved the sensitivity of the study, especially for the detection of structural and positional anomalies.

Conclusion

The prevalence and type of dental anomalies seemingly vary within and between populations, confirming the role played by racial factors. Genetic differences and the diagnostic criteria used may have led to differences between studies. Although the prevalence of dental anomalies varies within and between populations, the results of the present study were consistent with those of previous studies conducted into the same race.

Early diagnosis and timely management of dental anomalies can prevent further complications. It is therefore crucial to perform a careful radiographic examination in addition to the clinical examination. Population-specific studies will help clinicians to recognise the most common types of anomaly encountered in that region and enable patients to be informed about the effect and prognosis of dental anomalies as well as the treatment plan.

Conflicts of interest

The authors declare no conflicts of interest related to this study.

Author contribution

Dr Mediha Büyükgöze-Dindar contributed to the conceptualisation, methodology, data curation, formal analysis and draft preparation; Dr Meltem Tekbas-Atay contibuted to the conceptualisation, methodology, investigation, writing, review and editing of the manuscript.

(Received Jul 21, 2021; accepted Nov 4, 2021)

References

1. Bilge NH, Yeşiltepe S, Törenek Ağırman K, Çağlayan F, Bilge OM. Investigation of prevalence of dental anomalies by using digital panoramic radiographs. Folia Morphol (Warsz) 2018;77:323–328.
2. Celebi F, Taşkan MM, Turkal M. Dental anomaly prevalence in middle black sea population. Cumhuriyet Dent J 2015;18:343–350.
3. Almaz ME, Sönmez IS, Oba AA. Prevalence and distribution of developmental dental anomalies in pediatric patients. Meandros Med Dent J 2017;18:130–133.
4. Bu X, Khalaf K, Hobson RS. Dental arch dimensions in oligodontia patients. Am J Orthod Dentofacial Orthop 2008;134:768–772.
5. Laganà G, Venza N, Borzabadi-Farahani A, Fabi F, Danesi C, Cozza P. Dental anomalies: Prevalence and associations between them in a large sample of non-orthodontic subjects, a cross-sectional study. BMC Oral Health 2017;17:62.
6. Bassiouny DS, Afify AR, Baeshen HA, Birkhed D, Zawawi KH. Prevalence of maxillary lateral incisor agenesis and associated skeletal characteristics in an orthodontic patient population. Acta Odontol Scand 2016;74:456–459.
7. Yassin SM. Prevalence and distribution of selected dental anomalies among Saudi children in Abha, Saudi Arabia. J Clin Exp Dent 2016;8:e485–e490.
8. Anthonappa RP, King NM, Rabie AB, Mallineni SK. Reliability of panoramic radiographs for identifying supernumerary teeth in children. Int J Paediatr Dent 2012;22:37–43.
9. Dang HQ, Constantine S, Anderson PJ. The prevalence of dental anomalies in an Australian population. Aust Dent J 2017;62:161–164.
10. Baron C, Houchmand-Cuny M, Enkel B, Lopez-Cazaux S. Prevalence of dental anomalies in French orthodontic patients: A retrospective study. Arch Pediatr 2018;25:426–430.
11. Shilpa G, Gokhale N, Mallineni SK, Nuvvula S. Prevalence of dental anomalies in deciduous dentition and its association with succedaneous dentition: A cross-sectional study of 4180 South Indian children. J Indian Soc Pedod Prev Dent 2017;35:56–62.
12. Aren G, Guven Y, Guney Tolgay C, et al. The prevalence of dental anomalies in a Turkish population. J Istanb Univ Fac Dent 2015;49:23–28.
13. Patil SR, Maragathavalli G, Araki K, et al. Three-rooted mandibular first molars in a Saudi Arabian population: A CBCT study. Pesqui Bras Odontopediatria Clin Integr 2018;18:e4133.
14. Uslu O, Akcam MO, Evirgen S, Cebeci I. Prevalence of dental anomalies in various malocclusions. Am J Orthod Dentofacial Orthop 2009;135:328–335.
15. Altug-Atac AT, Erdem D. Prevalence and distribution of dental anomalies in orthodontic patients. Am J Orthod Dentofacial Orthop 2007;131:510–514.
16. Herrera-Atoche JR, Agüayo-de-Pau MD, Escoffié-Ramírez M, Aguilar-Ayala FJ, Carrillo-Ávila BA, Rejón-Peraza ME. Impacted maxillary canine prevalence and its association with other dental anomalies in a Mexican population. Int J Dent 2017;2017:7326061.
17. Thongudomporn U, Freer TJ. Prevalence of dental anomalies in orthodontic patients. Aust Dent J 1998;43:395–398.
18. Ezoddini AF, Sheikhha MH, Ahmadi H. Prevalence of dental developmental anomalies: A radiographic study. Community Dent Health 2007;24:140–144.
19. Gupta SK, Saxena P, Jain S, Jain D. Prevalence and distribution of selected developmental dental anomalies in an Indian population. J Oral Sci 2011;53:231–238.
20. Shokri A, Poorolajal J, Khajeh S, Faramarzi F, Kahnamoui HM. Prevalence of dental anomalies among 7- to 35-year-old people in Hamadan, Iran in 2012-2013 as observed using panoramic radiographs. Imaging Sci Dent 2014;44:7–13.
21. Afify AR, Zawawi KH. The prevalence of dental anomalies in the Western region of Saudi Arabia. ISRN Dent 2012;2012:837270.
22. Pallikaraki G, Sifakakis I, Gizani S, Makou M, Mitsea A. Developmental dental anomalies assessed by panoramic radiographs in a Greek orthodontic population sample. Eur Arch Paediatr Dent 2020;21:223–228.
23. Vastardis H. The genetics of human tooth agenesis: New discoveries for understanding dental anomalies. Am J Orthod Dentofacial Orthop 2000;117:650–656.
24. Muller TP, Hill IN, Peterson AC, Blayney JR. A survey of congenitally missing permanent teeth. J Am Dent Assoc 1970;81:101–107.
25. Rakhshan V. Congenitally missing teeth (hypodontia): A review of the literature concerning the etiology, prevalence, risk factors, patterns and treatment. Dent Res J (Isfahan) 2015;12:1–13.
26. Fekonja A. Hypodontia in orthodontically treated children. Eur J Orthod 2005;27:457–460.
27. De Coster PJ, Marks LA, Martens LC, Huysseune A. Dental agenesis: Genetic and clinical perspectives. J Oral Pathol Med 2009;38:1–17.
28. Subasioglu A, Savas S, Kucukyilmaz E, Kesim S, Yagci A, Dundar M. Genetic background of supernumerary teeth. Eur J Dent 2015;9:153–158.
29. Hurlen B, Humerfelt D. Characteristics of premaxillary hyperodontia. A radiographic study. Acta Odontol Scand 1985;43:75–81.
30. Shah A, Gill DS, Tredwin C, Naini FB. Diagnosis and management of supernumerary teeth. Dent Update 2008;35:510–512, 514–516, 519–520.
31. Witcher TP, Brand S, Gwilliam JR, McDonald F. Assessment of the anterior maxilla in orthodontic patients using upper anterior occlusal radiographs and dental panoramic tomography: A comparison. Oral Surg Oral Med Oral Pathol Oral Radiol Endod 2010;109:765–774.
32. Yilmaz HH, Türkkahraman H, Sayin MO. Prevalence of tooth transpositions and associated dental anomalies in a Turkish population. Dentomaxillofac Radiol 2005;34:32–35.

33. Ely NJ, Sherriff M, Cobourne MT. Dental transposition as a disorder of genetic origin. Eur J Orthod 2006;28:145–151.
34. Peck L, Peck S, Attia Y. Maxillary canine-first premolar transposition, associated dental anomalies and genetic basis. Angle Orthod 1993;63:99–109; discussion 110.
35. Vani NV, Saleh SM, Tubaigy FM, Idris A. Prevalence of developmental dental anomalies among adult population of Jazan, Saudi Arabia. Saudi J Dent Res 2016;7:29–33.
36. Pillai KG, Scipio JE, Nayar K, Louis N. Prevalence of taurodontism in premolars among patients at a tertiary care institution in Trinidad. West Indian Med J 2007;56:368–371.
37. Dash JK, Sahoo PK, Das SN. Talon cusp associated with other dental anomalies: A case report. Int J Paediatr Dent 2004;14:295–300.
38. Gadhia K, McDonald S, Arkutu N, Malik K. Amelogenesis imperfecta: An introduction. Br Dent J 2012;212:377–379.

Impact of Fracture Line Width on Radiographic Diagnosis of Vertical Root Fractures: Analysis of the Generalised Estimating Equation Model

Kaique LEITE DE LIMA[1], Lorena Rosa SILVA[1], Mozar ANDRADE MOTA NETO[2], Marcelo GUSMÃO PARAÍSO CAVALCANTI[3], Cláudio RODRIGUES LELES[1], Maria ALVES GARCIA SANTOS SILVA[1], Carlos ESTRELA[1], Brunno SANTOS DE FREITAS SILVA[1], Fernanda P YAMAMOTO-SILVA[1]

Objective: *To undertake a joint analysis of the influence of fracture width, dental thickness and distance of the fracture from the cortical bone on the radiographic diagnosis of vertical root fractures.*

Methods: *Thirty-six uniradicular bovine teeth were endodontically treated and distributed into three groups according to the remaining root dentine thickness: 1.2 mm, 1.5 mm and 1.8 mm. Each group comprised 12 teeth, six with vertical root fracture and six without. Scanning electron microscopy (SEM) images of the fractured tooth groups were obtained and the fracture lines were measured. All specimens were inserted into bone defects created in bovine ribs, at different distances from the external cortical bone. Digital periapical radiographs were randomly evaluated by three blinded examiners (presence or absence of fractures).*

Results: *The specificity for periapical radiography was found to be 89% and the accuracy rate was 57.4%. The mixed-model regression using the generalised estimating equation (GEE) model showed that the width of the fracture line and the thickness of the dental remnant play an important role in radiographic detection of vertical root fractures. There is a lower chance of correct diagnosis with fracture line widths < 0.2 mm (odds ratio [OR] 0.294, 95% confidence interval [CI] 0.103 to 0.836; P = 0.022) and tooth thicknesses < 1.2 mm (OR 0.342, 95% CI 0.157 to 0.747; P = 0.007).*

Conclusion: *Fracture line widths < 0.2 mm and smaller root thicknesses lead to a less accurate diagnosis of vertical root fractures on periapical radiographs.*

Key words: *diagnosis, endodontically treated teeth, radiograph, vertical root fracture*
Chin J Dent Res 2022;25(3):197–204; doi: 10.3290/j.cjdr.b3317977

Vertical root fracture (VRF) is characterised by a longitudinally orientated fracture plane that begins at the root apex and extends to the coronal part of the tooth[1].

Most signs and symptoms of VRF are nonspecific, thus limiting the reliability of the available methods for VRF detection[2]. CBCT has been suggested as a superior volumetric imaging system to periapical radiography in VRF diagnosis[3-6]; however, beam-hardening artefacts substantially reduce its performance[7] by hampering visualisation of or even mimicking the fracture line.

Incomplete root fractures are particularly difficult to detect on both periapical radiographs and CBCT[8]. Previous studies have compared periapical radiography and CBCT in assessing VRF[8-11] and revealed divergent and imprecise results for the two systems, thus hindering clear diagnosis of VRF and correct indication of the best system to use[1,12]. According to the American

1 Federal University of Goiás, Stomatological Sciences, Goiania, Brazil.
2 UniEVANGÉLICA University Centre of Anápolis, Anapolis, Brazil.
3 University of São Paulo, Sao Paulo, Brazil.

Corresponding author: Dr Brunno SANTOS DE FREITAS SILVA, Federal University of Goiás, Stomatological Sciences, Av. Primeira Avenida s/n, Goiania 74605-220, Brazil. Tel: 55-62-3209-6325. Email: brunno.santosfreitas@gmail.com

This study was funded in part by grants from the FUNADESP (#2020-21).

Academy of Oral and Maxillofacial Radiology, periapical radiography represents the initial imaging modality of choice in evaluating the suspected fractures[13] that may be observed on the root surface as a vertically orientated radiolucent line[8]. In fact, a fracture can only be visualised in radiographic examinations when the central beam of the x-rays is parallel to the fracture plane or within ± 4 degrees variation of it. Thus, a complementary approach recommends a horizontal angulation variation in radiographic images[15].

Several factors associated with image acquisition have been investigated for radiographic diagnosis of VRF, including the influence of root filling materials[16], the presence of metallic posts[9,17], comparison of different digital and conventional systems[18], the angulation in obtaining the radiographic images[15] and the influence of the fracture line width[3,4,10]. The results of these studies showed low accuracy of periapical radiography, especially because of the sensitivity of this examination method; however, these results should be interpreted with caution owing to the methodological differences across studies and the lack of simultaneous testing of the multiple predisposing factors that could influence the radiographic detection of VRF. For this reason, considering that periapical radiography is the main auxiliary method for diagnosing VRF and that current studies focus on individualised evaluation of the factors influencing its diagnosis, and are thus not very representative of clinical conditions, it is important to understand what dependent or joint factors are relevant to radiographic diagnosis of VRF. As such, this study aims to evaluate the influence of dental thickness, fracture width and the distance of fracture from the cortical bone in the radiographic diagnosis of VRF, using a methodology that considers the association of variables.

Materials and methods

This experimental study was approved by the Ethics Committee on Animal Research of our university (protocol no. 129/17).

Sample acquisition

Thirty-six single-rooted bovine teeth were acquired commercially from a specialist company (Mondelli Indústria de Alimentos, São Paulo, Brazil) for use as the study sample. The teeth were inspected microscopically (OPMI, Zeiss, Oberkochen, Germany) to examine the external root surfaces. Teeth exhibiting cracks, fractured cusps, pre-existing fractures (split tooth, complete or incomplete vertical root fracture), external resorptions, structural abnormalities or incomplete root formation were excluded.

Sample preparation

The crowns of the teeth were removed, leaving the remaining tooth at 15 mm in length. The samples were divided into three groups according to their visible dentine thickness: 1.2, 1.5 and 1.8 mm. These groups were based on the study by Katz and Tamse[19], who used a final mean thickness of 1.49 ± 0.16 mm after endodontic treatment. CBCT images (Orthopantomograph OP300, KaVo Dental, Tuusula, Finland) of the cervical, middle and apical regions were acquired and their thickness was measured using CS3D imaging software (v 3.1, Carestream Dental, Rochester, NY, USA). The final thickness of the dental remnant was established by taking the arithmetic mean of the three regions.

After random allocation of the groups, the sample units were worn using a #3 Peeso Reamer (Dentsply Maillefer, Ballaigues, Switzerland) in a motor at low rotation, guided by a digital caliper and periapical transoperative radiographs according to the group being studied. The root canals were then obturated using a thermoplastic technique with a McSpadden 0.50 condenser and gutta-percha cones (both Dentsply Maillefer) with epoxy amine resin cement (AH Plus, Dentsply Sirona, Charlotte, NC, USA).

Each group received 12 sample units, which were later divided randomly into six fractured and six non-fractured teeth. Simulation of the periodontal ligament for induction of VRF was performed according to the methodology proposed by Soares et al[20], after which fractures were induced using a universal test machine (Instron, TTDML, Canton, OH, USA) using a 2000 kg/force load cell at a speed of 0.05 mm/min.

Performing scanning electron microscopy (SEM)

SEM images of the fractured teeth were acquired to measure the fracture line (Figs 1 and 2). The teeth were dried at room temperature and scanned with a JEOL JSM IT300LV microscope (JEOL USA, Peabody, MA, USA) operating under a low vacuum, at a magnification of 15×. The image analysis was performed with ImageJ (National Institutes of Health, Bethesda, MD, USA), using the linear measurement tool in the cervical, middle and apical regions of the fracture tract. The final width was defined as the highest value found. The maximum fracture width in the sample ranged from 0.04 to 0.40 mm, with a mean of 0.14 ± 0.07 mm.

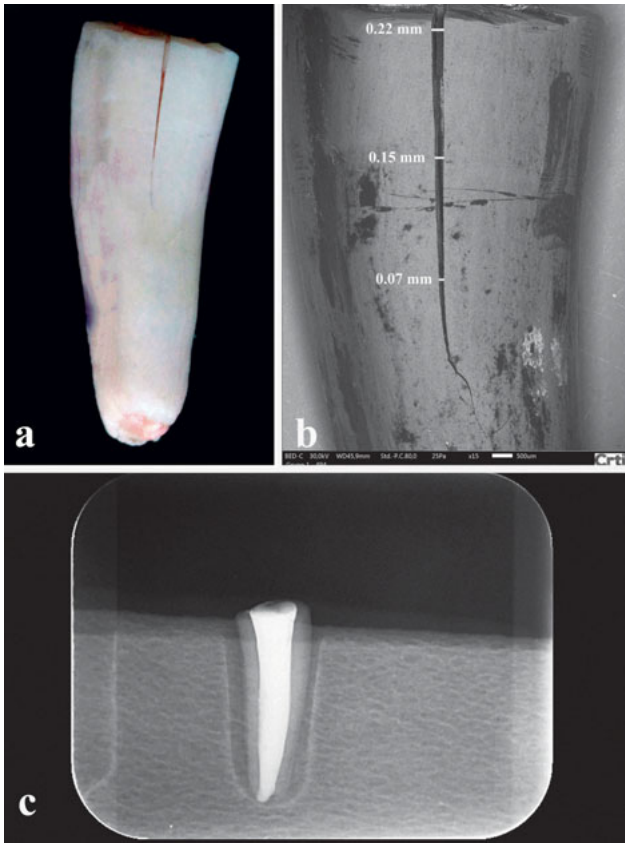

Fig 1 Dental remnant with fracture line < 0.2 mm. **(a)** Photograph of the fractured dental element. **(b)** SEM with 15× magnification, showing the fracture line. **(c)** Periapical radiograph with no evidence of VRF.

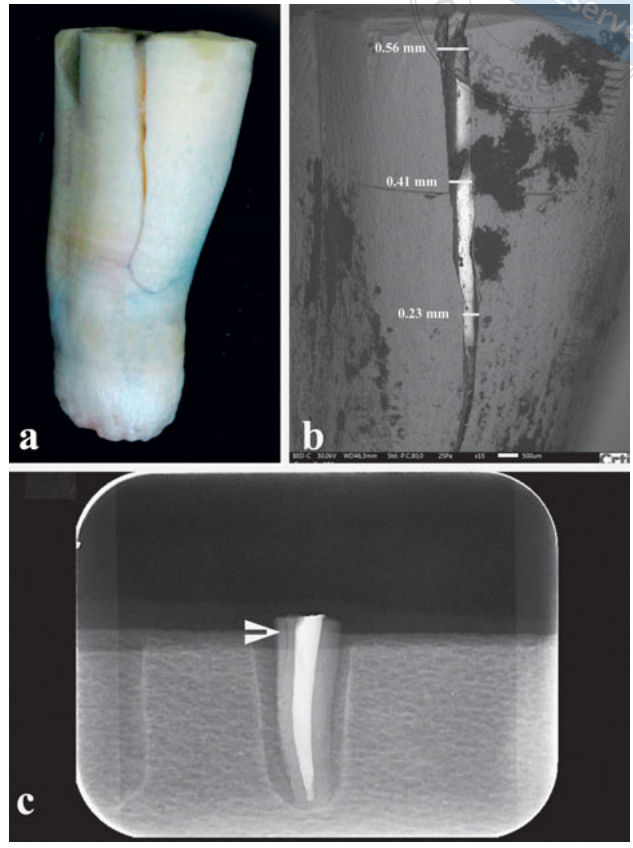

Fig 2 Dental remnant with fracture line > 0.2 mm. **(a)** Photograph of the fractured dental element. **(b)** SEM with 15× magnification, showing the fracture line. **(c)** Periapical radiograph with the radiolucent line on the proximal aspect compatible with VRF (arrowhead).

Phantom preparation

The cortical bone was simulated by using a bovine rib as a phantom. Bone defects were produced by simulating the dental alveoli (Fig 3). The phantom was prepared using a MaxiCut drill (American Burrs, Palhoça, Santa Catarina, Brazil) mounted on a low rotation motor to perform the scoring, which occurred at 1 mm on the cortical bone, and at a distance of 1 and 3 mm from the cortical bone.

Radiographic acquisition

Each tooth from each different group was radiographed individually in the three bovine rib bone defects being studied, which were surrounded by a thin layer of wax to simulate the attenuation of the x-ray beam. The images were acquired by positioning a phantom on an acrylic platform coupled to a transferor, as previously described by Nascimento et al[16].

All radiographic images were obtained using a Focus periapical unit (KaVo Dental) operating at 70 kVp and 7 mA and using size 2 phosphor plates (14.3 pl/mm, 886 × 1171 pixels) from the Express system (KaVo Dental). The exposure time was 0.2 s and a sensor-focus distance of 40 cm was used to obtain images at three horizontal angles, namely orthoradial, mesioradial and distoradial, with a variation of 15 degrees.

The images were analysed by simultaneously examining the three radiographs at different angulations of each tooth. Three calibrated and independent examiners, two radiologists and one endodontist, all with at least 5 years of experience, classified the images according to the evaluation presence of VRF using a 5-point scale: 1, VRF definitely present; 2, VRF probably present; 3, uncertain; 4, VRF probably absent; and 5, VRF definitely absent. All the images were evaluated in a low-light environment on an XPS X8700 computer with an Intel 3.4 GHz processor, 12 GB memory, 2 TB hard drive and a NVIDIA GeForce GTX 645 graphics

Fig 3 Bovine rib phantom used to evaluate the distance from the cortical bone. **(a)** 1 mm wear of cortical bone, **(b)** 1 mm from cortical bone and **(c)** 3 mm from cortical bone.

card (Dell, Austin, TX, USA) and a 28-inch colour monitor (UltraHD, Dell).

Data analysis

Data analysis was performed using SPSS software (version 24.0, IBM, Armonk, NY, USA). Descriptive statistics were used to summarise the data on VRF and independent factors. The VRF data classified by the raters were cross-tabulated with the dichotomous condition of the dental roots (whether fractured or not) to calculate the rates of the correct measures to be used in the overall measures, and by each of the raters, whose performance in the detection of VRF was expressed as accurate.

The outcome variable was labelled as a correct rating – code = 1 (true positive [TP] and true negative [TN] cases) or as an incorrect rating – code = 0 (false positive [FP] and false negative [FN] cases). Since the measurements were clustered among the raters and along the different distances of the cortical bone, there was a violation of the assumption of independence of data. Thus, correct identification of the root condition (fractured or not) was modelled by mixed-model regression using a generalised estimating equation (GEE).

The original database was changed to a format that rearranged the groups of related columns into groups of rows in the new data file using the "restructure" command in the software. The analysis was specified as a binomial distribution, and the Logit as the link function, in order to run the GEE model for the binary outcome. The independent factors in the regression model were the raters (three levels), the distance from the cortical bone (proximal, central and distal positions), the width of the fracture line (no fracture, < 0.2 mm and ≥ 0.2 mm) and the width of the remaining root structure (three levels). All the predictors were entered into the regression model using the forced entry method to test the main effects of each variable. GEE regression parameters were expressed as the odds ratio (OR) at a 95% confidence interval (CI). The significance of the model effects was tested using Wald chi-square statistics, and the statistical significance was set at $P < 0.05$.

Results

The sensitivity and specificity values, positive predictive value, negative predictive value and accuracy values for each examiner, in relation to the fracture diagnosed by periapical radiography, are presented in Table 1. The highest value found was for specificity, resulting in a greater ability to diagnose non-fractured teeth correctly according to 85% of all three evaluators. Periapical radiography presented a correct VRF detection rate of 57%.

Use of the GEE made it possible to establish that there was no statistically significant relation between the different evaluators or the distance of the cortical bone and the correct diagnosis of VRF (Table 2), considering $P < 0.05$ for all the variables. The width of the fracture line and the thickness of the dental remnant played an important role in detecting VRF, and the chance of correct diagnosis was lower when the fracture width was reduced (< 0.2 mm: OR 0.294, 95% CI 0.103 to 0.836; $P = 0.022$) or the remaining tooth was reduced (lower: OR 0.342, 95% CI 0.157 to 0.74; $P = 0.007$), except in non-fractured cases (OR 12.052, 95% CI 5.923 to 24.526; $P > 0.001$), which presented a greater chance of success than cases with width ≥ 0.2 mm.

Poor agreement was observed between the examiners in detecting VRF. Table 3 shows the interobserver kappa coefficients for VRF detection in periapical radiographs for each examiner. The intraexaminer kappa calculation indicated that substantial agreement was obtained in VRF detection, except for Examiner 1 (Table 4).

Discussion

In the present in vitro model, the width of the fracture line and the thickness of the dental remnant played important roles in VRF detection regardless of the distance from the tooth to the cortical bone. Fracture width seems to be a more determining factor for detection than dental remnant thickness, since larger fracture widths are more easily detected when the fracture plane is parallel to the central x-ray beam[14]. When the remaining tooth was reduced in dentine thickness, there was a smaller chance of correct VRF. This is because greater force was required to produce VRF in thicker teeth with the universal test machine, resulting in fractures with larger widths that favour their detection.

Table 1 Measurements taken from a 2 × 2 table applied to determine accuracy of assessment of teeth with possible VRF using periapical radiographs.

Rater	Number of images	Sensitivity	Specificity	Positive predictive value	Negative predictive value	Accuracy (%)
#1	108	0.51	0.61	0.57	0.55	0.56
#2	108	0.12	1.00	1.00	0.53	0.56
#3	108	0.22	0.96	0.85	0.55	0.59
Overall	324	0.29	0.85	0.67	0.54	0.57

Table 2 GEE parameters for the probability of correct diagnosis of VRF in radiographs.

Parameter		OR	95% CI		Significance
			Lower	Upper	
Intercept		1.301	0.473	3.581	0.610
Rater	#1	0.828	0.269	2.551	0.742
	#2	0.828	0.555	1.235	0.354
	#3	1.000	0.000	0.000	0.000
Distance to cortical bone	Proximal	0.647	0.355	1.177	0.154
	Central	1.066	0.586	1.939	0.834
	Distal	1.000	0.000	0.000	0.000
Width of fracture line	No fracture	12.052	5.923	24.526	> 0.001
	< 0.2 mm	0.294	0.103	0.836	0.022
	≥ 0.2 mm	1.000	0.000	0.000	0.000
Chance of correct diagnosis with remaining root structure width	Lower	0.342	0.157	0.747	0.007
	Intermediary	0.464	0.167	1.284	0.139
	Higher	1.000	0.000	0.000	0.000

Table 3 Kappa values for interexaminer agreement in interpreting periapical radiographs for VRF diagnosis.

	K value
Examiner 1 × Examiner 2	0.036
Examiner 1 × Examiner 3	0.072
Examiner 2 × Examiner 3	0.531

Table 4 Kappa values for intraexaminer agreement of VRF diagnosis.

	K value
Examiner 1	0.293
Examiner 2	0.730
Examiner 3	0.738

Several studies have investigated the accuracy of periapical radiographs in detecting an artificially made VRF and reported similar results, with low sensitivity and high specificity values[9-11]. Our main objective was not to confirm the difficulty of VRF radiographic detection, but rather to understand the impact of factors acting simultaneously to influence the formation/definition of the radiographic image in VRF diagnosis using a regression model.

The present authors formed three experimental groups composed of teeth with different thicknesses. The selection considered the influence of dentine thickness in the development of VRF[21] and the knowledge that VRF is more prevalent in teeth with a reduced dental structure, such as mandibular molars and maxillary premolars[22-24], often with endodontic treatment[25] and/or with intraradicular retainers[26,27]. The remaining tooth thickness may vary according to the type of teeth, the endodontic instrumentation technique (manual, rotary, etc.)[25,28] and the type of preparation made to receive an intraradicular retainer[29]. In this respect, reduced dental structure is associated with greater susceptibility to VRF[30] and greater radiographic sharpness. A smaller thickness offers less resistance to x-ray attenuation and may thus favour greater radiographic sharpness, facilitating radiographic detection of VRF[31]. Despite the greater sharpness of the radiographic image of the dental thickness, this did not facilitate correct diagnosis of VRF in the present study.

We also hypothesised that the distance from the tooth to the cortical bone would influence the radiographic detection of VRF. This could be an important factor to study since the different dental groups have distinctive positions in relation to the bone, e.g., anterior teeth are usually implanted closer to the cortical bone compared to the posterior teeth[32]. This hypothesis can be explained by the fact that superimposition of a thicker bone layer can make it difficult to visualise

radiolucent structures in radiographic images[33] since objects located along the long axis of an x-ray beam are projected to the same spot on the radiographic receptor. Thus, the proximity of fractured teeth to the cortical bone and the image receptor may increase the sharpness of the images, which could facilitate VRF diagnosis; however, the present data show that the distance of the cortical bone from the VRF was not a factor associated with VRF detection.

Our model also included an analysis of fracture width. Brady et al[10] compared the accuracy of periapical radiography and CBCT in detecting both complete (when fragments are separated) and incomplete VRF (when fragments are not separated) in endodontically untreated teeth in an ex vivo model. Comparison of complete versus incomplete VRF revealed that the area under the receiver operating characteristic curve was not significant, but that the sensitivity was significantly higher in the group with complete fracture than that with incomplete fracture. In our study, the accuracy of periapical radiography was low, corroborating previous studies[8,10,11]; however, our model of analysis did not separate the teeth into complete or incomplete fracture groups, because it was believed that fracture width does not necessarily imply that fragments are separated, but does influence their detection. The fracture width must be great enough for the x-ray beam to cross it in order to form a radiographic image[12]. Separated fragments would indeed aid in the diagnosis of VRF by revealing other radiographic signs, such as periradicular bone loss[34].

Patel et al[8] used a methodology similar to that of Brady et al[10] to create fractures in endodontically treated human teeth. They reported that no incomplete fracture (0.05 to 0.11 mm) was detected radiographically, and that only 19% of complete fractures (> 0.2 mm) were detected[8]. They also stated that both radiographically and CBCT-generated area under the curve values are inaccurate[8]. Özer[3] compared the ability of both CBCT and digital periapical radiography to diagnose VRF of different thicknesses (< 0.2 mm, 0.2 mm and 0.4 mm) and concluded that radiographs presented better results, concurrently with larger fracture thicknesses; moreover, 41.6% of the fractures < 0.2 mm were correctly diagnosed, and 60% of all the fractures were 0.4 mm thick. Corroborating their findings, we found that fractures > 0.2 mm were more likely to be diagnosed compared with fractures < 0.2 mm, regardless of the distance between the dental structure and the cortical bone or the thickness of the tooth.

This in vitro model with bovine teeth allowed the impact of cortical distance, tooth thickness and fracture width to be evaluated jointly and controllably in performing VRF diagnosis. Despite the limitations inherent to an in vitro study, use of the bovine model allowed standardisation of the tooth length, shape and age, thus reducing the bias related to these parameters. The chemical composition and tensile strength and modulus of elasticity of bovine tooth enamel and dentine are mostly similar to those of human teeth, making bovine alternatives the first choice when replacing human teeth for research purposes[35-37]. Despite the morphological differences between bovine and human teeth, studies with bovine teeth have presented results comparable to those obtained with extracted human teeth[35].

This study used high resolution SEM images to determine the fracture line width accurately, thus allowing microstructural visualisation and high image magnification[23], which enabled assigned limits to be evaluated clearly. The quantitative analysis from SEM images is a feasible technique conventionally performed with the ImageJ image processing tool[38].

Since periapical radiography is the first auxiliary method to evaluate a suspected fracture, it is important to understand its limitations in order to be more rational and specific in indicating the most suitable imaging option. The present results corroborate those of Özer[3] and Patel et al[8] and show that when the VRF cannot be identified radiographically, this is probably due to its small width. In this case, CBCT with a voxel size < 0.2 mm is indicated and increases the chance of VRF detection, even in the presence of artefacts.

Conclusion

In conclusion, diagnosis of VRF using digital periapical radiographs is influenced by the width of the fracture line. A distance > 0.2 mm between dental fragments tends to provide a greater number of correct diagnoses of VRF.

Conflicts of interest

The authors declare no conflicts of interest related to this study.

Author contribution

Drs Kaique LEITE DE LIMA, Lorena Rosa SILVA, Cláudio RODRIGUES LELES and Brunno SANTOS DE FREITAS SILVA contributed to the data analysis; Drs Kaique LEITE DE LIMA and Lorena Rosa SILVA contributed to the data gathering. All authors contributed to the writing and editing of the manuscript.

(Received Oct 20, 2021, accepted Apr 02, 2022)

References

1. Chang E, Lam E, Shah P, Azarpazhooh A. Cone-beam computed tomography for detecting vertical root fractures in endodontically treated teeth: A systematic review. J Endod 2016;42:177–185.
2. Patel S, Brown J, Pimentel T, Kelly RD, Abella F, Durack C. Cone beam computed tomography in Endodontics – A review of the literature. Int Endod J 2019;52:1138–1152.
3. Ozer SY. Detection of vertical root fractures of different thicknesses in endodontically enlarged teeth by cone beam computed tomography versus digital radiography. J Endod 2010;36:1245–1249.
4. Makeeva IM, Byakova SF, Novozhilova NE, et al. Detection of artificially induced vertical root fractures of different widths by cone beam computed tomography in vitro and in vivo. Int Endod J 2016;49: 980–989.
5. Khedmat S, Rouhi N, Drage N, Shokouhinejad N, Nekoofar MH. Evaluation of three imaging techniques for the detection of vertical root fractures in the absence and presence of gutta-percha root fillings. Int Endod J 2012;45:1004–1009.
6. Avsever H, Gunduz K, Orhan K, et al. Comparison of intraoral radiography and cone-beam computed tomography for the detection of horizontal root fractures: An in vitro study. Clin Oral Investig 2014;18:285–292.
7. Talwar S, Utneja S, Nawal RR, Kaushik A, Srivastava D, Oberoy SS. Role of cone-beam computed tomography in diagnosis of vertical root fractures: A systematic review and meta-analysis. J Endod 2016;42:12–24.
8. Patel S, Brady E, Wilson R, Brown J, Mannocci F. The detection of vertical root fractures in root filled teeth with periapical radiographs and CBCT scans. Int Endod J 2013;46:1140–1152.
9. Junqueira RB, Verner FS, Campos CN, Devito KL, do Carmo AM. Detection of vertical root fractures in the presence of intracanal metallic post: A comparison between periapical radiography and cone-beam computed tomography. J Endod 2013;39:1620–1624.
10. Brady E, Mannocci F, Brown J, Wilson R, Patel S. A comparison of cone beam computed tomography and periapical radiography for the detection of vertical root fractures in nonendodontically treated teeth. Int Endod J 2014;47:735–746.
11. Chavda R, Mannocci F, Andiappan M, Patel S. Comparing the in vivo diagnostic accuracy of digital periapical radiography with cone-beam computed tomography for the detection of vertical root fracture. J Endod 2014;40:1524–1529.
12. Tsesis I, Rosen E, Tamse A, Taschieri S, Kfir A. Diagnosis of vertical root fractures in endodontically treated teeth based on clinical and radiographic indices: A systematic review. J Endod 2010;36: 1455–1458.
13. Special Committee to Revise the Joint AAE/AAOMR Position Statement on use of CBCT in Endodontics. AAE and AAOMR joint position statement: Use of Cone Beam Computed Tomography in Endodontics 2015 Update. Oral Surg Oral Med Oral Pathol Oral Radiol 2015;120:508–512.
14. Pitts DL, Natkin E. Diagnosis and treatment of vertical root fractures. J Endod 1983;9:338–346.
15. Wenzel A, Kirkevang LL. High resolution charge-coupled device sensor vs. medium resolution photostimulable phosphor plate digital receptors for detection of root fractures in vitro. Dent Traumatol 2005;21:32–36.
16. Nascimento HA, Neves FS, de-Azevedo-Vaz SL, Duque TM, Ambrosano GM, Freitas DQ. Impact of root fillings and posts on the diagnostic ability of three intra-oral digital radiographic systems in detecting vertical root fractures. Int Endod J 2015;48:864–871.
17. Jakobson SJ, Westphalen VP, Silva Neto UX, Fariniuk LF, Schroeder AG, Carneiro E. The influence of metallic posts in the detection of vertical root fractures using different imaging examinations. Dentomaxillofac Radiol 2014;43:20130287.
18. Tofangchiha M, Bakhshi M, Fakhar HB, Panjnoush M. Conventional and digital radiography in vertical root fracture diagnosis: A comparison study. Dent Traumatol 2011;27:143–146.
19. Katz A, Tamse A. A combined radiographic and computerized scanning method to evaluate remaining dentine thickness in mandibular incisors after various intracanal procedures. Int Endod J 2003;36: 682–686.
20. Soares CJ, Pizi EC, Fonseca RB, Martins LR. Influence of root embedment material and periodontal ligament simulation on fracture resistance tests. Braz Oral Res 2005;19:11–16.
21. Silva LR, de Lima KL, Santos AA, et al. Dentin thickness as a risk factor for vertical root fracture in endodontically treated teeth: A case-control study. Clin Oral Investig 2021;25:1099–1105.
22. Cohen S, Berman LH, Blanco L, Bakland L, Kim JS. A demographic analysis of vertical root fractures. J Endod 2006;32:1160–1163.
23. PradeepKumar AR, Shemesh H, Jothilatha S, Vijayabharathi R, Jayalakshmi S, Kishen A. Diagnosis of vertical root fractures in restored endodontically treated teeth: A time-dependent retrospective cohort study. J Endod 2016;42:1175–1180.
24. Liao WC, Tsai YL, Wang CY, et al. Clinical and radiographic characteristics of vertical root fractures in endodontically and nonendodontically treated teeth. J Endod 2017;43:687–693.
25. Tang W, Wu Y, Smales RJ. Identifying and reducing risks for potential fractures in endodontically treated teeth. J Endod 2010;36:609–617.
26. Marchi GM, Mitsui FH, Cavalcanti AN. Effect of remaining dentine structure and thermal-mechanical aging on the fracture resistance of bovine roots with different post and core systems. Int Endod J 2008;41:969–976.
27. Junqueira RB, de Carvalho RF, Marinho CC, Valera MC, Carvalho CAT. Influence of glass fibre post length and remaining dentine thickness on the fracture resistance of root filled teeth. Int Endod J 2017;50:569–577.
28. Singla M, Aggarwal V, Logani A, Shah N. Comparative evaluation of rotary ProTaper, Profile, and conventional stepback technique on reduction in Enterococcus faecalis colony-forming units and vertical root fracture resistance of root canals. Oral Surg Oral Med Oral Pathol Oral Radiol Endod 2010;109:e105–e110.
29. Souza EM, do Nascimento LM, Maia Filho EM, Alves CM. The impact of post preparation on the residual dentin thickness of maxillary molars. J Prosthet Dent 2011;106:184–190.
30. Mireku AS, Romberg E, Fouad AF, Arola D. Vertical fracture of root filled teeth restored with posts: the effects of patient age and dentine thickness. Int Endod J 2010;43:218–225.
31. Patel S, Dawood A, Whaites E, Pitt Ford T. New dimensions in endodontic imaging: Part 1. Conventional and alternative radiographic systems. Int Endod J 2009;42:447–462.
32. Ohiomoba H, Sonis A, Yansane A, Friedland B. Quantitative evaluation of maxillary alveolar cortical bone thickness and density using computed tomography imaging. Am J Orthod Dentofacial Orthop 2017;151:82–91.
33. Bender IB, Seltzer S. Roentgenographic and direct observation of experimental lesions in bone: II. 1961. J Endod 2003;29:707–712; discussion 701.
34. Tamse A. Vertical root fractures in endodontically treated teeth: Diagnostic signs and clinical management. Endodontic Topics 2006;13:84–94.
35. Soares FZ, Follak A, da Rosa LS, Montagner AF, Lenzi TL, Rocha RO. Bovine tooth is a substitute for human tooth on bond strength studies: A systematic review and meta-analysis of in vitro studies. Dent Mater 2016;32:1385–1393.
36. Sano H, Ciucchi B, Matthews WG, Pashley DH. Tensile properties of mineralized and demineralized human and bovine dentin. J Dent Res 1994;73:1205–1211.

37. Teruel Jde D, Alcolea A, Hernández A, Ruiz AJ. Comparison of chemical composition of enamel and dentine in human, bovine, porcine and ovine teeth. Arch Oral Biol 2015;60:768–775.

38. Schneider CA, Rasband WS, Eliceiri KW. NIH Image to ImageJ: 25 years of image analysis. Nat Methods 2012;9:671–675.

Impact of Social Support on Perceived Stress in Latin American and Caribbean Dental Students and Dental Practitioners during Mandatory Social Isolation within the Coronavirus Pandemic in 2020

María Claudia GARCÉS-ELÍAS[1], Roberto A LEÓN-MANCO[1], Andrés A AGUDELO-SUÁREZ[2]

Objective: *To determine the impact of social support on perceived stress in Latin American and Caribbean dental students and dental practitioners during mandatory social isolation within the coronavirus (COVID-19) pandemic in 2020.*
Methods: *A cross-sectional study was conducted with a sample of 1812 dental students and dental practitioners from 21 Latin American and Caribbean countries. Perceived stress was assessed using the perceived stress scale (PSS-14), and the influence of social support was addressed using the Duke-UNC-11. Additionally, sociodemographic variables, knowledge of and preventive behaviour against COVID-19 and health status were considered. A descriptive, bivariate and multivariate analysis was performed through multiple linear regression.*
Results: *In the multivariate analysis, model 4 presented R2% = 21.20 (P < 0.001), a constant of 40.049; within the model, the social support variable had a non-standardised regression coefficient (b) of −4,527 (95% CI – 5.646 to −3,408; P < 0.001), the self-perceived level of concern regarding COVID-19 was b = 1.838 (95% confidence interval [CI] 0.887 to 2.790; P < 0.001), the self-perceived health status was b = −2.191(95% CI −2.944 to −1.437; P < 0.001), the number of days in compulsory isolation was b = −0.965 (95% CI −1.908 to −0.022; P = 0.045), while the level of confinement was b = 0.923 (95%CI: 0.106-1.740; P = 0.027), age was b = −1.743 (95% CI −2.625 to −0.860; P < 0.001), sex was b = 1.324 (95% CI 0.311 to 2.337; P = 0.011) and the economic income level was b = −1.539 (95% CI −2.434 to −0.644; P = 0.001).*
Conclusion: *An association was determined between perceived stress and social support, as well as the variables of concern about the disease, self-perceived health status, number of days and level of confinement, age, sex and economic income level, based on the experience of dental practitioners and dental students in mandatory isolation.*

Key words: *coronavirus, dental practitioners, dental students, psychological stress, social support*
Chin J Dent Res 2022;25(3):205–213; doi: 10.3290/j.cjdr.b3317983

The coronavirus (COVID-19) pandemic and the adoption of restrictive policies to control its spread, such as widespread quarantine, social distancing and self-isolation, modified the normal development of personal activities and habits. In addition, the increase in financial uncertainty and instability and the risk of contagion triggered, at a community level, a considerable increase in the levels of psychological stress, which may have been more prevalent in vulnerable groups such as women, unemployed people, individuals with a low socio-economic status and young adults. COVID-19 is also linked to cardiovascular and gastrointestinal diseases and depression[1-4].

1 Faculty of Dentistry, Universidad Peruana Cayetano Heredia. Lima, Peru.
2 Faculty of Dentistry, University of Antioquia, Medellin, Colombia.

Corresponding author: Dr María Claudia GARCÉS-ELÍAS, Universidad Peruana Cayetano Heredia - Av. Honorio Delgado 350, San Martín de Porres, 15102, Lima, Peru. Tel: 51-1-319-0000. Email: maria.garces@upch.pe

On the other hand, factors such as sex, socioeconomic level, self-acceptance, religious beliefs, culture and social support impact individuals' mental health. Social support is defined as the care and support received from third parties during challenging situations that allow the individual to modify their perception of the event; it is also an important strategy to facilitate stress reduction[5]. Likewise, during the health crisis, the population has had to experience physical distancing and faced low levels of social support; a lack of the latter is linked to reduced satisfaction with life, anxiety and depression. Social support helps to regulate stress levels and reduce work-related stress[6-8]; however, when it is not readily available, this has a negative impact on individuals' mental health[9]. As in previous epidemics, health care workers have presented high levels of stress during the current pandemic, having to deal with an increased workload and a high risk of contagion, and continued exposure to these factors could have a greater impact on mental health. As a mechanism for reducing work-related stress, social support is essential for health care workers, preventing psychological distress and psychiatric symptoms and improving their professional effectiveness[10].

Dental practitioners were also affected by the situation; their activities were interrupted drastically in the first months of the pandemic as they were restricted to performing urgent and emergency procedures to minimise possible risks of contagion, and job losses occurred; in addition, all academic and research activities were suspended; which resulted in situations of anxiety and psychological stress in this occupational group[11-13]. In contrast, in Latin America, there is little scientific evidence describing how the dental community is coping with the situation like other health professionals who have dealt with it throughout the pandemic.

As such, the objective of this study was to determine the impact of social support on perceived stress in Latin American and Caribbean dental students and practitioners during mandatory social isolation during the COVID-19 pandemic in 2020.

Materials and methods

Study design and population

A cross-sectional study was carried out by means of an anonymous survey, provided virtually to a convenience sample of dental students and professionals from 21 countries in Latin America and the Caribbean (Argentina, Bolivia, Brazil, Chile, Colombia, Costa Rica, Dominica, Dominican Republic, Ecuador, El Salvador, Grenada, Guatemala, Honduras, Mexico, Nicaragua, Panama, Paraguay, Peru, Puerto Rico, Uruguay and Venezuela), constituting an initial sample of 2442 respondents. Surveys with errors in the recording of information were discarded, resulting in a final sample of 1812 respondents (cooperation rate 83.4%).

Data collection techniques

Google Forms (Google, Mountain View, CA, USA) was used to design the questionnaire; subsequently, a pilot test was carried out with a sample of 30 participants to evaluate internal consistency and completion time. The time period allowed for the fieldwork was from 15 May to 26 August 2020. The online questionnaire was distributed through digital media such as Facebook groups, WhatsApp messages, emails and invitations sent to different dental schools. Additionally, the snowball technique was employed to increase the number of participants. The questionnaire collected sociodemographic data and incorporated questions about the COVID-19 pandemic and social support.

Variables

For this study, in addition to the dependent variable, four dimensions were defined to group the independent variables present in the study. For the dependent variable, the 14-item perceived stress scale (PSS-14) was applied to measure stress in participants[14]. This instrument comprises 14 items, seven of which are positive and seven are negative, rated on a five-point Likert scale (0 = not at all/never, 1 = rarely, 2 = sometimes, 3 = quite often, and 4 = very often). Positively worded statements were reverse scored prior to analysis. All items were aggregated and the total score ranged from 0 to 56 with the understanding that the higher the score, the higher the self-perceived stress.

The four dimensions for the independent variables were as follows:

- Social support: The Duke-UNC-11 Functional Social Support Questionnaire was used to assess social support received by the participants. This self-administered instrument is composed of 11 statements, using a five-point Likert-style response scale (1 = much less than I want, 2 = less than I want, 3 = neither a lot nor a little, 4 = almost as much as I want and 5 = as much as I want). This quantitative questionnaire is made up of two dimensions: confidential social support, when people receive information, advice or guidance or can share their concerns, and affective social support, defined as expressions of appreciation,

sympathy or belonging to a group[15]. A cut-off point was established at the 32-point level, suggesting that a score lower than this refers to a low level of social support whereas a score equal to or higher than this indicates an adequate level[16].

- Sociodemographic characteristics: These include the variables age, sex, type of academic training, speciality (for those who did postgraduate studies), place of origin, number of people at home during quarantine, children and older adults under responsibility during quarantine, work, academic and domestic responsibilities during quarantine, and level of economic income during quarantine.
- Knowledge and preventive behaviour variables: These comprised the number of days in mandatory isolation, level of confinement, knowledge of someone infected with COVID-19, self-perceived level of knowledge of COVID-19 and following of preventive measures for COVID-19.
- Health variables: These are made up of the variables body mass index (BMI)[17], defined as the weight of the individual in kilograms divided by their height in metres squared (kg/m^2) (underweight = BMI ≤ 18.50, normal weight = BMI between 18.50 and 24.99, overweight = BMI between 25.00 and 29.99 and obese = BMI ≥ 30.00), as well as self-perceived level of concern about COVID-19 and self-perceived health status.

Statistical analysis

A descriptive analysis was applied for the qualitative and quantitative variables; subsequently, the normality of the distribution of the dependent variable and the other quantitative variables involved in the four dimensions was determined using a Kolmogorov-Smirnov test; additionally, a non-parametric Mann-Whitney U test was applied in the case of dichotomous variables and a Kruskal-Wallis test for polytomous variables. On the other hand, a hierarchical multiple regression was developed to establish models between the independent variables and perceived stress, according to the dimensions to be analysed. It should be noted that a logarithmic transformation was first performed for the PSS-14 because it lacked a normal distribution. The confidence level in the study was 95%, and $P < 0.05$ was considered an indicator of statistical significance in all tests. SPSS v. 25.0 (IBM, Armonk, NY, USA) was used for the analysis.

Ethics

The study was approved by the Ethics Committee of the Faculty of Dentistry of the University of Antioquia, Medellin, Colombia (Act 9-2020). In accordance with international standards for online surveys, all participants in the survey completed an informed consent form on the first page of the questionnaire and had the option of declining to participate in the study. Confidentiality was assured throughout the entire research process, in accordance with the Declaration of Helsinki and the Council for International Organizations of Medical Sciences (CIOMS) norms for health research.

Results

The mean perceived stress level of the sample was 24.59 (SD 7.46); an association was observed between perceived stress level and age, biological sex, type of academic training, speciality, place of origin, number of people at home during quarantine, having children and older adults in one's care, level of work and academic responsibilities, and level of economic income during obligatory social isolation ($P < 0.05$) (Table 1). In addition, an association was found between perceived stress level and some variables that made up each of the four established dimensions, such as social support, nutritional status, self-perceived level of concern about COVID-19, self-perceived health status, level of confinement, level of knowledge about COVID-19 and adherence to recommendations to prevent COVID-19 ($P < 0.05$) (Table 2).

A multiple linear regression analysis was performed, hierarchically ordering the dimensions and their variables in four models, obtaining an R2% value of 8.00 in Model 1 ($P < 0.001$), an R2% of 15.50 in Model 2 ($P < 0.001$), an R2% of 17.20 in Model 3 ($P < 0.001$) and an R2% of 21.20 in Model 4 ($P < 0.001$); in this last model, the change in R2% was significant ($P < 0.001$) with a constant of 40.049; in addition, significance was found in self-perception of the level of concern regarding COVID-19 (unstandardised regression coefficient (b) of 1.838, 95% confidence interval (CI) 0.887 to 2.790, $P < 0.001$), self-perceived health status (b = −2.191, 95% CI −2.944 to −1.437, $P < 0.001$), number of days in mandatory isolation (b = −0.965, 95% CI −1.908 to −0.022, $P = 0.045$), level of confinement (b = 0.923, 95% CI 0.106 to 1.740, $P = 0.027$), age (b = −1.743, 95% CI −2.625 to −0.860, $P < 0.001$), sex (b = 1.324, 95% CI 0.311 to 2.337, $P = 0.011$) and level of economic income in quarantine (b = −1.539, 95% CI −2.434 to −0.644, $P = 0.001$) (Table 3).

Table 1 Perceived stress according to sociodemographic variables (N = 1812).

Variable		n (%)	Perceived stress level (PSS-14 score)		
			Mean value	Standard deviation	*P* value
Age, y	Mean ± standard deviation	32.44 ± 11.56			
	18–24	548 (30.24)	26.59	7.34	< 0.001*
	25–34	671 (37.03)	24.99	6.98	
	≥ 35	593 (32.73)	22.30	7.50	
Sex	Male	557 (30.74)	23.36	7.32	< 0.001**
	Female	1255 (69.26)	25.14	7.46	
Type of academic training	Dental student	655 (36.15)	26.64	7.18	< 0.001**
	Dental practitioner	1157 (63.85)	23.43	7.37	
Speciality?	Yes	791 (68.37)	22.96	7.46	0.001**
	No	366 (31.63)	24.47	7.06	
Place of origin	Mexico, Central America and the Caribbean	151 (8.33)	22.99	8.13	0.003**
	South America	1661 (91.67)	24.74	7.38	
Number of people at home during social isolation	Mean ± standard deviation	3.00 (1.83)			
	≤ 3	1217 (67.20)	24.30	7.43	0.019**
	> 3	594 (32.80)	25.20	7.50	
Caring for children during social isolation?	Yes	612 (33.77)	24.63	7.44	0.958**
	No	1200 (66.23)	24.57	7.47	
Caring for older adults during social isolation?	Yes	1282 (70.75)	24.52	7.41	0.593**
	No	530 (29.25)	24.76	7.60	
Work responsibilities during social isolation	Decreased	654 (45.35)	23.43	7.58	< 0.001*
	Equal	271 (18.79)	24.28	6.74	
	Increased	517 (35.85)	25.12	7.14	
Academic responsibilities during social isolation	Decreased	363 (23.93)	24.21	7.45	0.009*
	Equal	363 (23.93)	24.19	6.91	
	Increased	791 (52.14)	25.27	7.60	
Domestic (home) responsibilities during social isolation	Decreased	18 (1.00)	25.83	5.72	0.129*
	Equal	469 (26.10)	24.11	7.75	
	Increased	1310 (72.90)	24.80	7.35	
Income level during social isolation	Decreased	1018 (68.97)	24.70	7.51	0.016*
	Equal	393 (26.63)	23.40	6.91	
	Increased	65 (4.40)	25.29	6.73	
Total		1812 (100.00)	24.59	7.46	

*Kruskal-Wallis test.

**Mann-Whitney U test.

Discussion

The provisions put in place to control the spread of COVID-19 may have a negative impact on the mental health of the population, especially where situations such as loneliness and decreased social interaction are clear risk factors for some mental disorders. In addition, the emergence and persistence of concerns about one's own and one's family's health, along with anxiety about the future, could increase the risk of mental health pathologies such as anxiety, panic, stress and obsessive-compulsive disorder[18]. Health care workers are also directly affected by work circumstances such as the considerable increase in the number of cases, shortage of human resources, excessive workload and insufficient capacity to control the spread through health systems[19].

It is important to mention that the more variables incorporated into the present model, the more explanatory it was; in addition, it is evident that social support is significant in each of the models presented. A negative association was found between social support and perceived stress in dental practitioners and students during quarantine in the COVID-19 pandemic. Similarly, studies by Mak et al[20] and Ye et al[21] indicate that both in the SARS epidemic and currently in the COVID-19 pandemic, support from relatives, friends and health care workers plays a role in the ability to cope with stressful situations and the possible development of other conditions.

In relation to social support and health workers, a study conducted on paediatricians who experienced high levels of support during COVID-19 showed lower levels of stress compared to a second group[22]. With regard to the dental profession, evidence suggests that professionals who reported an excessive workload pre-

Table 2 Perceived stress level based on social support, health status and knowledge and preventive behaviours (N = 1812).

Variable			n (%)	Perceived stress level (PSS-14 score)		
				Mean value	Standard deviation	*P* value
Social support		Low	437 (24.12)	28.60	6.44	< 0.001**
		Adequate	1375 (75.88)	23.32	7.31	
Health status	BMI	Underweight	77 (4.25)	26.88	7.88	0.001*
		Normal	1123 (61.98)	24.90	7.44	
		Overweight	495 (27.32)	23.84	7.26	
		Obese	117 (6.46)	23.32	7.71	
	Self-perceived level of concern about COVID-19	Low	943 (52.04)	23.45	7.59	< 0.001**
		High	869 (47.96)	25.83	7.11	
	Self-perceived health status	Very poor	5 (0.28)	39.60	5.86	< 0.001*
		Poor	21 (1.16)	32.90	8.22	
		Fair	261 (14.40)	27.70	7.01	
		Good	1149 (63.41)	24.43	6.99	
		Excellent	376 (20.75)	22.26	7.87	
Knowledge and preventive behaviour	Number of days in mandatory social isolation	Mean ± standard deviation	60.80 ± 25.30			
		≤ 60	1010 (55.74)	24.77	7.17	0.259**
		> 60	802 (44.26)	24.37	7.81	
	Confinement level	I did not go out any day	200 (11.04)	26.16	7.61	0.016*
		I went out very little	1441 (79.53)	24.41	7.45	
		I went out frequently	95 (5.24)	24.23	7.64	
		I went out every day	76 (4.19)	24.47	6.65	
	Knowledge of someone infected with COVID-19	Yes	846 (46.69)	24.87	7.43	0.123**
		No	966 (53.31)	24.35	7.48	
	Self-perceived level of knowledge of COVID-19	Low	1449 (79.97)	24.89	7.29	< 0.001**
		High	363 (20.03)	23.39	8.02	
	Following of preventive measures for COVID-19	Never	2 (0.11)	29.00	0.00	< 0.001*
		Rarely	6 (0.33)	23.50	9.16	
		Usually	493 (27.21)	25.68	6.64	
		Sometimes	42 (2.32)	26.81	7.53	
		Always	1269 (70.03)	24.09	7.70	

*Kruskal-Wallis test.

**Mann-Whitney U test.

sented low levels of social support; Marklund et al[23] found that work-related responsibilities are key to the development of stress; however, this can be buffered by certain strategies such as social support. They also found that the different roles in the dental profession can experience different levels of stress[23].

It is evident that stress has an impact on personal health status and vice versa, coinciding with the results of the present study in which self-perceived health status and level of concern about COVID-19 show significant differences for the association between social support and perceived stress level; likewise, León-Manco et al[24] found that poor self-reported health led to an increase in perceived stress as measured using the PSS-14. In a study of nurses, Liao et al[25] stated that both physical and mental health are affected by one's degree of perceived stress, which could be regulated by means of social support and self-efficacy, since both variables are negatively correlated with stress.

Regarding knowledge of and adoption of preventive behaviour against COVID-19, the study showed that the number of days and level of isolation were factors to be considered in the association of perceived stress and social support. On the other hand, the concern and fear of infection felt by dental practitioners relegated to emergency work revealed high levels of stress in them, particularly caused by the possibility of transmitting the infection to family members, thus causing them to self-isolate for preventive reasons[26]. A previous study detailed the consequences of quarantines on the mental

Table 3 Hierarchical multiple regression models for the perceived stress scores in the study sample (N = 1812).

Variable			Determination coefficient % (R2%)	Change of R2%
Model 1	Social support		8.00	8.00
Model 2	Social support		15.50	7.50
	Health status variables	BMI		
		Self-perceived level of concern about COVID-19		
		Self-perceived health status		
Model 3	Social support		17.20	1.60
	Health status variables	BMI		
		Self-perceived level of concern about COVID-19		
		Self-perceived health status		
	Knowledge and preventive behaviours variables	Number of days in mandatory social isolation		
		Confinement level		
		Knowledge of someone infected with COVID-19		
		Self-perceived level of knowledge of COVID-19		
		Following of preventive measures for COVID-19		
Model 4	Social support		21.20	4.00
	Health status variables	BMI		
		Self-perceived level of concern about COVID-19		
		Self-perceived health status		
	Knowledge and preventive behaviours variables	Number of days in mandatory social isolation		
		Confinement level		
		Knowledge of someone infected with COVID-19		
		Self-perceived level of knowledge of COVID-19		
		Following of preventive measures for COVID-19		
	Sociodemographic variables	Age		
		Sex		
		Type of academic training		
		Speciality		
		Place of origin		
		Number of people at home during social isolation		
		Children under care during social isolation		
		Older adults under care during social isolation		
		Work responsibilities during social isolation		
		Academic responsibilities during social isolation		
		Domestic (home) responsibilities during social isolation		
		Income level during social isolation		

health of health workers, including acute stress reactions, which also relate to isolation and a lack of contact with their family[27].

On the other hand, the sociodemographic variables age, sex and level of economic income showed significant differences between social support and stress, suggesting that the more stable these factors are, the lower the perceived level of stress is. Mekhemar et al[12] noted that female dentists aged between 50 and 59 years with chronic pathologies, who worked in a private practice and who considered the COVID-19 pandemic as a financial risk obtained higher values for conditions such as depression, stress and anxiety.

Likewise, Massad et al[28] state that sex, social support and age were associated with the level of psychological stress in a sample evaluated in Jordan; because of the first aspect, the number of cases of domestic violence increased in women due to established governmental guidelines. They also note that among the aspects to be considered in the relationship between sex and anxiety,

	P value, change of R2%	Constant	Non-standardised regression coefficient (b)	Standardised regression coefficient	95% confidence interval	*P* value	*P* value model
	< 0.001	31.806	–4.840	–0.283	–5.994 to –3.685	< 0.001	< 0.001
	< 0.001	40.015	–4.377	–0.256	–5.493 to –3.261	< 0.001	< 0.001
			–0.805	–0.078	–1.477 to –0.134	0.019	
			1.925	0.135	0.991 to 2.860	< 0.001	
			–2.424	–0.215	–3.169 to –1.679	< 0.001	
	0.011	43.066	–4.327	–0.253	–5.444 to –3.210	< 0.001	< 0.001
			–0.856	–0.083	–1.531 to –0.182	0.013	
			2.143	0.150	1.197 to 3.089	< 0.001	
			–2.340	–0.208	–3.095 to –1.586	< 0.001	
			–1.011	–0.071	–1.951 to –0.071	0.035	
			0.655	0.053	–0.165 to 1.475	0.117	
			–0.333	–0.023	–1.272 to 0.605	0.486	
			–0.411	–0.025	–1.524 to 0.702	0.469	
			–0.568	–0.067	–1.137 to 0.001	0.051	
	< 0.001	40.049	–4.527	–0.265	–5.646 to –3.408	< 0.001	< 0.001
			–0.392	–0.038	–1.089 to 0.306	0.271	
			1.838	0.129	0.887 to 2.790	< 0.001	
			–2.191	–0.194	–2.944 to –1.437	< 0.001	
			–0.965	–0.067	–1.908 to –0.022	0.045	
			0.923	0.074	0.106 to 1.740	0.027	
			–0.09	–0.006	–1.028 to 0.848	0.851	
			–0.081	–0.005	–1.189 to 1.027	0.886	
			–0.401	–0.047	–0.966 to 0.164	0.164	
			–1.743	–0.137	–2.625 to –0.860	< 0.001	< 0.001
			1.324	0.088	0.311 to 2.337	0.011	
			–1.385	–0.073	–2.158 to 0.348	0.071	
			–0.215	–0.013	–1.312 to 0.882	0.700	
			–0.466	–0.022	–1.882 to 0.950	0.518	
			0.716	0.044	–0.411 to 1.843	0.213	
			0.481	0.033	–0.530 to 1.492	0.350	
			0.368	0.023	–0.698 to 1.435	0.498	
			0.563	0.072	–0.037 to 1.162	0.066	
			–0.001	0.001	–0.641 to 0.640	0.998	
			0.692	0.040	–0.453 to 1.836	0.236	
			–1.539	–0.120	–2.434 to –0.644	0.001	

social support is important, as the more members of a social network that a person has during social isolation, the lower the degree of anxiety they experience; for age, also evaluated in the study, a correlation with stress was observed during quarantine, suggesting that older people are less likely to be affected due to their greater economic and emotional stability[28].

With regard to the limitations of the present study, the possible emergence of selection bias during the recruitment of participants, carried out through digital media such as email and social networks, is important. Likewise, the participants in the study came from various different countries in Latin America and the Caribbean, meaning that each of them had experienced different cultural, economic and health contexts during the pandemic; these could have an impact on their responses to the surveys, and consequently on the results of the study. Another aspect to consider is that due to the cross-sectional nature of the study, it is not possible to define a cause-and-effect relationship

between the variable studies; thus, the findings should not be extrapolated to the general population.

It is evident that during the COVID-19 health crisis, dental practitioners and students faced complex circumstances that had an impact on their mental health, specifically on their perceived level of stress. The support, value and sense of belonging provided by those closest to them, translated as social support, which was scarce during this time due to the promotion of individualistic behaviour to preserve collective health; all this within Latin America and the Caribbean, regions that experienced crisis situations both in the health system and at an economic level.

Conclusion

The findings of this study show that social support was a factor associated with perceived stress levels in dental students and general dental practitioners during the COVID-19 quarantine period. In addition, variables such as concern about illness, self-perceived health status, number of days and level of confinement, as well as age, sex and income level, had an impact on the findings.

Acknowledgements

The authors thank all the dental practitioners who participated in the survey.

Conflicts of interest

The authors declare no conflicts of interest related to this study.

Author contribution

Drs María Claudia Garcés-Elías, Roberto A. León-Manco and Andrés A. Agudelo-Suárez contributed to the conception, design, acquisition and interpretation of the data, critically reviewed the manuscript, gave final approval, and agreed to be accountable for all aspects of the work in ensuring accuracy and integrity.

(Received Jun 24, 2021; accepted Nov 8, 2021)

References

1. Ghafari R, Mirghafourvand M, Rouhi M, Osouli Tabrizi S. Mental health and its relationship with social support in Iranian students during the COVID-19 pandemic. BMC Psychol 2021;9:81.
2. Williams CYK, Townson AT, Kapur M, et al. Interventions to reduce social isolation and loneliness during COVID-19 physical distancing measures: A rapid systematic review. PLoS One 2021;16:e0247139.
3. Moriarty T, Bourbeau K, Fontana F, McNamara S, Pereira da Silva M. The relationship between psychological stress and healthy lifestyle behaviors during COVID-19 among students in a US midwest university. Int J Environ Res Public Health 2021;18:4752.
4. Teh WL, Shahwan S, Abdin E, et al. Confirmatory factor analysis and measurement invariance of the multidimensional scale of perceived social support in young psychiatric and non-psychiatric Asians. Ann Acad Med Singap 2019;48:314–320.
5. Babore A, Lombardi L, Viceconti ML, et al. Psychological effects of the COVID-2019 pandemic: Perceived stress and coping strategies among healthcare professionals. Psychiatry Res 2020;293:113366.
6. Mo Y, Deng L, Zhang L, et al. Work stress among Chinese nurses to support Wuhan in fighting against COVID-19 epidemic. J Nurs Manag 2020;28:1002–1009.
7. Szkody E, Stearns M, Stanhope L, McKinney C. Stress-buffering role of social support during COVID-19. Fam Process 2021;60: 1002–1015.
8. Bekele F, Mechessa DF, Sefera B. Prevalence and associated factors of the psychological impact of COVID-19 among communities, health care workers and patients in Ethiopia: A systematic review. Ann Med Surg (Lond) 2021;66:102403.
9. Zhang H, Shi Y, Jing P, Zhan P, Fang Y, Wang F. Posttraumatic stress disorder symptoms in healthcare workers after the peak of the COVID-19 outbreak: A survey of a large tertiary care hospital in Wuhan. Psychiatry Res 2020;294:113541.
10. Alnazly E, Khraisat OM, Al-Bashaireh AM, Bryant CL. Anxiety, depression, stress, fear and social support during COVID-19 pandemic among Jordanian healthcare workers. PLoS One 2021;16:e0247679.
11. Cotrin P, Moura W, Gambardela-Tkacz CM, et al. Healthcare workers in Brazil during the COVID-19 pandemic: A cross-sectional online survey. Inquiry 2020;57:46958020963711.
12. Mekhemar M, Attia S, Dörfer C, Conrad J. The psychological impact of the COVID-19 pandemic on dentists in Germany. J Clin Med 2021;10:1008.
13. Sarialioglu Gungor A, Donmez N, Uslu YS. Knowledge, stress levels, and clinical practice modifications of Turkish dentists due to COVID-19: A survey study. Braz Oral Res 2021;35:e048.
14. De la Rubia JM, de León FC. Validation of the perceived stress scale (PSS-14) in the population of registered dentists of Monterrey [in Spanish]. Anxiety and Stress 2014;20:193–209.
15. Broadhead WE, Gehlbach SH, de Gruy FV, Kaplan BH. The Duke-UNC functional social support questionnaire. Measurement of social support in family medicine patients. Med Care 1988;26:709–723.
16. Bellón Saameño JA, Delgado Sánchez A, Luna del Castillo JD, Lardelli Claret P. Validity and reliability of the Duke-UNC-11 questionnaire of functional social support [in Spanish]. Aten Primaria 1996;18:153–156, 158-163.
17. World Health Organization. Body mass index – BMI. https://www.euro.who.int/en/health-topics/disease-prevention/nutrition/a-healthy-lifestyle/body-mass-index-bmi. Accessed 10 June 2021.
18. Fiorillo A, Gorwood P. The consequences of the COVID-19 pandemic on mental health and implications for clinical practice. Eur Psychiatry 2020;63:e32.
19. Shah K, Chaudhari G, Kamrai D, Lail A, Patel RS. How essential is to focus on physician's health and burnout in coronavirus (COVID-19) pandemic? Cureus 2020;12:e7538.
20. Mak WWS, Law RW, Woo J, Cheung FM, Lee D. Social support and psychological adjustment to SARS: The mediating role of self-care self-efficacy. Psychol Health 2009;24:161–174.

21. Ye Z, Yang X, Zeng C, et al. Resilience, social support, and coping as mediators between COVID-19-related stressful experiences and acute stress disorder among college students in China. Appl Psychol Health Well Being 2020;12:1074–1094.
22. Di Filippo P, Attanasi M, Dodi G, et al. Evaluation of sleep quality and anxiety in Italian pediatric healthcare workers during the first wave of COVID-19 pandemic. BMC Res Notes 2021;14:219.
23. Marklund S, Huang K, Zohouri D, Wahlström J. Dentists working conditions – Factors associated with perceived workload. Acta Odontol Scand 2021;79:296–301.
24. León-Manco RA, Agudelo-Suárez AA, Armas-Vega A, et al. Perceived stress in dentists and dental students of Latin America and the Caribbean during the mandatory social isolation measures for the COVID-19 pandemic: A cross-sectional study. Int J Environ Res Public Health 2021;18:5889.
25. Liao C, Guo L, Zhang C, et al. Emergency stress management among nurses: A lesson from the COVID-19 outbreak in China – A cross-sectional study. J Clin Nurs 2021;30:433–442.
26. Consolo U, Bellini P, Bencivenni D, Iani C, Checchi V. Epidemiological aspects and psychological reactions to COVID-19 of dental practitioners in the Northern Italy districts of Modena and Reggio Emilia. Int J Environ Res Public Health 2020;17:3459.
27. Torales J, O'Higgins M, Castaldelli-Maia JM, Ventriglio A. The outbreak of COVID-19 coronavirus and its impact on global mental health. Int J Soc Psychiatry 2020;66:317–320.
28. Massad I, Al-Taher R, Massad F, Al-Sabbagh MQ, Haddad M, Abufaraj M. The impact of the COVID-19 pandemic on mental health: Early quarantine-related anxiety and its correlates among Jordanians. East Mediterr Health J 2020;26:1165–1172.

EXPERT DEFINITIVE GUIDE

NEW

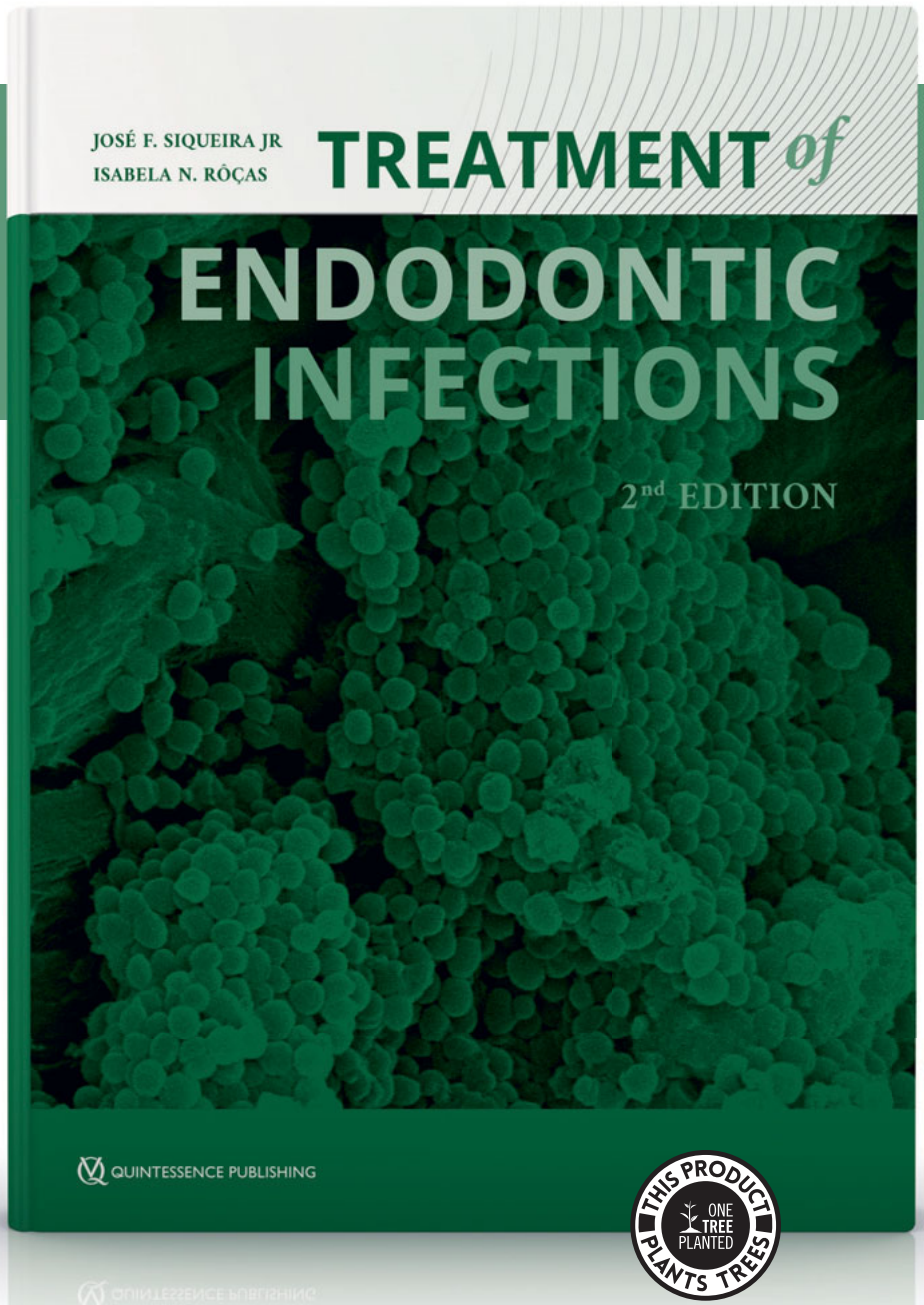

José F. Siqueira Jr | Isabela N. Rôças

Treatment of Endodontic Infections

576 pages, 717 illus
ISBN 978-1-78698-112-7
€198

Apical periodontitis is one of the most common inflammatory diseases that affect humans and is caused by microbial infection of the dental root canal system. A thorough understanding of the etiology and pathogenesis of apical periodontitis is essential for high-quality endodontic practice based on a solid scientific foundation. The first section of this book deals with microbiologic and pathophysiologic aspects of the different manifestations of apical periodontitis, while the second section describes the best evidence for predictable treatment and prevention of the disease. Clinical techniques and protocols to treat endodontic infections are described in detail. This new edition boasts a team of renowned authorities in the field that contribute state-of-the-art evidence about the biology and practice of the endodontic treatment of teeth with infected root canals. The content is supplemented with numerous full-color illustrations and radiographs. This book is a definitive guide to those involved with the prevention and treatment of endodontic infections.

www.quint.link/
endodontic-infections

books@quintessenz.de

+49 (0)30 761 80 667

QUINTESSENCE PUBLISHING

Scanning Accuracy of 10 Intraoral Scanners for Single-crown and Three-unit Fixed Denture Preparations: An In Vitro Study

Xin Yue ZHANG[1,2#], Yue CAO[1,2,3#], Zhe Wen HU[1,4], Yong WANG[1,2], Hu CHEN[1,2], Yu Chun SUN[1,2]

Objective: *To evaluate the accuracy of 10 intraoral scanners for single-crown and three-unit preparation models.*

Methods: *A maxillary partially edentulous model was fabricated. A dental cast scanner was used to obtain standard tessellation language (STL) data. Ten intraoral scanners, namely Trios 2 (TR2; 3Shape, Copenhagen, Denmark), True Definition (TD; 3M, Saint Paul, MN, USA), CEREC AC Omnicam (OM; Dentsply Sirona, Charlotte, NC, USA), Organical Scan Oral (OS; R+K, Berlin, Germany), PlanScan (PS; Planmeca, Helsinki, Finland), DWIOP (DW; Dental Wings, Montreal, Canada), Xianlin (XL; Hangzhou Xianlin, Hangzhou, China), DL-100 (DL; Guangzhou Longcheng, Guangzhou, China), Trios 3 (TR3; 3Shape) and i500 (MD; MEDIT, Seoul, South Korea) were used to obtain stereolithography data as test groups. Trueness, precision and surface accuracy were evaluated by deviation analysis using 3D image processing software. One tooth with a three-unit preparation for each test group was registered with the reference scan data, and the absolute distance from another tooth was calculated as the absolute accuracy. The data were analysed using a Mann-Whitney U test and Dunn-Bonferroni test ($\alpha = 0.05$).*

Results: *The best trueness, precision and surface accuracy of scanning single crown preparation were recorded with TD (trueness 2.9 μm and precision 1.9 μm) and XL (surface accuracy 20.3 ± 2.9 μm). The best trueness, precision, surface accuracy and absolute accuracy of three-unit preparations were recorded with TD (2.6 μm), XL (1.9 μm), OM (27.1 ± 5.2 μm) and TR3 (79.2 ± 19.6 μm), respectively. There was no statistically significant difference in trueness between single- and multiple-unit preparations for any of the intraoral scanners ($P > 0.05$). A statistically significant difference in the surface accuracy between single and multiple preparations was found for TR2, TD, OM, DW, XL, DL and MD ($P < 0.05$).*

Conclusion: *The trueness and precision of intraoral scanners for scanning three-unit preparations were nearly the same as those for single-crown preparations; however, with the exception of OS, PS and TR3, the surface accuracy of single-crown preparations was significantly better than that for three-unit preparations.*

Key words: *intraoral scanner, scanning accuracy, single crown preparation, surface accuracy, three-unit fixed denture preparation*

Chin J Dent Res 2022;25(3):215–222; doi: 10.3290/j.cjdr.b3317959

1 Centre of Digital Dentistry, Peking University School and Hospital of Stomatology, National Engineering Research Centre of Oral Biomaterials and Digital Medical Devices, NHC Key Laboratory of Digital technology of stomatology, Beijing Key Laboratory of Digital Stomatology, National Clinical Research Centre for Oral Diseases, Beijing, P.R. China.

2 Department of Prosthodontics, Peking University School and Hospital of Stomatology, Beijing, P.R. China.

3 Institute for Clinical Research and Application of Sunny Dental, Beijing, P.R. China.

4 Department of VIP dental service, Peking University School and Hospital of Stomatology, Beijing, P.R. China.

# These two authors contributed equally to this work.

Corresponding authors: Dr Hu CHEN and Dr Yu Chun SUN, Centre of Digital Dentistry, Department of Prosthodontics, Peking University School and Hospital of Stomatology, #22 Zhongguancun South Avenue, Haidian District, Beijing 100081, P.R. China. Tel: 86-10-82195379. Email: ccen@bjmu.edu.cn; kqsyc@bjmu.edu.cn.

This work was supported by the Capital Science and Technology Leading Talent Project (grant no. Z191100006119022); National Key R&D Programme of China (grant no. 2018YFB1107200); Joint Fund of Ministry of Education of China for Equipment Preresearch (grant no. 6141A0202604); the Capital's Funds for Health Improvement and Research (grant no. 2018-2-4103); Programme for New Clinical Techniques; Therapies of Peking University School and Hospital of Stomatology (grant no. PKUSSNCT-18G01) and PKU-Baidu Fund (grant no. 2019BD021).

Fig 1 Multi-angle images of the partially edentulous maxillary model. The model can be regarded as eight single-crown preparations or six three-unit fixed denture preparations. (Single crown preparation: the left and right central incisors, canine, second premolar and second molar were abutment preparations; three-unit fixed denture preparation: left and right second molar and second premolar, second premolar and canine, canine and central incisor preparations.)

Digital dental technology has recently gained considerable popularity and is being incorporated into the workflow for fixed prosthodontics. The quality and accuracy of scanning data are crucial to digital dental restorations. Compared with dental cast scanners, intraoral scanners need to be placed in the patient's mouth. The range of scanning focal length is limited by the structure of the scanning head and the adjacent teeth. The scanning blind zone decreases the scanning quality, and the number of images stitched together is much greater than that for dental cast scanners, which increases the number of data processing errors.

Evaluation of the accuracy of intraoral scanners is often carried out using the scan data from the model scanner[1-3]. Previous related studies have often obtained trueness and precision by taking multiple scans of measured objects[4-9]. Accuracy consists of both precision and trueness; however, the trueness can only reflect the consistency of the scan data and the overall size of the scanned object but cannot reflect the consistency of the surface morphology. The consistency of the surface morphology is critical for accurate matching between the oral prosthesis and the remaining oral tissue, such as the fitness of the outer margin of the full crown preparation shoulder and the corresponding area of the zirconia full crown margin. In the present study, scanning accuracy was evaluated using three indexes: trueness, precision and surface accuracy. Trueness refers to the degree of agreement between the mean and reference values obtained from many test results, indicating the systematic error of the measurement results; precision refers to the degree of agreement between independent test results under specified conditions, indicating the random error of the measurement process[9,10]; and surface accuracy refers to the degree of coincidence of the scanned data points with the surface morphology of the scanned object.

The present study sought to measure the scanning trueness, precision, surface accuracy and other indexes to evaluate the accuracy of 10 intraoral scanners for scanning single-crown preparations and three-unit fixed denture preparation models, ignoring the impact of the oral environment, to provide a reference for relevant research into evaluation criteria and clinical application.

Materials and methods

Experimental materials, equipment and software

A maxillary standard dentition plaster model (Stone, Heraeus Kulzer, Hanau, Germany) was selected to pre-

Table 1 Characteristics of scanners used in the study.

Scanner type	Model	Manufacturer	Software	Country	Imaging principle
Intraoral	Trios 2	3Shape	1.3.4.3	Denmark	Confocal microscopy
Intraoral	True Definition	3M	4.2.1	United States	Active wavefront sampling
Intraoral	CEREC AC Omnicam	Dentsply Sirona	Cerec SW 4.4.1	Germany	Triangulation
Intraoral	Organical Scan Oral	R+K	Exocad DentalDB 2012.12	Germany	Confocal microscopy
Intraoral	PlanScan	Planmeca	4.1.1.0	Finland	Triangulation
Intraoral	DWIOP	Dental Wings	1.8.0.038	Canada	Triangulation
Intraoral	Xianlin	Hangzhou Xianlin	V1.1.2	China	Triangulation
Intraoral	DL-100	Guangzhou Longcheng	V1.1.3	China	Triangulation
Intraoral	Trios 3	3Shape	1.4.7.5	Denmark	Confocal microscopy
Intraoral	i500	MEDIT	2.0.3	South Korea	Triangulation
Dental cast	Activity880	Smart Optics	2.6	Germany	Triangulation

pare the partially edentulous maxillary model; the left and right lateral incisors, first premolars and first molars were missing and the left and right central incisors, canines, second premolars and second molars were abutment preparations. A dental cast scanner (10 μm; Activity 880, SmartOptics, Bochum, Germany) was used to obtain standard tessellation language (STL) data for the model, and computer-aided design (CAD) software (Dental System 2013, 3Shape, Copenhagen, Denmark) was used to design the prototype, which was then printed using a high precision resin printer (VisiJet SL e-Stone, Projet 6000, 3D Systems, Rock Hill, SC, USA) to obtain a reference model (Fig 1). The 10 intraoral scanners used, namely Trios 2 (TR2), True Definition (TD), CEREC AC Omnicam (OM), Organical Scan Oral (OS), PlanScan (PS), DWIOP(DW), Xianlin (XL), DL-100 (DL), Trios 3 (TR3) and i500 (MD), and the dental cast scanner used in the study, are listed in Table 1.

Research methods

Obtain the STL scan data of the partially edentulous maxillary model

The dental cast scanner was used once to obtain STL data as a reference scan, then 10 intraoral scanners were used three times to obtain STL data for test groups by the same trained experimenter who was skilled in use of all the intraoral scanners, under the same experimental environment. The scanning path of the scanning head was a single optical path, that is, it scanned the occlusal surface first and then the lingual side to the buccal side.

Evaluation of scanning accuracy

With regard to trueness and precision, in Geomagic Studio 2013 software (3D Systems), the authors selected the surface of each preparation as a common area and registered the scan data with the reference data using the best-fit alignment command. The deviation analysis of the command was used to obtain the mean distance (Formula a), analysing the deviation of every point between the test group and reference group. The average value for mean distance (absolute value) was calculated as trueness for scanning single-crown preparations and three-unit fixed denture preparations (Formula b), and the standard deviation of the trueness per group was calculated as precision (Formula c).

$$md = \frac{\sum_{i=1}^{n} x_i - x_{i-actual}}{n} \quad \text{a}$$

$$tr = \frac{\sum_{i=1}^{m} |md_i|}{m} \quad \text{b}$$

$$pr = \sqrt{\sum_{i=1}^{m} \frac{(|md_i| - tr)^2}{m}} \quad \text{c}$$

m, number of subjects; md, mean distance; n, number of points of subjects; pr, precision; tr, trueness; x_i, test value; $x_{i\text{-actual}}$, reference value.

Surface accuracy

In Geomagic Studio, we used the deviation analysis of the software command to calculate the root mean square (RMS) (Formula d) and calculated the mean value and

standard deviation (SD) of the RMS to obtain surface accuracy (Formulae e and f).

$$RMS = \sqrt{\sum_{i=1}^{n} \frac{(x_i - x_{i-actual})^2}{n}} \quad \text{d}$$

$$sa_{av} = \frac{\sum_{i=1}^{m} RMS_i}{m} \quad \text{e}$$

$$sa_{sd} = \sqrt{\sum_{i=1}^{m} \frac{(RMS_i - sa_{av})^2}{m}} \quad \text{f}$$

m, number of subjects; n, number of points of subjects; $s\alpha_{av}$, average value of surface accuracy;$s\alpha_{sd}$, standard deviation of surface accuracy; x_i, test value; $x_{i\text{-actual}}$, reference value.

Absolute accuracy

The left second molar was selected as the common area, each test group was superimposed over the reference scan data and deviation analysis was performed using the best-fit method. We calculated the distance of the occlusal surface, mesial surface, distal surface, buccal side and lingual side of the left second premolar in the test group from the reference scan data and obtained five distances for each tooth preparation. The offset distance of the faces was the absolute accuracy of scanning three-unit fixed denture preparations.

Statistical methods

A Shapiro-Wilk normality test was performed, and some data were abnormally distributed. A Dunn-Bonferroni test was used to compare ten groups in pairs. Statistical differences between the accuracy indexes of the single-crown preparation and the three-unit fixed denture preparation of 10 scanners were analysed using an independent samples Mann-Whitney U test. Statistical analyses were conducted using SPSS (v20.0; IBM, Armonk, NY, USA) ($\alpha = 0.05$).

Results

The representative deviation patterns of single-crown preparations and three-unit fixed denture preparations are presented in Figs 2 and 3. The colour distribution showed the positive and negative distribution of deviation; green represents the area with a small amount of deviation, red represents positive deviation and blue represents negative deviation. The overall deviation of the 10 scanners was relatively small, but OS showed a greater negative deviation of the occlusal surface of the posterior teeth and the lingual fossa of the anterior teeth. It also showed greater positive deviation of the incisal end of the anterior teeth and the cusp of the posterior teeth. Negative deviations may cause the manufactured restorations to not fit properly on the preparation, and positive deviations may lead to poor retention of the restorations.

An overview of the results and statistics is presented in Tables 2 to 4. The trueness of 10 scanners for scanning single-crown preparations ranged from 2.9 to 24.7 μm, precision ranged from 1.9 to 18.4 μm and surface accuracy ranged from 22.0 ± 5.0 μm to 89.3 ± 58.3 μm. The trueness of scanning three-unit fixed denture preparations ranged from 2.6 to 19.2 μm, precision ranged from 1.9 to 15.1 μm and surface accuracy ranged from 27.1 ± 5.2 μm to 102.6 ± 41.6 μm. TD showed the best trueness for scanning single-crown preparations and three-unit fixed denture preparations, TD and XL showed the best precision and TD showed the best accuracy in general. OS displayed the worst surface accuracy but was clinically acceptable. Absolute accuracy ranged from 79.2 ± 19.6 μm to 333.9 ± 68.7 μm. Absolute accuracy of scanning three-unit fixed denture preparations for PS and DW was over 300 μm, showing that the suitability of the outer margin of the full crown preparation may beyond the tolerance range.

The Dunn-Bonferroni test results showed that OS was significantly worse than the other groups in terms of mean distance for scanning single-crown and three-unit fixed denture preparations ($P < 0.05$). XL was significantly better than the other groups except for TD and OM, whereas OS and PS were significant worse than the others in terms of surface accuracy for scanning single-crown preparations ($P < 0.05$). TR3 was significantly better than TR2, OS, PS and DL, whereas OS was significantly worse than the other groups in surface accuracy for scanning three-unit fixed denture preparations ($P < 0.05$). TR3 performed significantly better than the other groups except for MD, whereas PS and DW were significantly worse than the other groups in absolute accuracy for scanning three-unit fixed denture preparations ($P < 0.05$). Statistical analysis showed that there was no significant difference in trueness between single-crown preparations and three-unit fixed denture preparations in any of the intraoral scanners ($P > 0.05$). For surface accuracy between the single-crown preparation and the three-unit fixed denture preparation, the differences for TR2, TD, OM, DW, XL, DL and MD were statistically significant ($P < 0.05$).

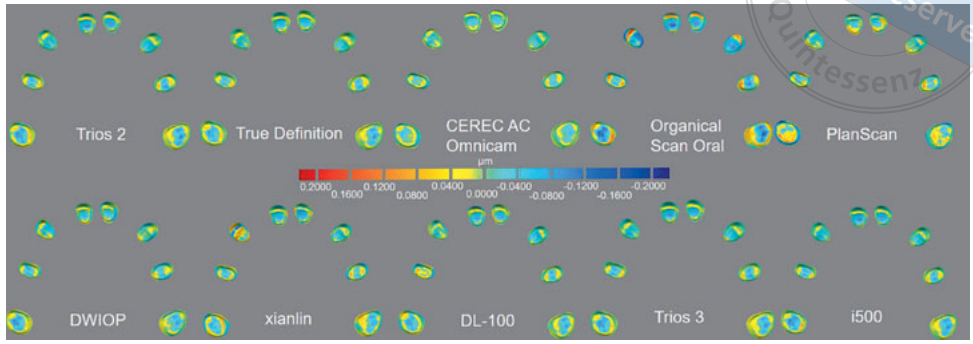

Fig 2 Colour-coded deviation maps of single-crown preparation. The range of deviation is colour-coded from –200 mm (blue) to 200 mm (red).

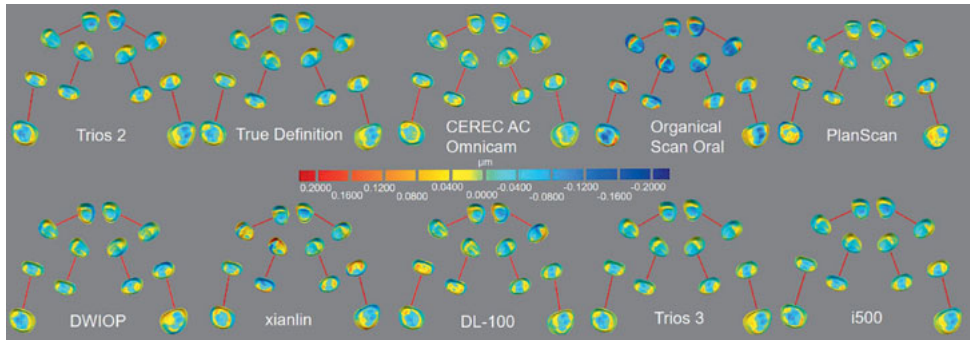

Fig 3 Colour-coded deviation maps of three-unit fixed denture preparation. The range of deviation is colour-coded from –200 mm (blue) to 200 mm (red).

Table 2 Accuracy indexes for scanning single-crown preparations and three-unit fixed denture preparations (micron).

Group		TR2	TD	OM	OS	PS	DW	XL	DL	TR3	MD
Intraoral scanner		Trios 2	True Definiton	CEREC AC Omnicam	Organical Scan Oral	PlanScan	DWIOP	Xianlin	DL-100	Trios 3	i500
Single-crown	Trueness (n = 24)	4.4	2.9	4.1	24.7	10.8	4.3	4.1	5.2	5.7	7.4
	Precision (n = 24)	2.2	1.9	2.0	18.4	9.5	2.9	3.2	4.2	3.9	5.8
	Surface accuracy (n = 24)	25.7 ± 4.2	22.0 ± 5.0	22.3 ± 3.4	89.3 ± 58.3	40.8 ± 9.9	24.8 ± 0.4	20.3 ± 2.9	36.4 ± 39.5	24.7 ± 4.2	24.9 ± 4.0
Three-unit fixed denture	Trueness (n = 18)	4.3	2.6	3.6	19.2	6.8	3.7	3.0	3.4	4.8	5.6
	Precision (n = 18)	2.2	2.0	2.2	15.1	7.5	2.8	1.9	2.1	3.4	4.3
	Surface accuracy (n = 18)	36.8 ± 8.0	31.3 ± 9.3	27.1 ± 5.2	102.6 ± 41.6	46.1 ± 12.3	31.0 ± 7.1	44.1 ± 25.2	37.8 ± 20.4	27.8± 4.8	31.0 ± 5.0
	Absolute accuracy (n = 15)	200.7 ± 34.6	176.6 ± 49.3	135.7 ± 26.1	182.4 ± 63.9	316.5 ± 19.9	333.9 ± 68.7	131.8 ± 29.1	164.1 ± 32.8	79.2 ± 19.6	101.4 ± 41.4

Discussion

The existing intraoral scanning technology is mainly a non-contact measurement method, and the main working principles include confocal microscopy, active wavefront sampling, triangulation, laser-based visual and optical coherence tomography technology[11-13]. This study involved three scanning principles: confocal microscopy for TR2, OS and TR3, active wavefront sampling for TD and triangulation for OM, PS, DW, XL, DL and MD. No common law between scanning principle and accuracy was found; OS performed worse than the other two scanners with the same scanning principle. The nominal scanning accuracy and evaluation methods given by different manufacturers are different. This study evaluated the accuracy of the scanners from single-crown and three-unit fixed denture preparations to the local microscopic data points, providing a more objective evaluation for clinical use. The trueness values were all smaller than those for surface accuracy. This was because when calculating trueness, the mean deviation between the test group and the reference group was positive or negative, causing a certain positive and negative offset.

The results of the statistical analysis showed that there was no statistically significant difference in the

Table 3 A Dunn-Bonferroni test examined the differences among the ten groups. The first value for each group is the *P* value of mean distance for scanning single-crown preparations, the second is the *P* value of surface accuracy for scanning single-crown preparations, the third is the *P* value of mean distance for scanning three-unit fixed denture preparations, the fourth is the *P* value of surface accuracy for scanning three-unit fixed denture preparations and the last is the *P* value of absolute accuracy for scanning three-unit fixed denture preparations.

Group	TR2	TD	OM	OS	PS	DW	XL	DL	TR3
TD	0.071, 0.009*, 0.037*, 0.056, 0.336								
OM	0.720, 0.015*, 0.336, 0.001*, 0.000*	0.148, 0.870, 0.259, 0.207, 0.123							
OS	0.000*, 0.000*, 0.001*, 0.000*, 0.365	0.000*, 0.000*, 0.000*, 0.000*, 0.955	0.000*, 0.000*, 0.000*, 0.000*, 0.110						
PS	0.055, 0.000*, 0.873, 0.170, 0.017*	0.000*, 0.000*, 0.054, 0.001*, 0.001*	0.023*, 0.000*, 0.423, 0.000*, 0.000*	0.001*, 0.225, 0.000*, 0.027*, 0.001*					
DW	0.633, 0.563. 0.352. 0.051, 0.011*	0.184, 0.044*, 0.247, 0.968, 0.000*	0.905, 0.064, 0.976, 2.222, 0.000*	0.000*, 0.000*, 0.000*, 0.000*, 0.001*	0.017*, 0.000*, 0.441, 0.001*, 0.876				
XL	0.427, 0.000*, 0.117, 0.285, 0.006*	0.312, 0.292, 0.603, 0.398, 0.074	0.663, 0.223, 0.543, 0.035*, 0.807	0.000*, 0.000*, 0.000*, 0.000*, 0.065	0.007*, 0.000*, 0.159, 0.015*, 0.000*	0.752, 0.002*, 0.523, 0.376, 0.000*			
DL	0.974, 0.565, 0.280, 0.409, 0.157	0.076, 0.002*, 0.313, 0.276, 0.651	0.744, 0.003*, 0.906, 0.019*, 0.275	0.000*, 0.000*, 0.000*, 0.000*, 0.508	0.051, 0.001*, 0.358, 0.028*, 0.000*	0.656, 0.249, 0.882, 0.259, 0.000*	0.446, 0.000*, 0.625, 0.807, 0.182		
TR3	0.653, 0.466, 0.880, 0.003*, 0.000*	0.024*, 0.062, 0.053, 0.296, 0.000*	0.419, 0.089, 0.417, 0.828, 0.012*	0.000*, 0.000*, 0.000*, 0.000*, 0.000*, 0.000*	0.143, 0.000*, 0.992, 0.000*, 0.000*	0.353, 0.879, 0.435, 0.315, 0.000*	0.213, 0.002*, 0.156, 0.059, 0.024*	0.630, 0.192, 0.353, 0.033*, 0.000*	
MD	0.325, 0.530, 0.863, 0.086, 0.000*	0.005*, 0.049*, 0.024*, 0.843, 0.002*	0.179, 0.072, 0.257, 0.144, 0.117	0.000*, 0.000*, 0.002*, 0.000*, 0.006*	0.352, 0.000*, 0.739, 0.002*, 0.000*	0.144, 0.960, 0.270, 0.812, 0.000*	0.075, 0.000*, 0.082, 0.518, 0.186	0.309, 0.229, 0.210, 0.373, 0.008*	0.593, 0.919, 0.747, 0.214, 0.347

*$P < 0.05$.

mean distance for scanning single-crown preparation and three-unit fixed denture preparations with 10 scanners. This indicates that the trueness and precision of 10 scanners can reach the same level as scanning a single crown when scanning a three-unit fixed denture preparation.

The numerical comparison showed that the surface accuracy of three-unit fixed denture preparations was

Table 4 A Mann-Whitney U test was used to examine the differences between the accuracy indexes of 10 scanners between scanning single-crown preparations and three-unit fixed denture preparations.

	TR2	TD	OM	OS	PS	DW	XL	DL	TR3	MD
Mean distance	$Z = -0.165$, $P > 0.05$	$Z = -0.611$, $P > 0.05$	$Z = -0.776$, $P > 0.05$	$Z = -1.207$, $P > 0.05$	$Z = -1.627$, $P > 0.05$	$Z = -0.496$, $P > 0.05$	$Z = -0.789$, $P > 0.05$	$Z = -1.106$, $P > 0.05$	$Z = -0.572$, $P > 0.05$	$Z = -0.559$, $P > 0.05$
Surface accuracy	$Z = -4.500$, $P < 0.05$	$Z = -3.482$, $P < 0.05$	$Z = -2.899$, $P < 0.05$	$Z = -1.906$, $P > 0.05$	$Z = -1.081$, $P > 0.05$	$Z = -3.102$, $P < 0.05$	$Z = -4.844$, $P < 0.05$	$Z = -2.631$, $P < 0.05$	$Z = -1.691$, $P > 0.05$	$Z = -3.750$, $P < 0.05$

Mean distance denotes the mean distance when scanning the single-crown preparation and the 3-unit fixed denture preparation; surface accuracy denotes the surface accuracy when scanning the single-crown preparation and the three-unit fixed denture preparation.

larger than single-crown preparations. The differences between groups were statistically significant except for OS, PS and TR3. The calculation method for surface accuracy avoids the offset of the scanning errors of the two abutments, indicating that the surface accuracy of the fixed bridge was inferior to that of the single crown, which explains that surface accuracy is more representative for the measurement of the overall surface morphology.

At present, there is no uniform international standard for the evaluation of the accuracy of intraoral scanners. To avoid the interference of intraoral factors, the accuracy studies are usually performed in vitro[2,6,8,14-16]. Previous accuracy studies often used repeated measurements to obtain systematic and random errors but ignored the floating degree of point cloud data relative to real data in a single scan[2,8,15], which was the surface accuracy proposed in the present study. This is especially important for the suitability of all digital restorations based on this data (e.g., undercut area, shoulder margin). Thus, in the previous study, we evaluated two intraoral scanners and proposed the concept and evaluation method of trueness of the scanner and precision of the scanned data[3] and evaluated the data of the scanned single-crown preparation. In the present study, the same method was used to evaluate the trueness and precision of scanning the single-crown preparation and the three-unit fixed denture preparation with 10 intraoral scanners. At the same time, the concept of surface accuracy was proposed to represent the degree of consistency between the scanned data points and the surface morphology of the scanned object. For fixed dentures, in addition to the aforementioned accuracy indexes, absolute accuracy is closely related to clinical suitability, that is, the suitability between the fixed retainer and the preparation after the fixed denture has been fully seated on the one-sided abutment. It is closely related to inaccuracies such as warping that often occurs when clinical fixed dentures are in place. Thus, it is also one of the indicators of this study.

The results showed that the deviation of absolute accuracy in the 10 intraoral scanners was higher than the surface accuracy. This was because surface accuracy considered the three-unit fixed denture preparation as a whole and there was an overall error cancellation phenomenon in the deviation analysis, whereas the absolute accuracy was based on one of the three-unit fixed denture preparations as the reference, and the mean distance of the other preparation from the reference group, therefore there was no error cancellation.

Conclusion

This study proved that 10 scanners can scan single-crown preparations and three-unit fixed denture preparations successfully and reach clinical requirements. TD, TR2, XL, TR3 and OM showed good scanning accuracy, but OS and PS performed poorly. This study initially explored the accuracy evaluation methods of 10 intraoral scanners scanning single-crown and three-unit fixed denture preparations. In future studies, more units of preparation should be evaluated to explore the maximum unit span to meet clinical needs. The accuracy indicators of this study can correspond to different types of clinical significance and guide the clinical selection of appropriate scanning equipment to meet clinical needs.

Conflicts of interest

The authors declare no conflicts of interest related to this study.

Author contribution

Dr Xin Yue ZHANG contributed to the experiments, study design, data analyses and manuscript writing; Dr Yue CAO contributed to the data analyses, visualisation and manuscript writing; Dr Zhe Wen HU contributed to the data analyses and conceptualisation; Dr Hu CHEN and Prof Yu Chun SUN contributed to the study

design, manuscript revision and editing. All the authors reviewed the manuscript.

(Received April 01, 2021; accepted Nov 08, 2021)

References

1. Boeddinghaus M, Breloer ES, Rehmann P, Wöstmann B. Accuracy of single-tooth restorations based on intraoral digital and conventional impressions in patients. Clin Oral Investig 2015;19:2027–2034.
2. Ender A, Mehl A. Full arch scans: Conventional versus digital impressions--An in-vitro study. Int J Comput Dent 2011;14:11–21.
3. Zhang XY, Li H, Zhao YJ, Wang Y, Sun YC. Evaluation of the quality of three-dimensional data acquired by using two kinds of structure light intra-oral scanner to scan the crown preparation model [in Chinese]. Zhonghua Kou Qiang Yi Xue Za Zhi 2016;51:432–436.
4. Patzelt SB, Vonau S, Stampf S, Att W. Assessing the feasibility and accuracy of digitizing edentulous jaws. J Am Dent Assoc 2013;144:914–920.
5. Carbajal Mejía JB, Wakabayashi K, Nakamura T, Yatani H. Influence of abutment tooth geometry on the accuracy of conventional and digital methods of obtaining dental impressions. J Prosthet Dent 2017;118:392–399.
6. Nedelcu RG, Persson AS. Scanning accuracy and precision in 4 intraoral scanners: An in vitro comparison based on 3-dimensional analysis. J Prosthet Dent 2014;112:1461–1471.
7. Song Y, Sun YC, Zhao YJ, Wang Y, Lv PJ. Quantitative evaluation for the accuracy of dental model three-dimensional scanner [in Chinese]. Beijing Da Xue Xue Bao Yi Xue Ban 2013;45:140–144.
8. Ender A, Mehl A. Accuracy of complete-arch dental impressions: a new method of measuring trueness and precision. J Prosthet Dent 2013;109:121–128.
9. Marghalani A, Weber HP, Finkelman M, Kudara Y, El Rafie K, Papaspyridakos P. Digital versus conventional implant impressions for partially edentulous arches: An evaluation of accuracy. J Prosthet Dent 2018;119:574–579.
10. International Organization for Standardization. ISO-5725-1. Accuracy (trueness and precision) of measurement methods and results. Part 1: General principles and definitions. 1994-12. http://www.iso.org/iso/store.htm. Accessed 8 November 2021.
11. Güth JF, Keul C, Stimmelmayr M, Beuer F, Edelhoff D. Accuracy of digital models obtained by direct and indirect data capturing. Clin Oral Investig 2013;17:1201–1208.
12. Kravitz ND, Groth C, Jones PE, Graham JW, Redmond WR. Intraoral digital scanners. J Clin Orthod 2014;48:337–347.
13. Mörmann WH. The evolution of the CEREC system. J Am Dent Assoc 2006;137 suppl:7S–13S.
14. Ender A, Mehl A. Influence of scanning strategies on the accuracy of digital intraoral scanning systems. Int J Comput Dent 2013;16:11–21.
15. Kim RJ, Park JM, Shim JS. Accuracy of 9 intraoral scanners for complete-arch image acquisition: A qualitative and quantitative evaluation. J Prosthet Dent 2018;120:895-903.e1.
16. Hayama H, Fueki K, Wadachi J, Wakabayashi N. Trueness and precision of digital impressions obtained using an intraoral scanner with different head size in the partially edentulous mandible. J Prosthodont Res 2018;62:347–352.

Comparison of the Relationship between Temporomandibular Disorder and Oral Habits or Quality of Life in Dentistry Students in Different Years of Education

Ravza ERASLAN[1], Taner OZTURK[2]

Objective: *To evaluate the prevalence of temporomandibular disorder (TMD) in dental faculty students in different years of education and investigate the relationship between TMD and oral habits or quality of life.*
Methods: *The Fonseca Anamnestic Index (FAI) questionnaire was used to determine the prevalence and severity of TMD, the Oral Behaviors Checklist (OBC) questionnaire served to determine the severity of harmful oral habits/parafunctions and the Oral Health Impact Profile-14 (OHIP-14) questionnaire was used to evaluate the quality of life in a total of 452 dentistry students (269 women and 183 men) in different years of education.*
Results: *With regard to incidence of TMD, a total of 215 women had TMD (215/269, 79.9%), which was significantly higher than that in men (87/183, 47.5%) ($P < 0.001$). According to the OBC and OHIP-14 questionnaire results, harmful oral habits and quality of life showed a low to moderately significant correlation with TMD ($P < 0.05$).*
Conclusion: *The Fonseca, OHIP-14 and OBC questionnaires allow early and inexpensive determination of oral habits that increase the prevalence of TMD. The prevalence of TMD in dentistry students at the clinical education stage is higher than those who have not progressed to the clinical education stage.*

Key words: *Fonseca questionnaire, oral behaviours checklist, oral health impact profile-14, temporomandibular disorder*
Chin J Dent Res 2022;25(3):223–232; doi: 10.3290/j.cjdr.b3317985

The temporomandibular joint (TMJ) is a part of the chewing system, which fulfils important functions such as chewing, speaking, swallowing, tasting and breathing[1]. The TMJ is anatomically and biomechanically different from other movable joints in the body. It is the only movable joint among those that make up the head and neck system. The TMJ is located between the hood of the mandible of the mandibular condyle and the mandibular fossa of the temporal bone and consists of the condyle in the lower jawbone, the mandibular fossa in the temporal bone, and the joint disc that separates these two bone surfaces from each other[2,3].

Although there are several definitions of TMJ dysfunction, or temporomandibular disorder (TMD), it is commonly expressed as a combination of problems related to the masticatory muscles, the TMJ and related structures[2,4-6]. Malocclusion, trauma, bruxism, parafunctional habits, pathophysiology of the masticatory

1 Department of Prosthodontics, Faculty of Dentistry, Erciyes University, Kayseri, Türkiye.
2 Department of Orthodontics, Faculty of Dentistry, Erciyes University, Kayseri, Türkiye.

Corresponding author: Dr Taner OZTURK, Department of Orthodontics, Faculty of Dentistry, Erciyes University, 38039, Kayseri, Türkiye. Tel: 90-533-168-04-66; Fax: 90-352-428-06-57. Email: tanertr35@gmail.com

muscles, emotional stress, psychosocial factors, age and sex are implicated in the aetiologies of TMD[4-10].

Symptoms indicative of TMD include TMJ pain when chewing and clicking and popping sounds in the TMJ[11,12]. TMJ pain, one of the most common symptoms, limits jaw movements and causes joint sounds, as well as symptoms such as headache, earache, tinnitus, toothache and vertigo[13]. These symptoms can be observed alone or together[9].

Results from different clinical trials have shown that more reliable tools are needed to determine the severity of TMD in the population. The determination of aetiological factors and the role of several factors in TMD help prevent the standardisation of samples[6]. Due to the need for widely valid and simple evaluation procedures that standardise research samples including TMD patients, questionnaires have been developed that identify the main clinical findings of TMD and classify patients according to their severity level[14].

One of the indices used to diagnose TMD patients in the healthy population is the Fonseca Anamnestic Index (FAI). The low cost and easy applicability of the FAI make it preferable for the diagnosis of TMD in patients. The FAI is a questionnaire consisting of 10 questions that determine the presence of pain in the head and back regions, pain on chewing, parafunctional habits, limitation of movement, clicking sounds, malocclusion and emotional stress[14].

The Oral Behaviours Checklist (OBC) indicates oral activities such as chewing, swallowing and speaking. Oral parafunctional habits, on the other hand, reflect other sorts of habits, such as gnashing teeth while awake or sleeping; activities like chewing gum or biting the lips, cheeks, nails or a pen; or playing a wind instrument, all of which create a load on the arches[15,16].

Parafunctional habits affect the masticatory system at various levels owing to repetitive trauma. These factors are considered critical during the onset of TMD strongly related to TMJ pain. Additionally, significant psychosocial stress can cause TMD, and it may be related to chronic TMJ pain[17,18].

This study evaluates the prevalence of TMD, oral habits and quality of life using the FAI, OBC and Oral Health Impact Profile-14 (OHIP-14) questionnaires applied to dentistry students and revealing the relationship between severity of TMD, oral habits and quality of life.

Materials and methods

This observational cross-sectional study was conducted among students of the Faculty of Dentistry at Erciyes University, Kayseri, Turkey, and approved by the Erciyes University Clinical Research Ethics Committee (approval no. 2021/87). Informed consent was obtained from all participants included in the study. At the beginning of the study, 650 students were sent questionnaires, 120 could not be contacted and 78 declined to answer the questions. A total of 452 volunteer dentistry students (mean age 21.18 ± 2.08 years, mean height 169.40 ± 12.50 m, mean weight 65.74 ± 13.68 kg, mean body mass index [BMI] 23.49 ± 7.09 kg/m^2) participated in the study. Of these, 103 were men (mean age 21.14 ± 2.42 years, mean height 178.57 ± 6.35 m, mean weight 77.03 ± 12.32 kg, mean BMI 24.11 ± 3.38 kg/m^2) and 269 were women (mean age 21.20 ± 1.82 years, mean height 169.78 ± 13.23 m, mean weight 58.05 ± 8.08 kg, mean BMI 23.59 ± 3.70 kg/m^2). The online questionnaire was created using Google Forms (Mountain View, CA, USA) and emailed to the registered students in the dentistry faculty student office database. Before the questionnaire was administered, the purpose of the study and the questions were explained, and informed consent was obtained from all participants.

FAI

Various questionnaires have been conducted to date for the classification of TMD[14]. In the early 1990s, Fonseca et al developed a questionnaire that was easy to apply and understand, thus allowing a simple classification of TMD[5]. In the present study, a questionnaire designed by Fonseca was used to classify the severity of TMD. This questionnaire was used due to its ability to collect epidemiological data. It comprises 10 questions that provide a versatile assessment of the presence of pain on chewing, parafunctional habits, limitation of movement, joint sounds, malocclusion and emotional stress in the joint area, head and neck. The participants could only provide one of the following answers (without any time limitation) to the questions: yes (10 points), sometimes (5 points) and no (0 points). After adding up the scores, the participants were classified into four categories: TMD-None (0 to 15 points), Mild-TMD (20 to 40 points), Moderate-TMD (45 to 60 points) and Severe-TMD (70 to 100 points).

OBC

The OBC is a self-reporting questionnaire used to determine any parafunctional disorder of the oral structures and associated muscles. Like in previous studies[19,20], two questions on singing and playing a musical instrument in the original 21-question OBC checklist were

removed, and the checklist was changed. Thus, a 19-question questionnaire was used for evaluation[19,20]. The participants answered each item according to the frequency of complaints (4 = always, 3 = most of the time, 2 = sometimes, 1 = several times or 0 = none). The total score for the OBC was used for analysis. The overall score can range from 0 to 76. A total of three groups (0 points = none; 1 to 16 points = low; 17 to 76 points = high OBC group) were formed for all patients according to the total score obtained from the OBC[19].

OHIP-14

The OHIP is one of the instruments used to assess quality of life related to oral or dental health. The instrument was developed by Slade and Spencer[21]. Its validity and reliability have been demonstrated, and it is commonly used in dentistry.

The OHIP-14, which consists of 14 items (two for each of seven dimensions) and is shorter than the original OHIP, was then developed. The answers to the items were assessed on a Likert-type scale as follows: no = 0, rarely = 1, occasionally = 2, often = 3 and always = 4.

Fourteen questions were asked regarding functional activity, disability, pain, psychological state and physical dimension, as well as social insufficiency, and the aim was to measure oral functional disorders or limitations extensively[22]. The lowest score for the OHIP-14 was 0, whereas the highest was 56. As the score reached the maximum, oral health and quality of life decreased[23].

To determine the awareness of the individuals participating in the study about possible TMD or previous treatments they received, the following three questions were asked by the researchers: "Do you think you have a problem with the jaw or jaw joint?" "Have you been to the dentist for jaw joint pain within the last year?" and "Have you had any treatment (mouthpiece, exercise, medicine, etc.)?" They were asked to answer the three questions with a "yes" or "no".

Sample size calculation

According to the study by Karaman and Sapan24, considering the OHIP-14 scores that varied with different years of education and the power analysis performed, using GPower software (v 3.1.9.4, Heinrich Heine Universität Düsseldorf, Düsseldorf, Germany)25 at 90% power, for alpha = 0.05, d = 0.54 (large) effect value, it was determined that we should recruit 60 participants at least for each education year in the present study.

Statistical analysis

The data for the obtained results were stored and processed using Microsoft Excel (Microsoft Office 365, Microsoft, Redmond, WA, USA). Statistical analysis of the data was carried out using SPSS (v 24.0, IBM, Armonk, NY, USA). Chi-square and Fisher exact tests were used to examine the relationship between sex and classes of distribution of the TMD score, and a Mann-Whitney U test was used to compare the OBC scores by sex and class. A Kendall tau-b correlation test was used to evaluate the relationship between the OBC, OHIP-14 and FAI. The strengths of the correlation between the variables were defined as follows: 0.00 to 0.10, negligible; 0.10 to 0.39, weak; 0.40 to 0.69, medium; 0.70 to 0.89, strong; and 0.90 to 1.00, very strong[26]. $P < 0.05$ denoted statistical significance.

Results

It was determined that 66.8% of the students participating in the questionnaire had TMJ problems at any level (Table 1). The proportion was found to be 77.9% for women and 47.5% for men. The OBC questionnaire scores and BMI values were more statistically significant in women than men (Table 1).

The total score for the FAI was significantly higher in women than in men (Table 2; $P < 0.001$). The prevalence of TMD differed significantly in first-, second-, third-, fourth- and fifth-year students ($P = 0.017$). It was determined that the FAI scores for the individuals in the fourth ($P = 0.027$) and fifth ($P = 0.045$) years were significantly higher than those for the individuals in the first year. At the same time, the OBC ($P < 0.001$) and OHIP-14 ($P = 0.002$) scores were found to be significantly higher in women than in men (Table 2). The BMI scores did not have a statistically significant effect on the total scores obtained from the FAI ($P = 0.52$), OHIP-14 ($P = 0.17$) and OBC ($P = 0.85$) questionnaires (Table 2). When the FAI scores were evaluated according to year of education, there was a statistically significant difference (Table 3; $P = 0.008$). A statistical relationship could not be established between the groups based on the OBC ($P = 0.32$) and BMI ($P = 0.61$) scores as well as the years of education (Table 3).

A statistically significant relationship was established between the groups based on the FAI results and the groups based on the BMI scores (Table 4; $P = 0.028$). There was no statistically significant relationship between the groups based on the OBC and BMI scores (Table 4; $P = 0.15$).

Table 1 Distribution and comparison of FAI, OBC and BMI scores according to sex.

Score		Female, n (%)	Male, n (%)	Total	*P* value
FAI	TMD-None	54 (20.1)	96 (52.5)	150 (33.2)	< 0.001*
	TMD-Mild	149 (55.4)	74 (40.4)	223 (49.3)	
	TMD-Moderate	42 (15.6)	10 (5.5)	52 (11.5)	
	TMD-Severe	24 (8.9)	3 (1.6)	27 (6.0)	
OBC	None	1 (0.4)	3 (1.6)	4 (0.9)	0.002**
	Low	42 (15.6)	50 (27.3)	92 (20.4)	
	High	226 (84.0)	130 (71.0)	352 (78.8)	
BMI group	Underweight	29 (10.8)	4 (2.2)	33 (7.3)	< 0.001*
	Normal	210 (78.1)	117 (63.9)	327 (72.3)	
	Overweight	28 (10.4)	54 (29.5)	82 (18.1)	
	Obese	2 (0.7)	8 (4.4)	10 (2.2)	

*Pearson chi-square test.
**Fisher exact test.
The level of statistical significance was set at $P < 0.05$.

Table 2 Comparison of FAI, OBC and OHIP-14 total scores among the education years and genders.

Group		FAI total	OBC total	OHIP-14
		Mean ± SD	Mean ± SD	Mean ± SD
Year of education	First year (n = 123)	24.59[a] ± 16.30	25.73 ± 10.45	8.22 ± 5.99
	Second year (n = 60)	27.17[a,b] ± 16.03	25.20 ± 8.70	9.00 ± 6.72
	Third year (n = 72)	29.93[a,b] ± 20.97	23.14 ± 9.68	9.31 ± 8.14
	Fourth year (n = 88)	34.55[b] ± 24.10	25.72 ± 11.68	10.25 ± 7.34
	Fifth year (n=109)	33.39[b] ± 21.99	26.22 ± 12.23	8.83 ± 6.80
	P value*	0.017*	0.565*	0.421*
Sex	Female	35.54 ± 20.89	27.60 ± 10.58	9.77 ± 6.95
	Male	21.48 ± 16.62	22.08 ± 10.38	7.97 ± 6.78
	P value	< 0.001**	< 0.001**	0.002**
BMI group	Underweight (n = 33)	38.03 ± 28.67	27.97 ± 8.18	11.48 ± 10.78
	Normal (n = 327)	29.13 ± 18.87	25.09 ± 10.55	8.92 ± 6.62
	Overweight (n = 82)	29.33 ± 22.25	25.38 ± 12.63	8.51 ± 6.25
	Obese (n = 10)	30.50 ± 20.61	25.70 ± 12.23	9.30 ± 5.60
	P value	0.518*	0.165*	0.848*
Total		29.85 ± 20.46	25.36 ± 10.83	9.04 ± 6.93

*Kruskal–Wallis test.
**Mann-Whitney U test.
SD, standard deviation.
The level of statistical significance was set at $P < 0.05$.

Table 3 Distribution and comparison of FAI, OBC and BMI scores according to education years.

Score		Year group, n (%)						*P* value
		1	2	3	4	5	Total	
FAI	TMD-None	49 (39.8)	19 (31.7)	23 (31.9)	28 (31.8)	31 (28.4)	150 (33.2)	0.008*
	TMD-Mild	66 (53.7)	34 (56.7)	37 (51.4)	36 (40.9)	50 (45.9)	223 (49.3)	
	TMD-Moderate	5 (4.1)	7 (11.7)	8 (11.1)	15 (17.0)	17 (15.6)	52 (11.5)	
	TMD-Severe	3 (2.4)	0 (0.0)	4 (5.6)	9 (10.2)	11 (10.1)	27 (6.0)	
OBC	None	0 (0.0)	0 (0.0)	2 (2.8)	1 (1.1)	1 (0.9)	4 (0.9)	0.323**
	Low	22 (17.9)	8 (13.3)	18 (25.0)	21 (23.9)	23 (21.1)	92 (20.4)	
	High	101 (82.1)	52 (86.7)	52 (72.2)	66 (75.0)	85 (78.0)	352 (78.8)	
BMI group	Underweight	5 (4.1)	6 (10.0)	6 (8.3)	11 (12.5)	5 (4.6)	33 (7.3)	0.614**
	Normal	93 (75.6)	41 (68.3)	50 (69.4)	61 (69.3)	82 (75.2)	327 (72.3)	
	Overweight	23 (18.7)	11 (18.3)	13 (18.1)	15 (17.0)	20 (18.3)	82 (18.1)	
	Obese	2 (1.6)	2 (3.3)	3 (4.2)	1 (1.1)	2 (1.8)	10 (2.2)	

*Pearson chi-square test.
**Fisher exact test.
The level of statistical significance was set at $P < 0.05$.

Table 4 Distribution and comparison of FAI and OBC scores according to BMI group.

Score		BMI group, n (%)					*P* value
		Underweight	Normal	Overweight	Obese	Total	
FAI	TMD-None	10 (30.3)	107 (32.7)	29 (35.4)	4 (40.0)	150 (33.2)	0.028*
	TMD-Mild	11 (33.3)	173 (52.9)	36 (43.9)	3 (30.0)	223 (49.3)	
	TMD-Moderate	6 (18.2)	32 (9.8)	11 (13.4)	3 (30.0)	52 (11.5)	
	TMD-Severe	6 (18.2)	15 (4.6)	6 (7.3)	0 (0.0)	27 (6.0)	
OBC	None	0 (0.0)	2 (0.6)	2 (2.4)	0 (0.0)	4 (0.9)	0.149*
	Low	2 (6.1)	70 (21.4)	17 (20.7)	3 (30.0)	92 (20.4)	
	High	31 (93.9)	255 (78.0)	63 (76.8)	7 (70.0)	352 (78.8)	

*Fisher exact test.
The level of statistical significance was set at $P < 0.05$.

Table 5 Scores for the individual OBC items and their Spearman rho correlations with the total FAI score and OHIP-14 score.

Item	Score, mean ± SD	FAI	OHIP-14
		Correlation coefficient	Correlation coefficient
1. Clench or grind teeth when asleep based on any information you may have	1.21 ± 1.27	0.513**	0.138**
2. Sleep in a position that puts pressure on the jaw	1.19 ± 1.23	0.483**	0.169**
3. Grind teeth during waking hours	0.55 ± 0.93	0.286**	0.105*
4. Clench teeth during waking hours	1.15 ± 1.08	0.382**	0.166*
5. Press, touch or hold teeth together other than while eating	1.83 ± 1.16	0.366**	0.146**
6. Hold, tighten or tense muscles without clenching or bringing teeth together	1.03 ± 1.16	0.555**	0.229**
7. Hold or jut jaw forward or to the side	0.59 ± 0.95	0.243**	0.176**
8. Press tongue forcibly against teeth	1.31 ± 1.22	0.186**	0.174**
9. Place tongue between teeth	0.86 ± 1.10	0.093*	0.093*
10. Bite, chew or play with your tongue, cheeks or lips	0.62 ± 0.92	0.093*	0.038
11. Hold jaw in rigid or tense position, such as to brace or protect the jaw	2.04 ± 1.28	0.091*	0.066
12. Hold between the teeth or bite objects such as hair, pipe, pencil, pens, fingers or fingernails	0.89 ± 1.05	0.066	0.089
13. Use chewing gum	1.64 ± 1.02	0.060	0.001
14. Lean with your hand on the jaw, such as cupping or resting the chin in the hand	2.07 ± 1.17	0.312**	0.133**
15. Chew food on one side only	1.93 ± 1.11	0.321**	0.236**
16. Eating between meals (food that requires chewing)	2.31 ± 1.09	0.209**	0.185**
17. Sustained talking (for example teaching, sales or customer service)	0.98 ± 1.00	0.147**	0.146**
18. Yawning	2.23 ± 0.94	0.158**	0.089
19. Holding telephone between head and shoulders	0.95 ± 1.11	0.023	0.001

*Correlation is significant at the $P < 0.05$ level (2-tailed).
**Correlation is significant at the $P < 0.01$ level (2-tailed).
SD, standard deviation.
Correlation coefficients were Kendall tau-b correlation coefficients.

Significant correlations were found between the questions in the OBC (except for questions 10, 11, 12, 13, 18 and 19), as well as the FAI and OHIP-14 scores (Table 5). While moderate correlations were established between OBC questions 1, 2 and 6, as well as the FAI questionnaire, a low-grade correlation with the OBC questionnaire was found (Table 5; $P < 0.01$).

Various correlations were found between the responses to the questions in the OHIP-14 questionnaire, as well as the FAI and OBC scores. Notably, a moderate correlation was found between the response to question 6 of the OHIP-14 and the FAI and OBC scores (Table 6; $P < 0.01$).

When the bivariate correlations among the FAI, OHIP-14 and OBC questionnaire total scores were examined, a moderate correlation was found between the FAI and OBC questionnaire scores, although there were significant correlations between them (Table 7; $P < 0.01$). When stratified by education, a moderate correlation was found between the FAI and OBC questionnaire scores, except for first-year students (Table 7; $P < 0.05$). In addition, only a moderate correlation was

Table 6 Scores for the individual OHIP-14 items and their Spearman rho correlations with the total FAI score and OBC score.

Item	Score, mean ± SD	FAI	OBC
		Correlation coefficient	Correlation coefficient
1. Have you had trouble pronouncing any words because of problems with your mouth or dentures?	0.31 ± 0.59	0.103*	0.100*
2. Have you felt that your sense of taste has worsened because of problems with your mouth or dentures?	0.15 ± 0.45	0.015	0.084
3. Have you had painful aching in your mouth?	0.91 ± 0.97	0.337**	0.265**
4. Have you found it uncomfortable to eat any foods because of problems with your mouth or dentures?	0.67 ± 0.86	0.206**	0.171**
5. Have you felt self-conscious because of your mouth or dentures?	1.73 ± 1.18	0.018	0.012
6. Have you felt tense because of problems with your mouth or dentures?	1.12 ± 1.06	0.427**	0.322**
7. Has your diet been unsatisfactory because of problems with your mouth or dentures?	0.49 ± 0.81	0.147**	0.073
8. Have you had to interrupt meals because of problems with your mouth or dentures?	0.50 ± 0.74	0.083	0.039
9. Have you found it difficult to relax because of problems with your mouth or dentures?	0.51 ± 0.78	0.330**	0.297**
10. Have you felt a bit embarrassed because of problems with your mouth or dentures?	0.73 ± 0.99	0.039	0.046
11. Have you been a bit irritable with other people because of problems with your mouth or dentures?	0.57 ± 0.84	0.241**	0.169**
12. Have you had difficulty doing your usual job because of problems with your mouth or dentures?	0.53 ± 0.81	0.158**	0.156**
13. Have you felt that life in general was less satisfying because of problems with your mouth or dentures?	0.66 ± 0.93	0.197**	0.141**
14. Have you been totally unable to function because of problems with your mouth or dentures?	0.17 ± 0.44	0.096*	0.085

*Correlation is significant at the $P < 0.05$ level (2-tailed).
**Correlation is significant at the $P < 0.01$ level (2-tailed).
SD, standard deviation.
Correlation coefficients were Kendall tau-b correlation coefficients.

found between the OHIP-14 and FAI for the third-year students (Table 7; $P < 0.05$). When evaluated according to BMI groups, strong correlations were observed between the Fonseca and OBC questionnaires in individuals whose scores were not within normal values (Table 7; $P < 0.05$).

Discussion

The present study assessed the impact of oral habits, both in terms of the joints and quality of life, on TMD in 452 dental students. With this cross-sectional study, it was determined that the prevalence of TMD in dentistry students was 66.8%. One of the most important findings was that all students had at least one oral parafunction and 16 of the 19 questions correlated with their FAI score.

The FAI provides valuable data for the early detection and low-cost evaluation of TMD. Ayali and Ramoglu[27] conducted a study on 409 dentistry students and found that 38.6% had mild TMD, 13.4% had moderate TMD and 4.4% had severe TMD. Habib et al[28] administered the FAI to 400 people and found that 36.1% had mild TMD, 9.6% had moderate TMD and 1.1% had severe TMD. Among the 452 students in the present study, 33.2% did not have TMD, whereas 49.3% had mild TMD, 11.5% had moderate TMD and 6.0% had severe TMD. Considering the distribution of years of education, the fourth and fifth-year students' average FAI TMD scores were significantly higher than those for other years (especially the first-year students). Similarly, Karaman and Sapan[24] found that the prevalence of TMD was higher among senior students in the faculty of dentistry.

The frequency of TMD detected by the FAI varies between 37% and 81% in similar studies conducted on students[19,20,27-31]. Mild TMD (49.3%) was the most prevalent level of TMD in the population assessed in

Table 7 Relationship between FAI, OBC and OHIP-14 scores by year group, sex and BMI group.

Variable		FAI–OBC	FAI–OHIP-14	OBC–OHIP-14
Year group	First year	0.327**	0.146	0.192*
	Second year	0.436**	0.282*	0.316*
	Third year	0.505**	0.514**	0.352**
	Fourth year	0.706**	0.348**	0.293**
	Fifth year	0.567**	0.347**	0.185
Sex	Female	0.551**	0.327**	0.282**
	Male	0.311**	0.249**	0.137
BMI group	Underweight	0.848**	0.759**	0.691**
	Normal	0.428**	0.264**	0.211**
	Overweight	0.691**	0.290**	0.292**
	Obese	0.740*	0.022	0.061
Total		0.517**	0.318**	0.249**

*$P < 0.05$; **$P < 0.01$.
The data presented are Kendall tau-b correlation coefficients.

the present study. This is in line with the results reported by Pedroni et al[32] and Karthik et al[33], all of whom used the FAI to evaluate TMD. In a Turkish population, Özdinç et al[31] and Emel Dervis[34] reported a prevalence similar to the current study (47.3%). On the other hand, Türken et al[29] reported a higher prevalence of TMD (79%) than that reported in the present study. These results may be due to differences in the populations, such as varying sex distribution or sociodemographic characteristics. In addition, since all the participants in the present study were students, stress-related psychological factors caused by school-related factors like busy class schedules and anxiety about the possibility of failure may have caused variations in severity of TMD[35].

A study conducted by Ahuja et al[36] with 450 students studying at faculties of dentistry indicated that women suffer from joint disorders more than men. Minghelli et al[37] studied Portuguese children aged between 5 and 19 years and found that the prevalence of TMD was higher in females. Karaman and Buyuk[38] found that females' mean FAI TMD scores were significantly higher than males'. Hongxing et al[39], Karibe et al[40] and Kim et al[41] found that symptoms of masticatory disorders were more frequent among women in comparison to men. Wieckiewicz et al[42] and Kim et al[41] stated that this frequency arose from biological differences, including hormonal and psychosocial factors. Poveda et al[43] and Nomura et al[5] noted that this higher prevalence of TMD among women could be related to their physiological characteristics, hormonal variations and structures in connective tissues and muscles. Landi et al[44] indicated that the serum value of 17-beta-estradiol among TMD patients was higher than that in patients who did not suffer from TMD. This study indicated that the prevalence of TMD in women was significantly higher than its prevalence in men (77.9% vs 47.5%)[44], which was in line with the findings of previous studies.

Ingle et al[45] reported that the OHIP-14 score was higher among women. Gonzales-Sullcahuamán et al[46] found no statistically significant relationship between OHIP-14 score and year of academic education, and no difference between the sexes. Karaman and Buyuk[38] found that the mean OHIP-14 score for women was significantly higher than that for men. This study suggests that the OHIP-14 score is higher in women than men, and there was no statistically significant relationship between years of education and OHIP-14 score[38].

In the present study, the OBC was used to evaluate oral parafunctions. The OBC is a self-administered tool designed to evaluate oral activities such as grinding and other oral parafunctions during sleep or awake hours[47,48]. Perrotta et al[49] aimed to explain the relationships between parafunctional habits and TMD and reported a relationship between them. Van der Meulen et al[50] found no significant difference regarding total OBC scores between male and female participants. Chow and Cioffi[51] reported that women's OBC scores were higher than those of men. Karaman and Buyuk[38] stated that mean OBC scores were higher for women than men. Paduano et al[52], meanwhile, found no relationship between sex and oral parafunctions. A moderately significant relationship was found between the FAI questionnaire results and OBC scores[52]. The OBC scores for female participants were statistically higher than those for male participants, and there was no significant relationship between academic year and OBC score[52].

According to Jordani et al[53], obesity and a sedentary lifestyle were not found to be associated with TMD pain

in adolescents. Rhim et al[54] found TMD to be associated with low BMI and abdominal obesity in women, whereas BMI was not associated with TMD in men, and they stated that further prospective studies are required to determine the causal relationship and mechanism between TMD and obesity. In Turkish society, individuals of normal weight have more joint problems[55]. The same was found to be true in the present study; it would therefore be incorrect to conclude that severity of TMJ disorders increases in overweight and obese people. The reason for this may be because the number of people in those groups was fewer than the number of individuals of a normal weight.

The present study found that increasing oral parafunctional habits assessed with the OBC were associated with TMJ problems. In addition, a moderate correlation was found between severity of TMD and responses to the following questions related to oral parafunctional habits evaluated by the OBC questionnaire: "Do you clench or grind your teeth while sleeping?", "Do you put pressure on your jaw while sleeping?" and "Is there pain or tension in your jaw muscles while awake?" These results are similar to those reported by Yeler et al[30], who showed that TMD is associated with unilateral chewing and bruxism. In addition, Karthik et al[33] reported that TMD symptoms were more common in university students who defined themselves as tense. Moreover, in a study on Nepalese students, Royaka et al[35] detected that 20% of the participants exhibited grinding. Similarly, Lövgren et al[47] found that oral parafunctional habits were more prevalent in students diagnosed with TMD in a study involving dentistry students, and they suggested that this result was associated with bruxism, which was frequently observed in participants.

A moderate correlation was found between the response to question 6 in the OHIP-14 questionnaire ("Do you feel tension due to problems with your teeth, mouth or prosthesis?") and the FAI and OBC questionnaire scores. This shows that the high results obtained from the FAI and OBC questionnaires can be interpreted as representative of the high level of tension in the person.

When evaluated according to BMI groups, there were strong correlations between the FAI and OBC questionnaires in individuals whose scores were not normal. The existence of problems, such as those related to eating habits, in individuals whose scores were not normal may cause a difference between oral parafunction and an increase in TMD severity in these groups.

An early diagnosis of TMD and the factors that cause it (occlusal factors developed because of oral parafunctions) is vital in dentistry. Early diagnosis and treatment of problems prevents them from progressing further and becoming complicated and thus improves individuals' quality of life. These questionnaire studies, which seem simple, will increase the chance of treating individuals early by increasing the prevalence, awareness and early diagnosis of TMD in this respect.

Limitations

An important limitation of this study is the use of questionnaires for the evaluation. Although objective measurement tools would be more beneficial, this limitation can be ignored because the validity and reliability of all the questionnaires used in the present study have been established. Only specific subclinical symptoms related to TMJ problems can be obtained when only one questionnaire is used. Considering the data obtained, it is necessary to diagnose TMD precisely based on clinical and radiological examination, followed by prompt treatment. This study involved only students in the dentistry faculty. The proportions of students differed by sex; however, the literature shows that the prevalence of TMD is higher in women. This situation may have affected the results of the study and made it difficult to generalise the results. It is therefore necessary to evaluate TMJ problems and clinical and radiological examinations in future studies with similar but more participants, and various student populations should be involved.

Conclusion

This study revealed that the prevalence of TMD was higher among fourth- and fifth-year students of the dentistry faculty, especially compared with the first-year students. Additionally, prevalence of TMD was higher among the female students than the male students. TMD, quality of life and oral habits were related to each other. Necessary measures should be taken in the dental education system to improve students' quality of life, improve joint disorders and eliminate detrimental oral habits.

Acknowledgements

The authors thank the faculty staff for their help with the data collection.

Conflicts of interest

The authors declare no conflicts of interest related to this study.

Author contribution

Dr Ravza ERASLAN contributed to the study conceptualisation, methodology, data collection and writing (original draft and editing) and Dr Taner OZTURK contributed to the methodology, statistical analysis and writing (reviewing and editing).

(Received Sep 06, 2021; accepted Nov 03, 2021)

References

1. Okeson JP. Bell's Orofacial Pains, ed 6. Chicago: Quintessence, 2005.
2. Ramoglu S, Ozan O, Aydın M. Conservative treatment approaches in temporomandibular joint disorders: Occlusal splints [in Turkish]. ADO Journal of Clinical Sciences 2011;5:913–923.
3. Okeson JP. Management of Temporomandibular Disorders and Occlusion. St. Louis: Mosby, 2008.
4. Kuvvetli Selvi S, Sandallı N. Temporomandibular disorders in children and adolescents: Literature review [in Turkish]. J Dent Fac Ataturk Univ 2007;(suppl 2):1–9.
5. Nomura K, Vitti M, Oliveira AS, et al. Use of the Fonseca's questionnaire to assess the prevalence and severity of temporomandibular disorders in Brazilian dental undergraduates. Braz Dent J 2007;18:163–167.
6. de Oliveira AS, Dias EM, Contato RG, Berzin F. Prevalence study of signs and symptoms of temporomandibular disorder in Brazilian college students. Braz Oral Res 2006;20:3–7.
7. Almoznino G, Zini A, Zakuto A, et al. Cervical muscle tenderness in temporomandibular disorders and its associations with diagnosis, disease-related outcomes, and comorbid pain conditions. J Oral Facial Pain Headache 2020;34:67–76.
8. Baran I, Nalcacı R, Ucar S. Temporomandibular disorders in older denture-wearing people. Turk J Geriatr 2008;11:26–32.
9. Bagis B, Ayaz EA, Turgut S, Durkan R, Özcan M. Gender difference in prevalence of signs and symptoms of temporomandibular joint disorders: a retrospective study on 243 consecutive patients. Int J Med Sci 2012;9:539–544.
10. Benoliel R, Sela G, Teich S, Sharav Y. Painful temporomandibular disorders and headaches in 359 dental and medical students. Quintessence Int 2011;42:73–78.
11. Kim YK, Kim SG, Im JH, Yun PY. Clinical survey of the patients with temporomandibular joint disorders, using Research Diagnostic Criteria (Axis II) for TMD: Preliminary study. J Craniomaxillofac Surg 2012;40:366–372.
12. Mobilio N, Casetta I, Cesnik E, Catapano S. Prevalence of self-reported symptoms related to temporomandibular disorders in an Italian population. J Oral Rehabil 2011;38:884–890.
13. Hilgenberg PB, Saldanha ADD, Cunha CO, Rubo JH, Conti PC. Temporomandibular disorders, otologic symptoms and depression levels in tinnitus patients. J Oral Rehabil 2012;39:239–244.
14. Bevilaqua-Grossi D, Chaves TC, de Oliveira AS, Monteiro-Pedro V. Anamnestic index severity and signs and symptoms of TMD. Cranio 2006;24:112–118.
15. Schiffman E, Ohrbach R, Truelove E, et al. Diagnostic criteria for temporomandibular disorders (DC/TMD) for clinical and research applications: Recommendations of the International RDC/TMD Consortium Network and Orofacial Pain Special Interest Group. J Oral Facial Pain Headache 2014;28:6–27.
16. Lobbezoo F, Ahlberg J, Glaros AG, et al. Bruxism defined and graded: An international consensus. J Oral Rehabil 2013;40:2–4.
17. Ohrbach R, Bair E, Fillingim RB, et al. Clinical orofacial characteristics associated with risk of first-onset TMD: The OPPERA prospective cohort study. J Pain 2013;14(12, suppl):T33–T50.
18. Ohrbach R, Fillingim RB, Mulkey F, et al. Clinical findings and pain symptoms as potential risk factors for chronic TMD: Descriptive data and empirically identified domains from the OPPERA case-control study. J Pain 2011;12(11, suppl):T27–T45.
19. Al Hayek SO, Al-Thunayan MF, AlGhaihab AM, AlReshaid RM, Omair A. Assessing stress associated with temporomandibular joint disorder through Fonseca's anamnestic index among the Saudi physicians. Clin Exp Dent Res 2018;5:52–58.
20. Karabicak GO, Hazar Kanik Z. Temporomandibular disorder prevalence and its association with oral parafunctions, neck pain, and neck function in healthcare students: A cross-sectional study. Cranio 2020:1–7.
21. Slade GD, Spencer AJ. Development and evaluation of the Oral Health Impact Profile. Community Dent Health 1994;11:3–11.
22. Slade GD. Derivation and validation of a short-form oral health impact profile. Community Dent Oral Epidemiol 1997;25:284–290.
23. Liu Z, McGrath C, Hägg U. Changes in oral health-related quality of life during fixed orthodontic appliance therapy: An 18-month prospective longitudinal study. Am J Orthod Dentofacial Orthop 2011;139:214–219.
24. Karaman A, Sapan Z. Evaluation of temporomandibular disorders, quality of life, and oral habits among dentistry students. Cranio 2020:1–7.
25. Faul F, Erdfelder E, Lang AG, Buchner A. G*Power 3: A flexible statistical power analysis program for the social, behavioral, and biomedical sciences. Behav Res Methods 2007;39:175–191.
26. Schober P, Boer C, Schwarte LA. Correlation coefficients: Appropriate use and interpretation. Anesth Analg 2018;126:1763–1768.
27. Ayalı A, Ramoglu S. Assessment of prevalence and severity of temporomandibular disorders in North Cyprus dentistry students [in Turkish]. J Dent Fac Ataturk Univ 2014;24:367–372.
28. Habib SR, Al Rifaiy MQ, Awan KH, Alsaif A, Alshalan A, Altokais Y. Prevalence and severity of temporomandibular disorders among university students in Riyadh. Saudi Dent J 2015;27:125–130.
29. Türken R, Büyük SK, Yaşa Y. Evaluation of temporomandibular joint disorders and oral habits in dentistry faculty students [in Turkish]. ACU Sağlık Bil Derg 2020;11:208–213.
30. Yalçın Yeler D, Yılmaz N, Koraltan M, Aydın E. A survey on the potential relationships between TMD, possible sleep bruxism, unilateral chewing, and occlusal factors in Turkish university students. Cranio 2017;35:308–314.
31. Özdinç S, Ata H, Selçuk H, Can HB, Sermenli N, Turan FN. Temporomandibular joint disorder determined by Fonseca anamnestic index and associated factors in 18- to 27-year-old university students. Cranio 2020;38:327–332.
32. Pedroni CR, De Oliveira AS, Guaratini MI. Prevalence study of signs and symptoms of temporomandibular disorders in university students. J Oral Rehabil 2003;30:283–289.
33. Karthik R, Hafila MIF, Saravanan C, Vivek N, Priyadarsini P, Ashwath B. Assessing prevalence of temporomandibular disorders among university students: A questionnaire study. J Int Soc Prev Community Dent 2017;7(suppl 1):S24–S29.
34. Emel Dervis N. Prevalence of temporomandibular disorder in Turkish university students: A questionnaire study. Balk J Dent Med 2019;23:80–87.
35. Rokaya D, Suttagul K, Joshi S, Bhattarai BP, Shah PK, Dixit S. An epidemiological study on the prevalence of temporomandibular disorder and associated history and problems in Nepalese subjects. J Dent Anesth Pain Med 2018;18:27–33.
36. Ahuja V, Ranjan V, Passi D, Jaiswal R. Study of stress-induced temporomandibular disorders among dental students: An institutional study. Natl J Maxillofac Surg 2018;9:147–154.

37. Minghelli B, Cardoso I, Porfírio M, et al. Prevalence of temporomandibular disorder in children and adolescents from public schools in southern portugal. N Am J Med Sci 2014;6:126–132.
38. Karaman A, Buyuk SK. Evaluation of temporomandibular disorder symptoms and oral health-related quality of life in adolescent orthodontic patients with different dental malocclusions. Cranio 2022;40:55–63.
39. Hongxing L, Astrøm AN, List T, Nilsson IM, Johansson A. Prevalence of temporomandibular disorder pain in Chinese adolescents compared to an age-matched Swedish population. J Oral Rehabil 2016;43:241–248.
40. Karibe H, Shimazu K, Okamoto A, Kawakami T, Kato Y, Warita-Naoi S. Prevalence and association of self-reported anxiety, pain, and oral parafunctional habits with temporomandibular disorders in Japanese children and adolescents: A cross-sectional survey. BMC Oral Health 2015;15:8.
41. Kim TY, Shin JS, Lee J, et al. Gender difference in associations between chronic temporomandibular disorders and general quality of life in Koreans: A cross-sectional study. PLoS One 2015;10:e0145002.
42. Wieckiewicz M, Grychowska N, Wojciechowski K, et al. Prevalence and correlation between TMD based on RDC/TMD diagnoses, oral parafunctions and psychoemotional stress in Polish university students. Biomed Res Int 2014;2014:472346.
43. Poveda Roda R, Bagan JV, Díaz Fernández JM, Hernández Bazán S, Jiménez Soriano Y. Review of temporomandibular joint pathology. Part I: Classification, epidemiology and risk factors. Med Oral Patol Oral Cir Bucal 2007;12:E292–E298.
44. Landi N, Manfredini D, Lombardi I, Casarosa E, Bosco M. 17-beta-estradiol and progesterone serum levels in temporomandibular disorder patients [in English, Italian]. Minerva Stomatol 2004;53: 651–660.
45. Ingle NA, Chaly PE, Zohara CK. Oral health related quality of life in adult population attending the outpatient department of a hospital in Chennai, India. J Int Oral Health 2010;2:45–56.
46. Gonzales-Sullcahuamán JA, Ferreira FM, de Menezes JV, Paiva SM, Fraiz FC. Oral health-related quality of life among Brazilian dental students. Acta Odontol Latinoam 2013;26:76–83.
47. Lövgren A, Österlund C, Ilgunas A, Lampa E, Hellström F. A high prevalence of TMD is related to somatic awareness and pain intensity among healthy dental students. Acta Odontol Scand 2018;76: 387–393.
48. Kaplan SE, Ohrbach R. Self-report of waking-state oral parafunctional behaviors in the natural environment. J Oral Facial Pain Headache 2016;30:107–119.
49. Perrotta S, Bucci R, Simeon V, Martina S, Michelotti A, Valletta R. Prevalence of malocclusion, oral parafunctions and temporomandibular disorder-pain in Italian schoolchildren: An epidemiological study. J Oral Rehabil 2019;46:611–616.
50. van der Meulen MJ, Lobbezoo F, Aartman IH, Naeije M. Validity of the Oral Behaviours Checklist: Correlations between OBC scores and intensity of facial pain. J Oral Rehabil 2014;41:115–121.
51. Chow J, Cioffi I. Pain and orthodontic patient compliance: A clinical perspective. Semin Orthod 2018;24:242–247.
52. Paduano S, Bucci R, Rongo R, Silva R, Michelotti A. Prevalence of temporomandibular disorders and oral parafunctions in adolescents from public schools in Southern Italy. Cranio 2020;38:370–375.
53. Jordani PC, Campi LB, Braido GVV, Fernandes G, Visscher CM, Gonçalves DAG. Obesity, sedentarism and TMD-pain in adolescents. J Oral Rehabil 2019;46:460–467.
54. Rhim E, Han K, Yun KI. Association between temporomandibular disorders and obesity. J Craniomaxillofac Surg 2016;44:1003–1007.
55. Ekici Ö. Psychological profile and sleep quality of patients with temporomandibular joint dysfunction with or without bruxism. J Turk Sleep Med 2021;8:35–42.

A Single-Visit Technique for Fabricating Interim, Immediately Loaded Implant-supported Full-arch Prostheses with Prefabricated Rigid Connecting Bars: a Case Report

Yi Man TANG[1], Hua Jie YU[1], Li Xin QIU[1], Juan WANG[1]

Traditional techniques for fabricating interim, immediately loaded implant-supported full-arch prostheses are complex and time-consuming. The present study presents an efficient technique for fabricating interim prostheses with prefabricated multipurpose rigid connecting bars. This technique can minimise the misfit attributed to the polymerisation shrinkage of resin and expansion of the working cast, and simultaneously facilitate impression taking and occlusal records in one visit, thus reducing laboratory and chair time. Due to its ease of use and clinical efficiency, the present technique is considered particularly beneficial for immediate loading rehabilitation.

Key words: *dental implant, full-arch, immediate loading, implant impressions, interim prostheses*
Chin J Dent Res 2022;25(3):233–239; doi: 10.3290/j.cjdr.b3317973

Immediate loading of implant-supported interim prostheses has become a reliable treatment modality for completely edentulous patients. The interim prosthesis splints the implants together, which allows for favourable force distribution in the peri-implant tissues and minimises the micromovement of the implants[1,2]. Prosthesis misfit is particularly risky in immediate loading rehabilitations in the first 2 to 3 weeks after implant insertion.

1 4th Division, Peking University School and Hospital of Stomatology, National Clinical Research Centre for Oral Diseases, National Engineering Laboratory for Digital and Material Technology of Stomatology, Beijing Key Laboratory of Digital Stomatology, Beijing, P.R. China.

Corresponding author: Dr Juan WANG, 4th Division, Peking University School and Hospital of Stomatology, #22 Zhongguancun South Avenue, Haidian District, Beijing 100081, P.R. China. Tel: 86-10-85715955; Fax: 86-10-62173402. E-mail: wangjkq@126.com

This work was supported by the Programme for New Clinical Techniques and Therapies of Peking University School and Hospital of Stomatology (PKUSSNCT-19B05) and the National Natural Science Foundation of China (no. 82001013).

Several procedures have been used to fabricate an interim prosthesis immediately after surgery. The conventional method involves a preliminary impression being made in the clinic, followed by fabrication of a stone cast and personalised impression copings in the dental laboratory[3]. After splinting the impression copings in the mouth, a pickup impression with rigid impression materials is taken to fabricate an accurate final cast. This whole procedure is complex and time-consuming, and the fracture or distortion of the splint materials caused by polymerisation shrinkage may affect accuracy in the definitive impression[4]. The interim prosthesis can also be fabricated by direct conversion of an existing complete denture or using an intraorally welded titanium framework[5-6]; however, the intraoral connection processes are skill dependent and uncomfortable for patients. The resin used for connection may have a negative impact on soft tissue healing and increase the risk of wound swelling and infection. Moreover, with the development of CAD/CAM technology, a digital workflow has been considered an efficient modality to fabricate precise prostheses. Taking digital impressions using intraoral digitisers simplifies

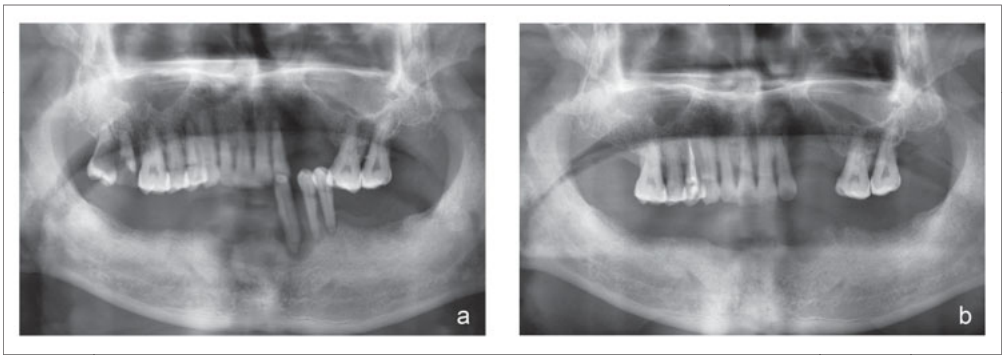

Fig 1 **(a)** Pretreatment panoramic radiograph; **(b)** panoramic radiograph of the patient before surgery.

the workflow greatly but presents disadvantages, namely the high initial economic investment and the steep learning curve for clinicians[7-8]. Thus, due to the limitations of conventional procedures, this article presents an immediate loading technique to facilitate the same-day adaptation of an implant-supported, screw-retained, full-arch prosthesis with prefabricated rigid connecting bars. With this technique, the non-tray pickup impression and occlusal records can be made simultaneously, reducing operative time and improving patient comfort.

Case report

A 64-year-old man presented with the chief complaint of difficulty chewing because he had lost most of his mandibular teeth. He had had diabetes for 5 years and was controlling it well with medication. Around 10 years previously, he had received a removable partial denture, but in recent years he had lost multiple teeth one after another and the old denture had come loose. On oral examination, the three remaining mandibular teeth, namely the left canine and first and second premolars, were extremely loose, and the periodontal probing depth was greater than 8 mm. A panoramic radiograph showed that the alveolar bone had been resorbed to the root apex (Fig 1a). In the maxilla, the left canine and first and second premolars were missing, and there were soft tissue and bone defects in both horizontal and vertical directions. The maxillary right second and third molars had hopeless residual crowns. A large cavity and periapical inflammation could be observed on the maxillary right first premolar. The other maxillary teeth had moderate periodontitis.

The patient was not satisfied with his old removable partial denture for both aesthetic and functional reasons and wanted a stable and functional outcome using implant-supported fixed restorations. He also wanted a denture to stay in place over the entire treatment period for professional reasons. Thus, a comprehensive treatment plan was proposed, which comprised the following steps:

- removal of the mandibular left canine and first and second premolars and the maxillary right second and third molars and relining the old removable partial denture;
- periodontal treatment of the remaining teeth and root canal treatment of the maxillary right first premolar;
- insertion of six implants (SPI Element RC; Thommen Medical, Grenchen, Switzerland) in the healed mandibular bone using the immediate loading technique;
- fabrication of an implant-supported fixed final prosthesis for the mandibular edentulous arch and a removable partial denture for the maxillary partially edentulous arch.

The patient's remaining mandibular teeth were extracted. After 3 months, a panoramic radiograph was taken to evaluate his residual alveolar bone (Fig 1b). Six implants were placed in the patient's edentulous mandible with a primary stability of 35 Ncm (Fig 2). The implants were cylindrical in shape with ISO 9268 trapezoidal threads, moderately rough sandblasted and acid-etched (SLA) surfaces and a 1.0-mm smooth collar. A complete set of stainless-steel rigid connecting bars of standardised size (thickness 1.5 mm, inner diameter 4.0 mm, outer diameter 6.0 mm) and different lengths (6 to 30 mm) were designed to accommodate varying distances between implants (Fig 3).

After the surgery, the multiunit abutments were screwed onto the implants. The implant cylinders were tightened to the multiunit abutments (Fig 4a). If the height of the implant cylinders interfered with the patient closing fully into occlusion, the cylinders were shortened accordingly. The interimplant distance was measured and connecting bars of optimal lengths were

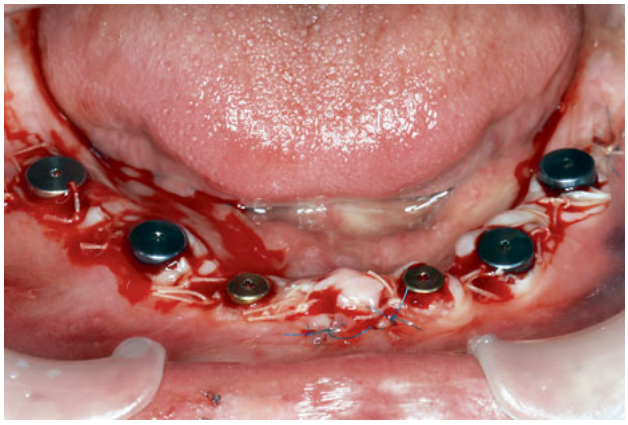

Fig 2 Edentulous mandible with six implants.

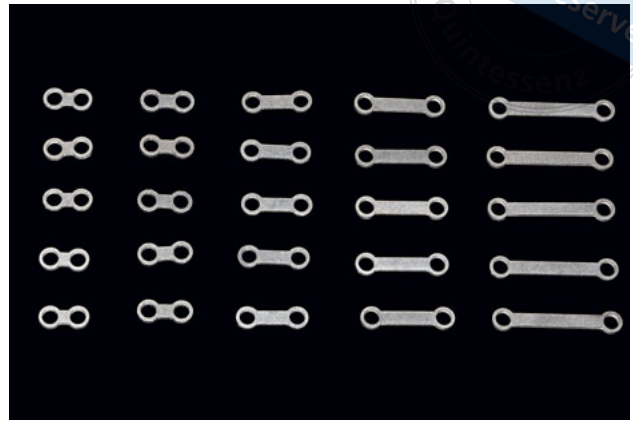

Fig 3 Prefabricated rigid connecting bars of various lengths.

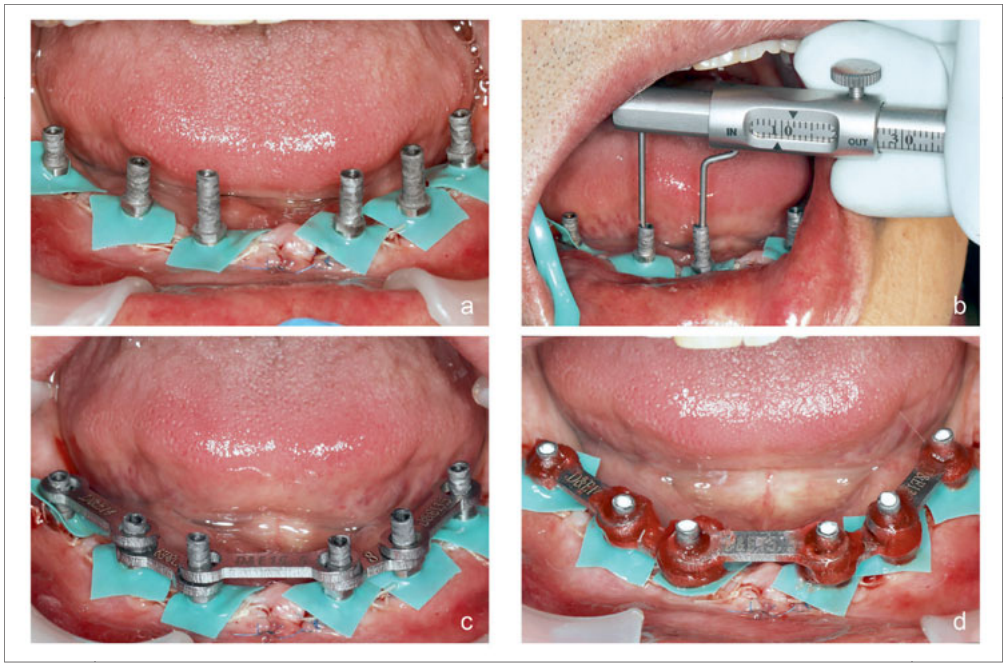

Fig 4 **(a)** Multiunit abutments and implant cylinders screwed into the implants; **(b)** measurement of the inter-abutment distance; **(c)** connecting bars of optimal lengths placed on the implant cylinders; **(d)** intraoral splinting of rigid connecting bars with a small amount of autopolymerising acrylic resin.

selected (Figs 4b and c). A small amount of autopolymerising acrylic resin (Pattern Resin; GC Corporation, Tokyo, Japan) was applied to connect the bars to the implant cylinders using a powder/liquid brush application technique (Fig 4d).

Light viscosity impression material (Express; 3M, Saint Paul, MN, USA) was injected underneath the splinting structure, and medium viscosity impression material (Express; 3M) was dispensed into the patient's mouth to ensure adequate exposure of all the screw channels (Fig 5a). Simutaneously, the patient's mandible was guided to the occlusal vertical dimension and occlusal registration was recorded (Fig 5b) at the same visit. Thereafter, the implant cylinders were unscrewed so that the splinted bars remained in the impression when it was removed (Fig 5c). Implant analogs were inserted into the impression and gingival mask material was injected around them (Fig 5d). The implant analogs were splinted with connecting bars and mounted on the articulator (Fig 6).

The interim prosthesis was fabricated using the conventional acrylic resin processing technique. The connecting bars were embedded as a reinforcing framework in the prosthesis (Fig 7). Three hours after surgery, the interim prosthesis was screwed to the implants with a torque of 15 Ncm (Fig 8a). A panoramic radiograph was taken to assess the passive fit of the prosthesis (Fig 8b). Denture base fracture was observed around 2 months

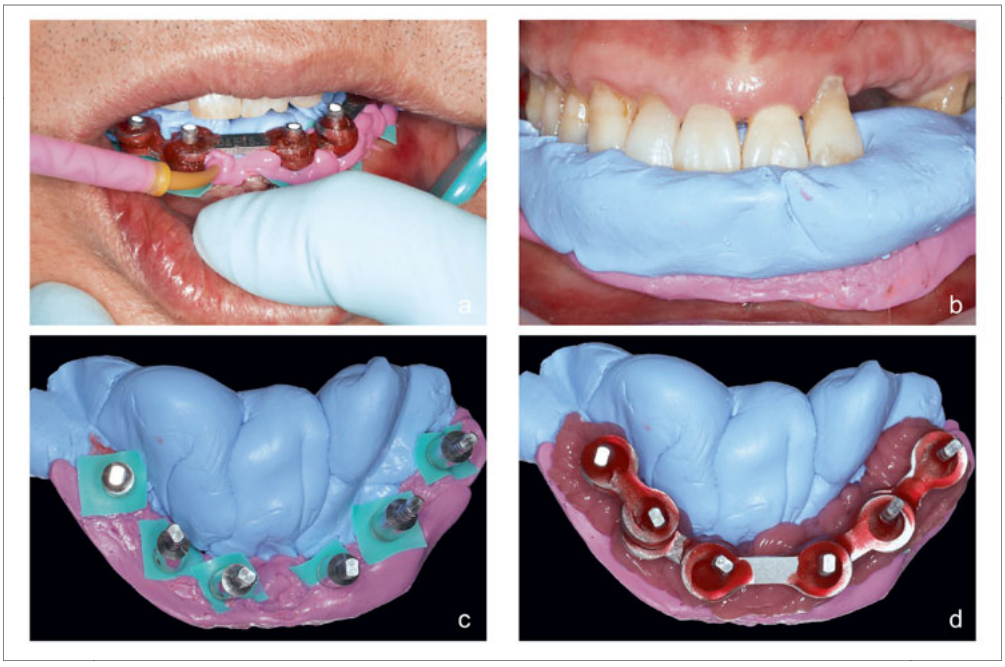

Fig 5 **(a)** Injection of impression material with no impression tray; **(b)** occlusal record of the patient over the splinting structure; **(c)** intaglio surface of the definitive impression with implant analogs inserted; **(d)** impression with a gingival mask and implant analogs splinted with rigid connecting bars.

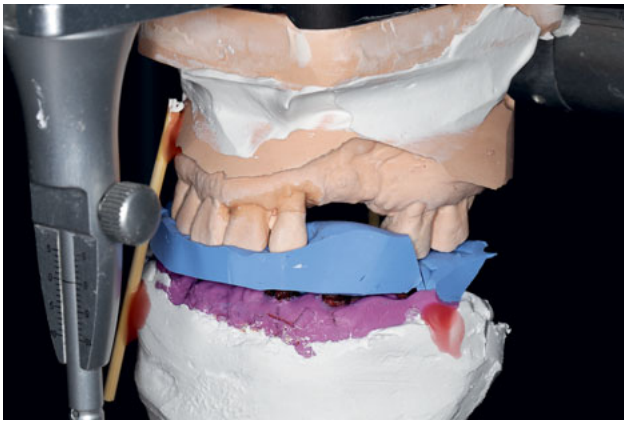

Fig 6 Gypsum casts on the articulator.

Fig 7 **(a)** Interim prosthesis with connecting bars embedded; **(b)** interim fixed implant-supported full-arch prosthesis.

after immediate restoration. The fracture occurred at the posterior edge of the denture rather than where the rigid connecting bars were embedded (Fig 9). The restoration was repaired and the patient was recalled 6 months after surgery to receive a final prosthesis. A new maxillary removable partial denture and mandibular metal-ceramic fixed full-arch prosthesis were fabricated and delivered (Fig 10).

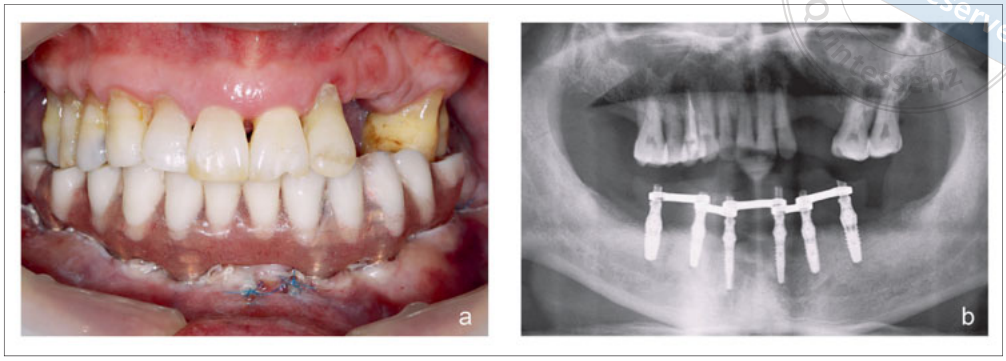

Fig 8 **(a)** Interim prosthesis in place immediately after implant surgery; **(b)** panoramic radiograph after immediate loading.

Fig 9 Denture base fracture of the interim prosthesis.

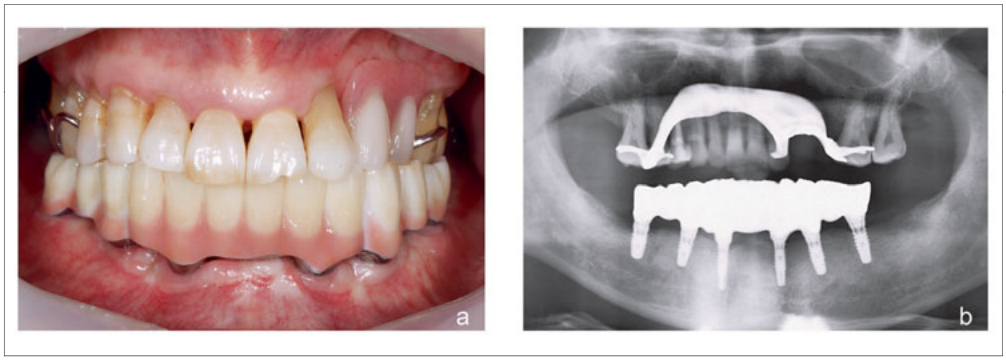

Fig 10 **(a)** Final prosthesis delivered 6 months after implant surgery; **(b)** panoramic radiograph after final prosthesis delivery.

Discussion

The present article describes a technique for fabricating interim, immediately loaded implant-supported full-arch prostheses with prefabricated rigid connecting bars. The main advantage of the technique is that it can simplify the process and improve the efficiency of the workflow. The prefabricated bars eliminate the time required for the fabrication of custom splinting structures and working cast preparation in the laboratory, reducing the waiting time and facilitating finishing of interim prostheses. In addition, edentulous patients who have lost occlusal contact points of natural teeth need their interocclusal relationship to be recorded prior to fabrication of the prosthesis. The technique described in this article makes it possible to take impressions and make occlusal records simultaneously, which can avoid the need to fabricate resin record bases in the laboratory and lower the risk of postoperative wound swelling. Compared with the conventional method, this technique can reduce chair time by around 1.5 hours. Time can be saved in impression taking, occlusal registration and pouring plaster models.

Acrylic resin polymerisation shrinkage has been considered a critical factor when taking impressions for multiple implants, especially for four or more implants

per dental arch[9-10]. Previous reports have proposed some innovative methods to solve this problem, such as the use of 3D printed splints and digital impression methods, the accuracy of which needs to be verified further[7,8,11]. In our proposed technique, the prefabricated bars minimise the mass of acrylic resin used and provide a homogeneous space between the joints, which can effectively prevent the impression error caused by polymerisation shrinkage.

Sufficient attention must be paid to the early complications that can occur in cases of immediate loading in edentulous full-arch restorations. Specifically, mechanical complications include prosthesis loosening, screw or abutment fracture, artificial tooth fracture and resin base fracture. Denture base fracture has been reported as a main complication during the time in function of immediate prostheses. Shen et al[12] reported that 28.1% of immediate prostheses fractured in 114 patients during 6 months of function. This type of complication was significantly related to bruxism, cantilever, the material used and maxillary rehabilitation[13]. Some studies utilised cast or milled metal bars and a CAD/CAM framework to reinforce the acrylic resin[6,14]; however, these techniques require extra time and make it difficult to complete the prosthesis within 24 hours. In contrast, the prefabricated bars can be used directly as a reinforcing framework in the poly(methyl methacrylate) denture base, which is a more economical and convenient method for reinforcement.

Immediate loading of an interim prosthesis increases the risk of misfit as well as adverse movement of the entire structure. The use of intermediate multiunit abutments allows the clinician to obtain an absolute passive fit of screw-retained full-arch prostheses, even in the presence of several angled implants. In addition, previous studies have shown that repeated screwing/unscrewing of the superstructure can result in permanent failure of the hemidesmosomal soft tissue connection around the implant[15]. Placement of intermediate abutments makes it possible to perform further restorative operations at the abutment level to protect the peri-implant soft tissues from damage and maintain bone tissue stability.

The present case report has several limitations. On one hand, taking an impression without using the tray causes the impression material to lose the support of the rigid tray, which may cause the material to become deformed when pouring a plaster model or mounting the articulator. On the other hand, this paper is susceptible to bias due to the weak strength of medical evidence as it is an individual case report. Well-designed randomised controlled trials with larger sample sizes are therefore necessary to further validate this method in the future.

Conclusion

This article presents an efficient technique for fabricating interim, immediately loaded implant-supported full-arch prostheses with prefabricated rigid connecting bars. The reduction of laboratory and chair time and the elimination of the possibility of errors are important contributing factors to achieving more predictable and successful prosthesis for both clinicians and patients.

Acknowledgements

The lab work was performed by Beijing Shengzhuo Dental Corporation.

Conflicts of interest

The authors declare no conflicts of interest related to this study.

Author contribution

Dr Yi Man TANG contributed to the data analysis and drafted the manuscript; Dr Hua Jie YU contributed to the data acquisition and interpretation; Prof Li Xin QIU and Dr Juan WANG contributed to the design of the case and the conduction of surgical and restoration procedures and critically revised the manuscript.

(Received April 18, 2021; accepted Oct 11, 2021)

References

1. Kofford B, Drago C, Nejat AH, Elshewy M. A novel approach for converting a mandibular complete denture to a fixed interim, screw-retained implant prostheses: A case report. J Prosthodont 2021;30:13–18.
2. Tealdo T, Menini M, Bevilacqua M, et al. Immediate versus delayed loading of dental implants in edentulous patients' maxillae: A 6-year prospective study. Int J Prosthodont 2014;27:207–214.
3. Stimmelmayr M, Beuer F, Edelhoff D, Güth JF. Implant impression techniques for the edentulous jaw: A summary of three studies. J Prosthodont 2016;25:146–150.
4. Rüttermann S, Alberts I, Raab WHM, Janda RR. Physical properties of self-, dual-, and light-cured direct core materials. Clin Oral Investig 2011;15:597–603.
5. Misch CM. Immediate loading of definitive implants in the edentulous mandible using a fixed provisional prosthesis: The denture conversion technique. J Oral Maxillofac Surg 2004;62:106–115.

6. Degidi M, Nardi D, Piattelli A. Immediate definitive rehabilitation of the edentulous patient using an intraorally welded titanium framework: A 3-year prospective study. Quintessence Int 2010;41: 651–659.
7. Menini M, Setti P, Pera F, Pera P, Pesce P. Accuracy of multi-unit implant impression: Traditional techniques versus a digital procedure. Clin Oral Investig 2018;22:1253–1262.
8. Pesce P, Pera F, Setti P, Menini M. Precision and accuracy of a digital impression scanner in full-arch implant rehabilitation. Int J Prosthodont 2018;31:171–175.
9. Ma J, Rubenstein JE. Complete arch implant impression technique. J Prosthet Dent 2012;107:405–410.
10. Papaspyridakos P, Kim YJ, Finkelman M, El-Rafie K, Weber HP. Digital evaluation of three splinting materials used to fabricate verification jigs for full-arch implant prostheses: A comparative study. J Esthet Restor Dent 2017;29:102–109.
11. Espona J, Roig E, Ali A, Roig M. Immediately loaded interim complete-arch implant-supported fixed dental prostheses fabricated with a completely digital workflow: A clinical technique. J Prosthet Dent 2020;124:423–427.
12. Shen H, Di P, Luo J, Lin Y. Clinical assessment of implant-supported full-arch immediate prostheses over 6 months of function. Clin Implant Dent Relat Res 2019;21:473–481.
13. Cercadillo-Ibarguren I, Sánchez-Torres A, Figueiredo R, Valmaseda-Castellón E. Early complications of immediate loading in edentulous full-arch restorations: A retrospective analysis of 88 cases. Int J Oral Maxillofac Implants 2017;32:1116–1122.
14. Crespi R, Vinci R, Capparé P, Romanos GE, Gherlone E. A clinical study of edentulous patients rehabilitated according to the “all on four” immediate function protocol. Int J Oral Maxillofac Implants 2012;27:428–434.
15. Ashurko I, Trofimov A, Tarasenko S, Mekhtieva S. Full-mouth screw-retained implant-supported rehabilitation with multiunit abutments using virtual guided surgery and digital prosthetics protocol. Case Rep Dent 2020;2020:3585169.

CLEAR NARRATIVE, STUNNING VISUALS

NEW

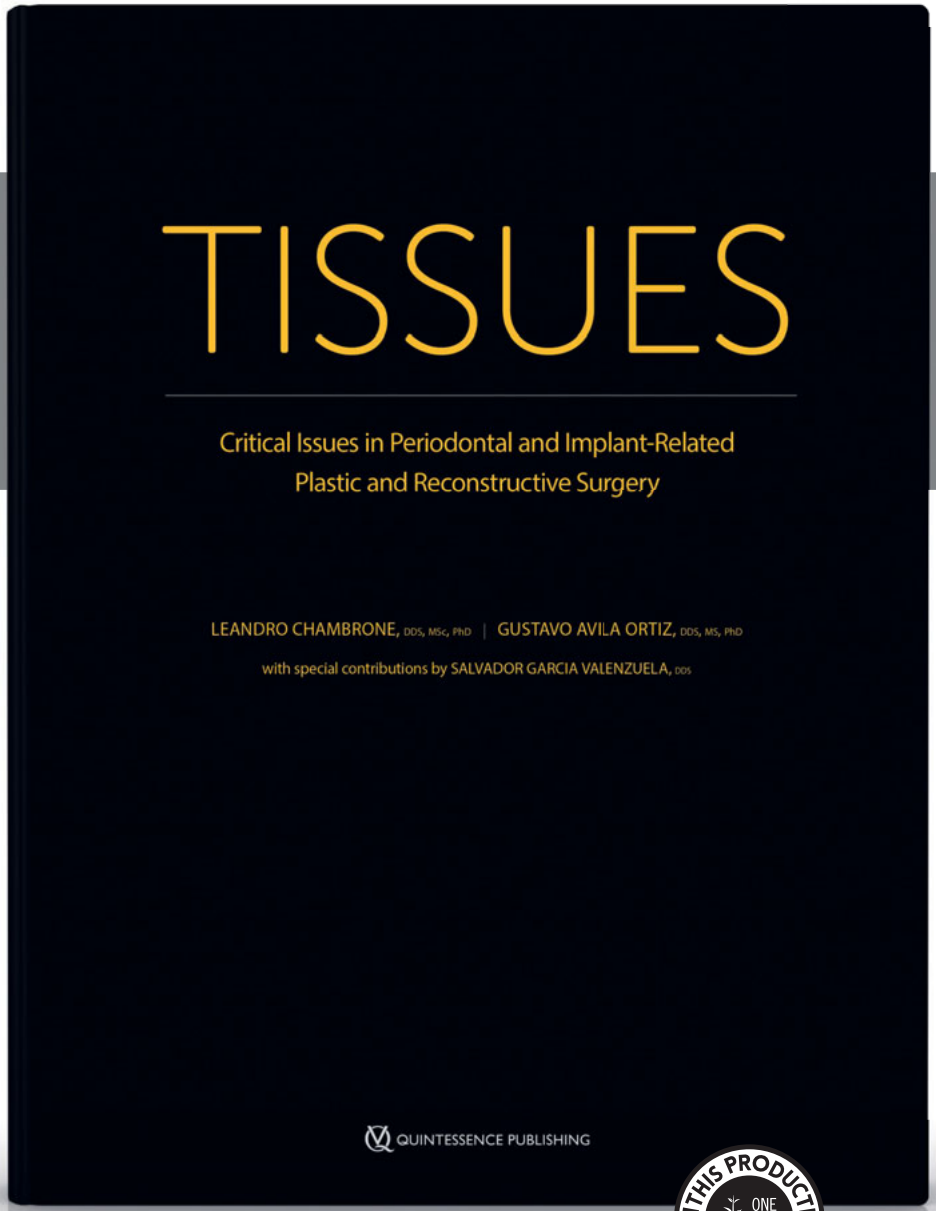

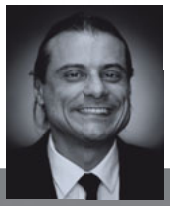

Leandro Chambrone | Gustavo Avila Ortiz

Tissues

Critical Issues in Periodontal and Implant-Related Plastic and Reconstructive Surgery

624 pages, 2,500 illus, ISBN 978-0-86715-963-9
€298

The success of periodontal and implant-related plastic and reconstructive surgical therapy is based on several fundamental principles, including an understanding of tissue characteristics in both health and disease, proper selection and use of surgical armamentarium, adequate flap design and management, and an understanding of the properties and indications of different graft materials. All of these elements are interconnected and must be considered in the process of treatment planning and patient care. This book beautifully weaves together clear narrative and stunning visuals to illustrate the five core components of periodontal and implant-related plastic and reconstructive surgical therapy—the tissues, the tools, the flaps, the grafts, and the surgeries—and how to manage them successfully in contemporary clinical practice. A true masterpiece in periodontology.

www.quint.link/tissues
books@quintessenz.de
+49 (0)30 761 80 667
QUINTESSENCE PUBLISHING

THE ART OF MOVING TEETH PREDICTABLY

NEW

Kwangchul Choy

Burstone's Biomechanical Foundation of Clinical Orthodontics

516 pages, 1,584 illus
ISBN 978-0-86715-949-3
€178

Dr Charles Burstone was a pioneer in orthodontic biomechanics, and his legacy lives on this second edition of his book, with Dr Kwangchul Choy at the helm. This textbook has taught thousands of orthodontists the importance of understanding biomechanics to ensure healthy, predictable movements in clinical practice, and this new edition will undoubtedly do the same for the new generations of students. Technology continues to advance in orthodontics, but no technology can replace a sound understanding of how the teeth move in their periodontal apparatus and how they can be pushed or pulled to get where they need to be. This book is the difference between an orthodontist who can move teeth and one who can plan cases with predictability and achieve the sought-after results.

www.quint.link/understanding-biomechanics

books@quintessenz.de

+49 (0)30 761 80 667

QUINTESSENCE PUBLISHING